

Transition metal containing supramolecular assemblies

Author:

Shen, Chao

Publication Date:

2015

DOI:

<https://doi.org/10.26190/unsworks/18459>

License:

<https://creativecommons.org/licenses/by-nc-nd/3.0/au/>

Link to license to see what you are allowed to do with this resource.

Downloaded from <http://hdl.handle.net/1959.4/55002> in <https://unsworks.unsw.edu.au> on 2024-05-03

Transition metal containing supramolecular assemblies

A thesis presented in partial fulfilment
of the requirements towards the degree of

Master of Philosophy

By

Chao Shen



UNSW
THE UNIVERSITY OF NEW SOUTH WALES

School of Chemistry

Faculty of Science

March 2015

Table of Contents

Contents

TABLE OF FIGURES.....	4
ABSTRACT	6
TABLE OF ABBREVIATIONS	7
ACKNOWLEDGEMENTS	8
1. CHAPTER 1	9
1.1. INTRODUCTION	9
1.1.1. <i>Molecular cages</i>	9
1.1.2. <i>Expanded ligands and metalloligands</i>	11
1.1.3. <i>Ru(II) polypyridyl complexes</i>	13
1.1.4. <i>Ru(II) complexes in cages, networks and polymers</i>	16
1.2. CHAPTER SUMMARY AND CONCLUSION	22
1.3. PROJECT AND ITS SIGNIFICANCE	22
2. CHAPTER 2	25
2.1. INTRODUCTION	25
2.2. LIGAND AND RUTHENIUM(II) COMPLEX SYNTHESIS AND CHARACTERIZATION	25
2.3. MASS SPECTROMETRY CHARACTERIZATION.....	28
2.4. NUCLEAR MAGNETIC RESONANCE(NMR) CHARACTERIZATION.....	28
2.5. STABILITY OF RUTHENIUM(II) COMPLEXES.....	30
2.6. EXAMPLES OF PROTONATION OF BROMO AND BORONIC ACID FUNCTIONALIZED RUTHENIUM(II) COMPLEX	32
2.7. CHAPTER SUMMARY AND CONCLUSION	34
2.8. EXPERIMENTAL SECTION	35
2.8.1. <i>General procedure</i>	35
2.8.2. <i>Ligand 1: 4'-(3-bromophenyl)-2,2':6',2''-terpyridine</i>	35
2.8.3. <i>Ligand 2: 4'-(4-bromophenyl)-2,2':6',2''-terpyridine</i>	35
2.8.4. <i>Ligand 3: 4'-(3-pyridyl)-2,2':6',2''-terpyridine</i>	35
2.8.5. <i>Ligand 4: 4'-(4-pyridyl)-2,2':6',2''-terpyridine</i>	35
2.8.6. <i>Ligand 7: 4'-(4-hydroxyphenyl)-2,2':6',2''-terpyridine</i>	35
2.8.7. <i>4'-[3-(5,5-dimethyl-1,3,2-dioxaborinan-2-yl)phenyl]-2,2':6',2''-terpyridine</i>	36
2.8.8. <i>4'-[4-(5,5-dimethyl-1,3,2-dioxaborinan-2-yl)phenyl]-2,2':6',2''-terpyridine</i>	36
2.8.9. <i>Ru(1)Cl₃ and Ru(2)Cl₃</i>	37
2.8.10. <i>Ru(5a)Cl₃ and Ru(6a)Cl₃</i>	37
2.8.11. <i>Synthesis of [Ru(2)(3)](PF₆)₂</i>	39
2.8.12. <i>Synthesis of [Ru(5b)(3)](PF₆)₂</i>	40
2.8.13. <i>Synthesis of [Ru(6b)(3)](PF₆)₂</i>	41
2.8.14. <i>Synthesis of [Ru(1)(4)](PF₆)₂</i>	41
2.8.15. <i>Synthesis of [Ru(2)(4)](PF₆)₂</i>	42
2.8.16. <i>Synthesis of [Ru(5b)(4)](PF₆)₂</i>	44
2.8.17. <i>Synthesis of [Ru(6b)(4)](PF₆)₂</i>	45
2.8.18. <i>Synthesis of [Ru(7)₂](PF₆)₂</i>	46
3. CHAPTER THREE: DINUCLEAR RU(II) COMPLEXES AS EXPANDED LIGANDS	47
3.1. INTRODUCTION	47
3.2. SYNTHESIS OF RUTHENIUM(II) DINUCLEAR COMPLEX.....	49
3.3. MASS SPECTROMETRY CHARACTERIZATION	54
3.4. NUCLEAR MAGNETIC RESONANCE (NMR) CHARACTERIZATION OF DINUCLEAR COMPLEX WITH TWO TERMINAL PENDENT PYRIDINES. ...	54
3.5. STABILITY OF RUTHENIUM(II) DINUCLEAR COMPLEX	57
3.6. EXAMPLE OF PROTONATION OF DINUCLEAR COMPLEX	57
3.7. ATTEMPTS TO BUILD LARGE MOLECULAR CAGES	58
3.8. CHAPTER SUMMARY AND CONCLUSION	63
3.9. EXPERIMENTAL SECTION	63

3.9.1.	<i>Ligand 8: 4'-(4-methylphenyl)-2,2':6',2''-terpyridine</i>	63
3.9.2.	$[Ru(2)(8)](PF_6)_2$	63
3.9.3.	$[Ru(9)(8)](PF_6)_2$	64
3.9.4.	$[Ru(10)(8)](PF_6)_2$	65
3.9.5.	$[Ru(9)(4)](PF_6)_2$	66
3.9.6.	$[Ru(10)(4)](PF_6)_2$	67
3.9.7.	$[Ru(6b)(9)](PF_6)_2$	68
3.9.8.	$[(8)Ru(12)Ru(8)](PF_6)_4$	69
3.9.9.	$[(8)Ru(13)(8)](PF_6)_4$	70
3.9.10.	$[(4)Ru(12)Ru(4)](PF_6)_4$	71
3.9.11.	$[(3)Ru(12)Ru(3)](PF_6)_4$	72
3.9.12.	$[(4)Ru(11)Ru(4)](PF_6)_4$	73
3.9.13.	$[(3)Ru(11)Ru(3)](PF_6)_4$	74
4.	CHAPTER FOUR	75
4.1.	INTRODUCTION	75
4.2.	SYNTHESIS OF PYRENE DERIVATIVES	77
4.2.1.	<i>Synthesis and hydrogenation of pyrene derivatives</i>	77
4.2.2.	<i>Suzuki or Sonogashira cross coupling reactions between tetrabromopyrene or tetraborylpyrene and functionalized ruthenium(II) complexes</i>	79
4.2.3.	<i>M₈L₆ cage synthesis via metal-template imine bond formation</i>	85
4.3.	SUMMARY AND CONCLUSION	97
4.4.	EXPERIMENTAL	98
4.4.1.	<i>1,3,6,8-tetrabromopyrene</i>	98
4.4.2.	<i>1,3,6,8-tetrakis(5,5-dimethyl-1,3,2-dioxaborinan-2-yl)pyrene</i>	98
4.4.3.	<i>1,3,6,8-Tetrakis(3-hydroxy-1-propynyl)pyrene</i>	99
4.4.4.	<i>Attempted hydrogenation of 1,3,6,8-Tetrakis(3-hydroxy-1-propynyl)pyrene</i>	100
4.4.5.	<i>Suzuki cross coupling reaction between 1,3,6,8-tetrabromopyrene and $[Ru(6b)(8)](PF_6)_2$</i>	100
4.4.6.	<i>Sonogashira cross coupling reaction between 1,3,6,8-tetrabromopyrene and $[Ru(10)(8)](PF_6)_2$</i>	101
4.4.7.	<i>Suzuki cross coupling reaction between 1,3,6,8-tetrabromopyrene and $[Ru(5b)(4)](PF_6)_2$</i>	102
4.4.8.	<i>Suzuki cross coupling reaction between 1,3,6,8-tetrakis(5,5-dimethyl-1,3,2-dioxaborinan-2-yl)pyrene and $Ru[1][4](PF_6)_2$</i>	103
4.4.9.	<i>Suzuki cross coupling reaction between 1,3,6,8-tetrakis(5,5-dimethyl-1,3,2-dioxaborinan-2-yl)pyrene and Ligand 1</i>	104
4.4.10.	<i>Tetrakis(4-nitrophenyl)ethene</i>	105
4.4.11.	<i>Tetrakis(4-aminophenyl)ethene</i>	105
4.4.12.	<i>TPE imine ligand (28)</i>	106
4.4.13.	<i>Self-assembled M₂L₃ cage</i>	107
5.	CONCLUSIONS AND FUTURE WORK	109
6.	REFERENCES	110

Table of Figures

Figure 1: A “diamantanoid” cage by Saalfrank’s group ^[2]	9
Figure 2: Representative tetrahedral cage by Raymond’s group ^[12]	10
Figure 3 : The expanded ligand for comparison.	11
Figure 4: Tris(bipyridine) ruthenium(II) complex, the prototypical photoactive coordination complex.	13
Figure 5: Ru(<i>bpy</i>) ₃ ²⁺ complex works as a catalyst in the visible light photocatalysis. ^[274]	14
Figure 6 : Energy level diagrams of [Ru(<i>bpy</i>) ₃] ²⁺ and [Ru(<i>tpy</i>) ₂] ²⁺ (MLCT = metal to ligand charge transfer, ISC = intersystem crossing, MC = metal-centered, GS = ground state, <i>bpy</i> = 2,2’-bipyridine, <i>terpy</i> = 2,2’:6’,2’’-terpyridine)	15
Figure 7: Homoleptic bis(terpyridine) ruthenium(II) complexes	16
Figure 8: Left: <i>fac</i> -[Ru(L) ₃](PF ₆) ₂ . Right: the adamantane-like Ru ₄ Ag ₆ cage. ^[34a]	17
Figure 9 : Left: Free ligand [Ru(L) ₃](PF ₆) ₂ . Middle: Ru ₄ Cd ₄ cubic cage showing geometric isomerism at all the vertexes (F = <i>fac</i> , M = <i>mer</i>) Right: metal center of the Ru ₄ Cd ₄ cubic cage. ^[34b]	18
Figure 10: The tristerpyridine ligand ^[34c] used to assemble dimeric cages with Ru(II) ions.	19
Figure 11: Left: tetrakis[4-(4’=phenyl-2,2’:6’,2’’-terpyridine)phenyl]methane ligand. Right: tetrahedral ligand coordinating to the ruthenium(II) center in the coordination network. ^[36]	19
Figure 12 : Left: Tris(phenanthroline) Ru(II) derived metalloligand. Right: metalloligand in the rhombododecahedral metal-organic cage ^[6c] .	20
Figure 13 : Homoleptic [Ru(<i>pytpy</i>) ₂] ²⁺ one dimensional polymer linked by coordination bond from silver(I).	21
Figure 14 : Left: Homoleptic 4’-(2,2’:6’,2’’-terpyridyl)hydrazones ruthenium(II) complex. Right: Banana shape heterometallomacrocyclic which forms part of a 1D coordination polymer chain.	21
Figure 15 : Examples of known heteroleptic pyridyl terpyridine ruthenium(II) complexes ^[30b, 31]	23
Figure 16 : Examples of dinuclear expanded ligand prepared in this project as a dimetallic analogue of small organic linkers used to self-assemble molecular spheres by Fujita ^[7]	24
Figure 17: Ligands used in this study and the numbering scheme adopted. Ligands 1, ^[50] 2, ^[51] 3, ^[52] 4, ^[53] 5a, ^[54] 5b, ^[34c] 6a, ^[47b] 6b ^[55] and 7 ^[50] have been previously reported.	26
Figure 18: Synthetic route to heteroleptic Ru(II) complexes prepared in this study. *Yields are given over 2 steps.	27
Figure 19: ¹ H NMR spectra (400 MHz, CD ₃ CN, 298K) for Ru(II) complexes synthesized in this study. Top to bottom: [Ru(1)(3)](PF ₆) ₂ ; [Ru(2)(3)](PF ₆) ₂ ; [Ru(5b)(3)](PF ₆) ₂ ; [Ru(6b)(3)](PF ₆) ₂ ; [Ru(1)(4)](PF ₆) ₂ ; [Ru(2)(4)](PF ₆) ₂ ; [Ru(5b)(4)](PF ₆) ₂ ; [Ru(6b)(4)](PF ₆) ₂ and [Ru(7)(2)](PF ₆) ₂ . See Figure 17 for labelling scheme adopted.	29
Figure 20 : NOESY (400 MHz, CD ₃ CN) spectrum of [Ru(6b)(3)](PF ₆) ₂	30
Figure 21 : ¹ H NMR (CD ₃ CN, 400 MHz) of (top to bottom): [Ru(7)(2)] ²⁺ ; [Ru(6b)(4)] ²⁺ precipitated with NH ₄ PF ₆ ; [Ru(5b)(4)] ²⁺ precipitated with NH ₄ PF ₆ (different sample) and (bottom) [Ru(5b)(4)] ²⁺ precipitated with KPF ₆ . The large 1:1:1 triplet at 6.1 ppm is NH ₄ ⁺ .	31
Figure 22: ¹ H NMR (CD ₃ CN, 400 MHz) of (top to bottom): deprotonated [Ru(1)(4)](PF ₆) ₂ ; protonated [Ru(1)(4)](PF ₆) ₂ by trace acid in solvent; Fully protonated [Ru(1)(4)](PF ₆) ₂ by TFA.	33
Figure 23: ¹ H NMR (CD ₃ CN, 300 MHz) of (top to bottom): deprotonated [Ru(6b)(4)](PF ₆) ₂ ; Protonated [Ru(6b)(4)](PF ₆) ₂ by trace amount of acid in the solvent; Protonated [Ru(6b)(4)](PF ₆) ₂ by adding TFA.	34
Figure 24: Bridging ligand, 6’,6’’-di(pyridin-2-yl)-2,2’:4’,4’’:2’’’,2’’’’-quaterpyridine and capping ligand, 4’-(4-methylphenyl)-2,2’:6’,2’’-terpyridine	47
Figure 25 : Coordination cage based on the banana shaped ligand, bis(pyridin-3-ylethynyl)benzene ^[77]	48
Figure 26: Ligands used in this study and the numbering scheme adopted.	49
Figure 27 : NMR spectra of [Ru(6b)(8)](PF ₆) ₂ and [(8)Ru(12)Ru(8)](PF ₆) ₄	51
Figure 28 : NMR spectra of [Ru(10)(8)](PF ₆) ₂ and [(8)Ru(13)Ru(8)](PF ₆) ₄	52
Figure 29 : Bridging ligand X and terminal ligand Y	53
Figure 30 : ¹ H NMR spectra (400 MHz, CD ₃ CN, 298K) for Ru(II) complexes synthesized in this study. Top to bottom: [(4)Ru(11)Ru(4)](PF ₆) ₄ ; [(4)Ru(12)Ru(4)](PF ₆) ₄ ; [(3)Ru(11)Ru(3)](PF ₆) ₄ ; [(3)Ru(12)Ru(3)](PF ₆) ₄ ; See Figure 26 for labelling scheme adopted.	55
Figure 31: new signals appear in the [(4)Ru(12)(4)](PF ₆) ₄ and protons of ring C’ shift upfield after Suzuki cross coupling reaction.	56
Figure 32 : NOESY spectrum of [(4)Ru(11)Ru(4)](PF ₆) ₄	57
Figure 33: ¹ H NMR (CD ₃ CN, 400 MHz) of (top to bottom): non-protonated [(4)Ru(11)Ru(4)](PF ₆) ₄ complex; Not fully protonated [(4)Ru(11)Ru(4)](PF ₆) ₄ complex; Fully protonated [(4)Ru(11)Ru(4)](PF ₆) ₄ complex.	58
Figure 34 : Top, free ligand in DMSO-d ₆ , [(4)Ru(12)Ru(4)](PF ₆) ₄ ; Bottom, free ligand, [(4)Ru(12)Ru(4)](PF ₆) ₄ in DMSO-d ₆ after treated with Pd(NO ₃) ₂ /Pd(CH ₃ CN) ₄ (BF ₄) ₂ at 80°C for 6 h.	59
Figure 35 Top, free ligand in CD ₃ CN, [(4)Ru(12)Ru(4)](PF ₆) ₄ ; Bottom, free ligand, [(4)Ru(12)Ru(4)](PF ₆) ₄ in CD ₃ CN after treatment with Pd(NO ₃) ₂ /Pd(CH ₃ CN) ₄ (BF ₄) ₂ at 80°C for 6 h.	60
Figure 36: COSY Spectrum of the supramolecular structure	61
Figure 37: NOESY Spectrum of the supramolecular structure	62
Figure 38: ¹ H- ¹³ C HSQC (600 MHz, CD ₃ CN) spectrum of the supramolecular structure.	63
Figure 39: (<i>bpy</i>) ₂ Ru(Pyr) ²⁺ ruthenium complex	75
Figure 40: Diagrams of [<i>bpy</i>] ₂ Ru(pyr) ²⁺ (MLCT = metal to ligand charge transfer, ISC = intersystem crossing, , GS = ground state, <i>bpy</i> = 2,2’-bipyridine, pyr = pyrene)	76
Figure 41 : Tetraphenylethene and an example of tetraphenylethene derivative as a fluorescent probe	76
Figure 42: ¹ H NMR (DMSO-d ₆ , 300MHz) spectrum of 1,3,6,8-tetrakis(3-hydroxy-1-propynyl)pyrene	78
Figure 43 : ¹ H NMR (DMSO-d ₆ , 300MHz) Comparison of starting materials, hydrogenation catalyzed by Pd/C and by PtO ₂	79
Figure 44: ¹ H NMR recorded spectra on 300MHz in CD ₃ CN, top, [Ru(6b)(8)](PF ₆) ₂ ; bottom, crude product of Suzuki cross coupling reaction between 1,3,6,8-tetrabromopyrene and [Ru(6b)(8)](PF ₆) ₂	81
Figure 45: ¹ H NMR recorded spectra on 300MHz in CD ₃ CN, top, [Ru(10)(8)](PF ₆) ₂ ; bottom, crude product of Sonogashira cross coupling reaction between 1,3,6,8-tetrabromopyrene and [Ru(10)(8)](PF ₆) ₂	82
Figure 46: Self-assembled M ₃ L ₆ cubic cage by Jonathan Nitschke’s group ^[95]	86
Figure 47: Left, tetrakis(4-aminophenyl)ethene; Right, TPE imine ligand.	86
Figure 48 : ¹ H NMR (CD ₃ CN, 300 MHz) spectra of (top): tetrakis(4-aminophenyl)ethene; (middle): 2-pyridine carboxaldehyde; (bottom): mixture of 2-pyridinecarboxaldehyde, FeBF ₄ ·6H ₂ O and tetrakis(4-aminophenyl) ethene (24:8:6) at 70°C in DMF for two days, followed by workup and dissolution in CD ₃ CN.	87
Figure 49: ¹ H NMR spectra recorded on 300MHz, top, tetrakis(4-aminophenyl)ethene in CD ₃ CN; middle, 2-pyridinecarboxaldehyde; bottom, mixture of 2-pyridinecarboxaldehyde (prepared the stock solution in DMF), FeBF ₄ ·6H ₂ O and tetrakis(4-aminophenyl)ethene at room temperature for 24 hours.	89
Figure 50: The proposed self-assembly of a M ₃ L ₆ cubic cage based on tetraanilineethene .	91
Figure 51: ¹ H NMR spectra (300 MHz, DMSO-d ₆) top to bottom: imine ligand 28, mixture of TPE imine ligand and FeBF ₄ ·6H ₂ O after heating at 70°C for 24 hours (middle) and 36h (bottom).	91
Figure 52: The structure of the Fe ₂ (29) ₃ cage formed by reaction of TPE with 2-pyridinecarboxaldehyde and Fe(BF ₄) ₂ ·6H ₂ O.	93
Figure 53 : ¹ H NMR (CD ₃ CN, 300MHz) spectra the reaction mixtures (in DMF) from different ratios (See Table 3) of 27, 2-pyridinecarboxaldehyde and Fe(BF ₄)·6H ₂ O, after workup.	93
Figure 54 : ¹ H NMR (CD ₃ CN, 300MHz), top, 27; middle, Fe ₂ L ₃ cage; bottom, 2-pyridinecarboxaldehyde.	94
Figure 55 : COSY spectrum (400 MHz, CD ₃ CN) of the Fe ₂ L ₃ Cage	95
Figure 56 : ¹ H- ¹³ C HSQC (600 MHz, CD ₃ CN) spectrum of the cage shows there is no cross peak of the peak in ¹ H NMR spectrum at 8.00 ppm.	95

Figure 57 : NOESY spectrum of the Fe₂L₃ cage

Figure 58 : ESI-MS of [Fe₂(29)₃]⁴⁺. Zoom of the 455.91 peak. Calc.455.91

96

108

Abstract

This thesis reports the synthesis of heteroleptic Ru(II) complexes featuring aryl bromide or boronic ester groups which are suitable for Pd(0)-catalysed cross-coupling reactions. These complexes are characterised in detail by ESI-MS, $^1\text{H-NMR}$, $^{13}\text{C-NMR}$ and several by elemental analysis. The reactivity and stability of these complexes is established allowing these to find applications as versatile building blocks for large metallocupramolecular structures. In particular their use as reagents for Suzuki coupling reactions are explored and reaction conditions and purification procedures are optimised. These complexes are then linked via Suzuki or Sonogashira coupling reaction to form very large dimetallic complexes. These dimetallic complexes feature pendant pyridyl groups and can therefore act as expanded analogues of the small bent organic molecules used by Fujita for forming large molecular cages with Pd(II) ions. A second goal is to prepare planar, tetrameric ruthenium(II) metalloligands which can act as molecular 'panels' to assemble large, box-like assemblies via self-assembly with palladium(II) ions, and preliminary results towards this goal are presented.

Table of Abbreviations

bpy	2,2'-bipyridine
Calcd	calculated
CH ₃ CN	acetonitrile
d	doublet
DMF	N,N-dimethylformamide
DMSO	dimethylsulfoxide
Et ₂ O	diethyl ether
EtOH	ethanol
g	gram(s)
h	hour(s)
Hz	Hertz
J	coupling constant
m	multiplet
mol	mole(s)
NMR	nuclear magnetic resonance (spectroscopy)
Pd/C	palladium on charcoal
phen	phenanthroline
q	quartet
s	singlet
t	doublet
TMS	trimethylsilyl
t	triplet
μ	micro
δ	chemical shift

Acknowledgements

I would like to thank Dr. Jonathon E. Beves for his supervision of the work presented in this thesis. I will always be grateful for the opportunity you gave me. I would also like to thank you for being so patient with my mistakes, for my Chinese accent, for the papers we will publish and for all the hours you have put into revising and discussing this thesis. Thank you for the support during the offshore period.

Big thank you to Tristan for his help in the lab as well as in the student offices during the early days. Thank you for chatting with me and sharing your understanding of the Australia.

A special thank you to Hasti for showing the trick of growing crystals, although the crystal we've got will not publish in this thesis.

A very special thank you to Jiajia Yang, for her great support and incentive in the middle days, especially, those ones in the lab. Thank you for showing the basic research skills about the stuff I worked with.

Thank you Pi Wang and Danyu Xia for putting up with me, for the coffee times and for the cooking time. Thank you for celebrating the Chinese New year in Australia and cooking the delicious I have ever had. I can never thank you enough for your friendship and support.

Thanks to my lovely parents and fiancée for their infinity love and encouragement even from so far away.

1. Chapter 1

1.1. Introduction

1.1.1. Molecular cages

Nature has exploited intermolecular interactions for the assembly of everything from lipid bilayers for compartmentalisation within cells to the formation of highly symmetrical clusters of proteins such as the clathrin protein^[1] which assembles into vesicle coats to transport cargoes. These self-assembled structures of Nature provide inspiration for the design and preparation of synthetic supramolecular architectures which may be capable of useful functions.

One of the most attractive classes of artificial containers is large, hollow cage molecules. These can be difficult to synthesize by conventional covalent methods. However, molecular cages can be readily prepared by self-assembly of preorganized small molecules using non-covalent interactions such as hydrogen bonds and coordinate bonds. The first synthetic molecular cage, a “diamantanoid” assembly^[2], was prepared by Saalfrank (see Figure 1) from dimethyl malonate, MeLi/MCl₂, oxalyl chloride, NH₄Cl and Mn(II), Co(II) and Ni(II) ions, which was characterized by X-ray crystallography.^[3] Understanding of the donor atom and coordination geometry preferences of metal ions and the geometric restrictions imposed by ligands is critical in design of molecular cages.

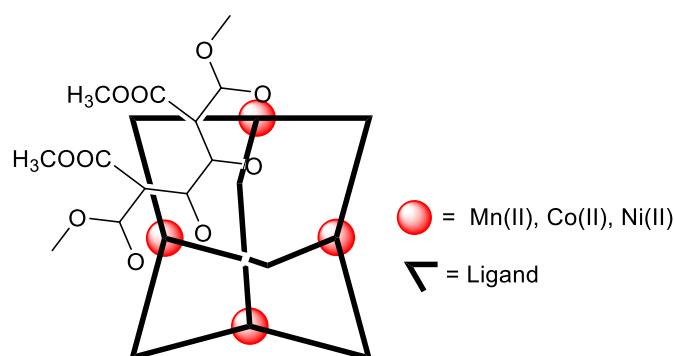


Figure 1 : A “diamantanoid” cage by Saalfrank’s group^[2]

The synthesis of a supramolecular cage is not always straightforward. The use of reversible reactions allows a degree of self-correction to occur in the assembly process through dissociation and

recombination, to allow thermodynamics to take control and drive the system to the lowest energy distribution of structures.^[4] Intermediate, high energy structures can rearrange during this process to form the lowest energy structure(s) as the final product can show greater thermodynamic stability among all intermediates.^[4a-c] Many coordination cages of different shapes such as tetrahedra^[5], octahedra,^[6] spheres,^[7] cubes,^[8] have been successfully synthesized by self-assembly and extensively studied. Of these, most rely on the combination of relatively labile metal ions with ligands of differing topologies and donor types. The most significant classes include Pd(II) ions with pyridyl ligands,^[6a, 9] Fe(II), Co(II) or Ni(II) ions with imine ligands^[10] and Al(III), Ga(III), In(III) Fe (III) and Ge(IV) with catechol based ligands^[5b, 11].

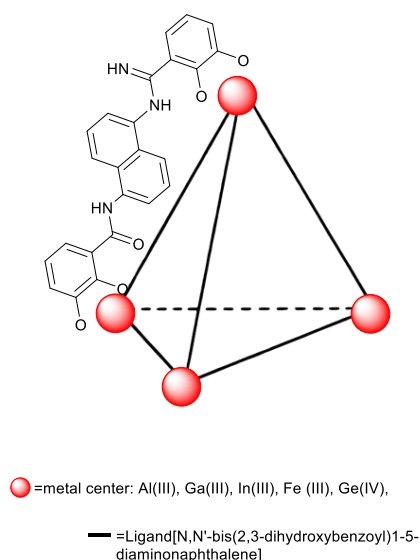


Figure 2 : Representative tetrahedral cage by Raymond's group^[12]

These cages can demonstrate selective guest binding based on size, shape and hydrophobic properties in particular. Due to the different environments inside and outside of the self-assembled host, guest molecules can have a significantly different chemical and physical behaviour inside the cage.^[5c] The isolated microenvironment of the cavity can make it possible for controlled molecular isomerization,^[13] for catalysis,^[8a, 14] to stabilize reactive species,^[5c, 15] or to generate of unusual reaction products.^[16]

Increasing attention is also being paid to enantiomeric purity of molecular cages,^[17] especially tetrahedral cages formed with octahedral metal centres which can have chiral configurations. In the solution or solid state, four octahedral metal ions with six bidentate ligands can result in a mixture of isomeric cages. Optically pure cages are required for uses such as enantioselective catalysis of organic reactions^[18] and chiral separations.^[19] One direct way to tackle this stereoselectivity problem is to decorate of the vertex of the ligands which chiral groups to direct the stereochemistry of the metal centres.^[17] Another way to resolve the cages is based on the formation of diastereomeric ion pairs. If the cage is anionic a cation resolving reagent such as an encapsulated guest is needed.^[18b, 20]

1.1.2. Expanded ligands and metalloligands

Expanded ligands^[21] could become one of the most useful design principles in supramolecular and metallosupramolecular chemistry. Expanded ligands and their parent ligands are structurally and topologically related (Figure 3) and can be used for the formation of large supramolecular structures.

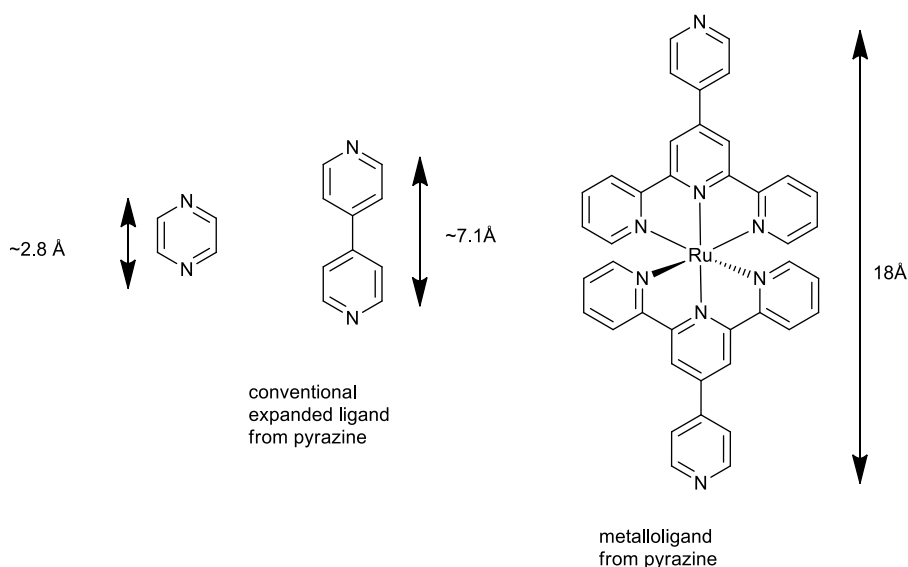


Figure 3 : The expanded ligand for comparison.

Expanded ligands are organic molecules containing metal-binding domains separated by spacer units such as aryl rings which extend the length of the ligands. In other words, the distance between donor sites to

donor sites is increased. Oxalic acid and terephthalic acid can be taken as an example, whose topologies are related. The utility of conventional spacers can be varied to form well-defined building blocks.

This concept has been widely applied in metallosupramolecular chemistry in the form of ‘metalloligands,’ also described as “complexes as metals, complexes as ligands”.^[21-22] The expansion of ligands relies on the addition of metal centres to link the multiple binding domains. It is worth mentioning even as metal-containing moieties are introduced the pendant pyridyl sites of expanded ligands still retain the geometry of the parent ligand. This introduction of a central metal-containing moiety, rather than conventional organic groups, in the expanded ligands delivers redox, magnetic, photophysical and other useful chemical properties to the ligand which can be exploited in larger structures.

There are chemical analogies between metalloligands and parent structures. One, two and three dimensional structures are formed based on the parent ligands. For example, it has been shown that 4,4'-bipyridine can be replaced by bis(4'-(4-pyridyl)-2,2':6',2''-terpyridine)ruthenium(II) complexes in the formation of macrocycles with 2,6-bis(bromomethyl)pyridine.^[23] Many other analogies can be found in the terpyridine based extended ligands such as phthalic acids,^[24] polyphosphines^[25] and polyacetylenes^[26] which are used for preparation of large metallosupramolecular structures.

1.1.3. Ru(II) polypyridyl complexes

Sunlight as an endless, green, non-toxic energy source has long been considered as an ideal ‘ingredient’ for chemical reactions. In conventional organic photochemical synthesis most reactions require the use of high energy UV light as most simple organic molecules do not absorb light in the visible part of the spectrum. This limitation has constrained development of visible light catalysed chemistry. However, a new strategy is to incorporate inorganic and organometallic compounds which are capable of catalysing organic reactions using visible light.

Among these transition metal complexes, ruthenium polypyridyl complexes have been especially well studied.^[27] Photochemical catalysis by tris(bipyridine) ruthenium(II) complex (Figure 4) takes advantages of the strong absorbance of visible light ($\lambda_{\text{max}} = 450 \text{ nm}$) by this complex, its predictable intermediates, functional group tolerance and stability to reaction conditions, such as high temperature or strongly acidic or basic conditions.

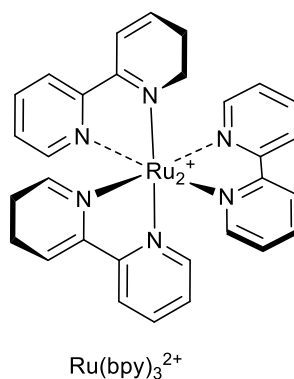


Figure 4 : Tris(bipyridine) ruthenium(II) complex, the prototypical photoactive coordination complex.

The key point here is that the triplet MLCT state of photoexcited ruthenium(II) complex can serve as an electron donor, which means the $[\text{Ru}^*(\text{bpy})_3]^{2+}$ is oxidized to $[\text{Ru}(\text{bpy})_3]^{3+}$. The ground state catalyst can be regenerated by accepting an electron from a sacrificial electron donor, typically an amine. For example, two decades ago research with $[\text{Ru}(\text{bpy})_3]^{2+}$ inspired the pioneering work of Fukuzumi.^[28] After $[\text{Ru}(\text{bpy})_3]^{2+}$ is excited an electron is transferred to an alkyl halide to form a Ru(III) complex. The halide group is lost as a negatively charged ion and the resulting organic radical is used for further reactions. The

Ru(III) complex can be reduced to Ru(II) complex by accepting an electron from the substrate or another reagent, either of which could act as electron donors.

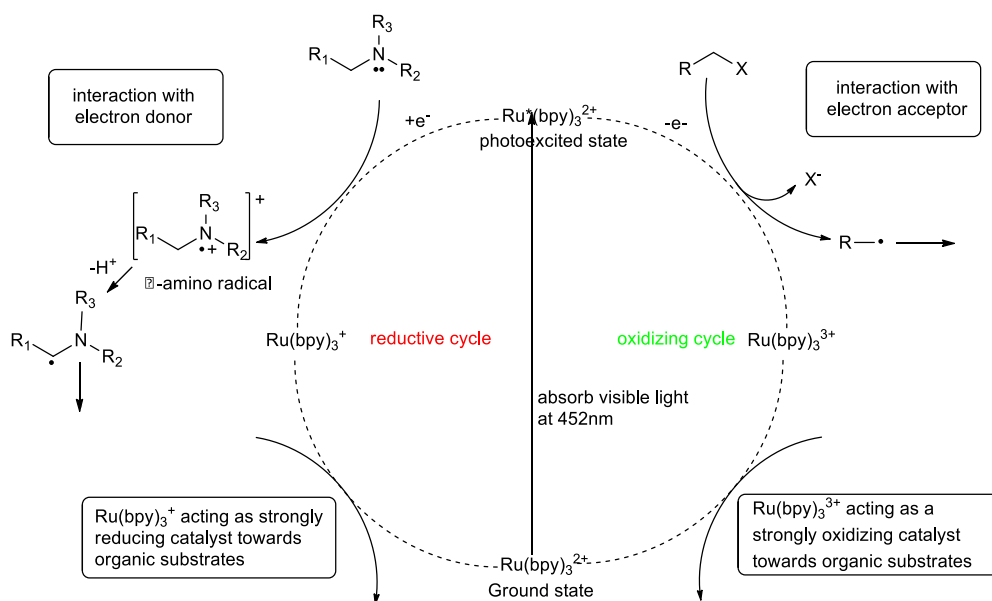


Figure 5 : $\text{Ru}[(\text{bpy})_3]^{2+}$ complex works as a catalyst in the visible light photocatalysis.^[27d]

Alternatively, a reductive cycle is possible where the photoexcited ruthenium(II) complex is reduced to $[\text{Ru}(\text{bpy})_3]^+$ by accepting an electron from electron donor. The amine intermediates can be further treated with acid to form amino radicals and iminium ions for other organic reactions (Figure 5).^[29] The regeneration of the ground state $\text{Ru}[(\text{bpy})_3]^{2+}$ from the reduced $[\text{Ru}(\text{bpy})_3]^+$ can be achieved by transferring an electron to another suitable substrate which acts as an electron acceptor. As it can be seen from the Figure 5, the $\text{Ru}[(\text{bpy})_3]^{2+}$ complex which can catalyse the organic reactions without being bound to any of the reactants.

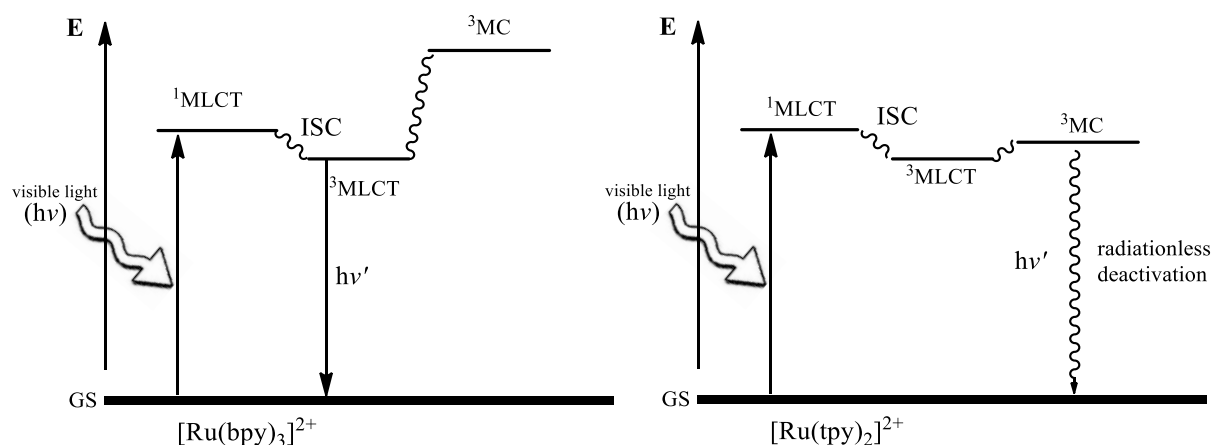


Figure 6 : Energy level diagrams of $[\text{Ru}(\text{bpy})_3]^{2+}$ and $[\text{Ru}(\text{tpy})_2]^{2+}$ (MLCT = metal to ligand charge transfer, ISC = intersystem crossing, MC = metal-centered, GS = ground state, bpy = 2,2'-bipyridine, terpy = 2,2':6',2''-terpyridine)

Apart from tris(2,2'-bipyridine)ruthenium(II), the related complex bis(terpyridine)ruthenium(II) $[\text{Ru}(\text{tpy})_2]^{2+}$ and its derivatives are one of the most prominent classes of ruthenium(II) complexes.^[30] Whether heteroleptic or homoleptic the formation of diastereomers is avoided due to the meridional coordination imposed by these tridentate rigid and planar ligands. Therefore, ruthenium(II) terpyridine based ligand units are used as potential building blocks for metallosupramolecular chemistry. Another significant difference between these two related complexes is the differences in their excited-state photophysical properties. $[\text{Ru}^*(\text{bpy})_3]^{2+}$ complexes have a less accessible ^3MC state due to a large energy gap between the $^3\text{MLCT}$ and ^3MC state (Figure 6). However, in the case of $[\text{Ru}^*(\text{tpy})_2]^{2+}$ the energy of these two states is similar, leading to a short excited state lifetime after being activated to the lowest excited $^3\text{MLCT}$ state. Most of the energy efficiently transfers to the ^3MC state from which deactivation to the ground state is rapid via a radiationless process. Extensive work has been done to improve the stability of $^3\text{MLCT}$ state or to increase the energy gap to the ^3MC state in $[\text{Ru}(\text{tpy})_2]^{2+}$ complexes. Additional electron-withdrawing groups such as COOH and COOEt^[30b, 31] on the 4'-position of terpyridine units stabilize the $^3\text{MLCT}$ state and lead to a longer excited lifetime. Another approach is to introduce an electron-donating group to destabilize the ^3MC state such as NH₂ and NHCOMe.^[30b, 31]

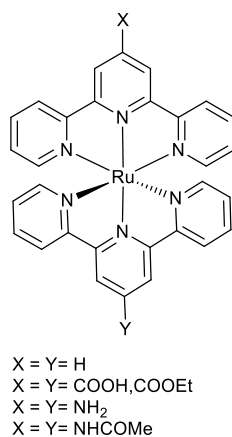


Figure 7 : Homoleptic bis(terpyridine) ruthenium(II) complexes

Strategies toward the long-lived and highly emissive excited state can be achieved by the introduction of a chromophore system on the terpyridine ligand which can stabilize the ³MLCT state.^[32] The phenyl ring attached to the 4'-position of the terpyridine ligand in the Ru complex has been realized to enhance the low quantum yield (less than 0.0007%).^[30b] While replacement of the phenyl rings with pyrimidine in the complex further improves the stability of ³MLCT state,^[30b] although both of their photo-properties are still far from that of Ru[(bpy)₃]²⁺. The straightforward approach to substantially extend the excited-state lifetimes can be achieved by enlargement of multichromophore system. Taking pyrene as an example, pyrene-based ruthenium complexes have been prepared which have triplet intraligand excited states (³IL)^[30b] with similar energies to the ³MLCT state. In this case, the ³IL state can work as an excited state reservoir for prolonging the excited time of ³MLCT state. As a result, the complex relax to the ground state via the phosphorescence.^[30b]

1.1.4. Ru(II) complexes in cages, networks and polymers

With the widespread interest in building large structures using metal directed self-assembly, kinetically inert ruthenium(II) complexes have been widely used in many areas.

There is a growing realization in self-assembling metal-organic cages incorporating ruthenium(II) metalloligands via binding other metal ions to form mixed-metal cages, although very few cages have been reported.^{[6c, 33],[34]} Two different approaches have been taken. The first is the expanded ligand

approach, where inert Ru(II) complexes are formed which act as ligands for labile metals to allow the self-assembly of cage structures under thermodynamic control. This method can prevent the scrambling of metal ion binding which would occur when only kinetically labile metal ions are used during the self-assembly. The second approach has been to use geometric restrictions to direct the formation of cages under kinetic control.

The Ward group have prepared bimetallic cages using pre-formed tris(bidentate) ruthenium complexes (Figure 8).^[34a] All of their cages rely on the stepwise assembly of cages by control of the coordination geometry of metal ions which occupy vertex positions in the cage structure. As an example, the adamantane-like Ru₄Ag₆ cage is formed from kinetically stable [Ru(L)₃]²⁺ units which have *fac* and *mer* configurations which must be separated before formation of mixed-metal cage. The geometrically pure metalloligands have three pendant bidentate binding sites, attached via flexible linkers, which are suitable for further coordination.

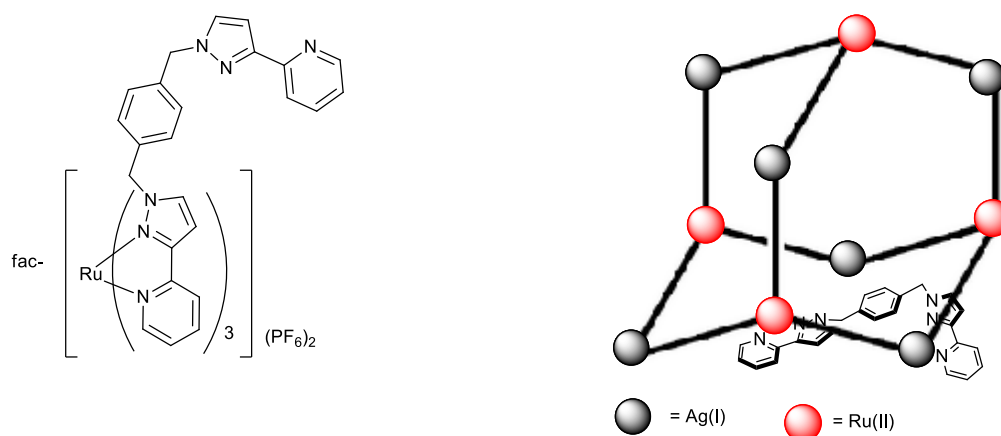


Figure 8 : Left: *fac*-[Ru(L)₃][PF₆]₂. Right: the adamantane-like Ru₄Ag₆ cage.^[34a]

The *fac*-[Ru(L)₃]²⁺ complexes are combined with Ag(I) ions to self-assemble into a Ru₄Ag₆ cage. The advantage of this stepwise method is that the Ag(I) ions cannot interact with the ruthenium binding domain during self-assembly to the expected cage.

Another bimetallic cage complex from the Ward group is based on Ru(II) and Cd(II) ions^[34b]. The ligand is similar to that mentioned above with kinetically labile Cd(II) ions instead of Ag(I) ions to form a

Ru_4Cd_4 cubic coordination cage which incorporates both *fac* and *mer* isomers of the Ru(II) complex. The synthesis of bis(pyrazolyl-pyridine) ruthenium(II) gives *fac/mer* isomers in a ratio of 1:3.^[34b] Therefore, no separation of the geometric isomers of the pre-formed $[\text{Ru}(\text{L})_3]^{2+}$ is needed in this case because one *fac* and three *mer* metalloligands meet the requirement of formation of the cage. The four Cd(II) ions have the same *fac* and *mer* ratio imposed by Ru(II) centres and are bound to the twelve remaining binding sites from ligands.

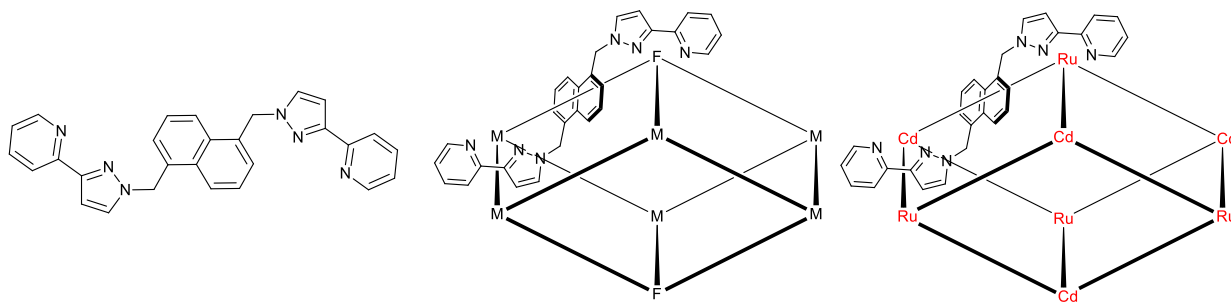


Figure 9 : Left: Free ligand $[\text{Ru}(\text{L})_3][\text{PF}_6]_2$. Middle: Ru_4Cd_4 cubic cage showing geometric isomerism at all the vertexes (F = *fac*, M = *mer*) Right: metal center of the Ru_4Cd_4 cubic cage.^[34b]

The first example of single-step self-assembly of a single nuclear ruthenium organic cage was reported recently, using tridentate terpyridine building blocks.^[34c] In this example, the assembly is under kinetic control and the high degree of preorganization and rigidity of the ligand is key to the synthesis. This 3D structure has a better stability towards strong acids and bases compared with bimetallic cages assembled with labile metal ions (such as those by Ward). The relatively low yield (35%) may be attributed to the inert nature of the Ru(II) centres, which offer little opportunity for error-correction during complex formation, which is of course the major drawback of attempting self-assembly directed by these ions.

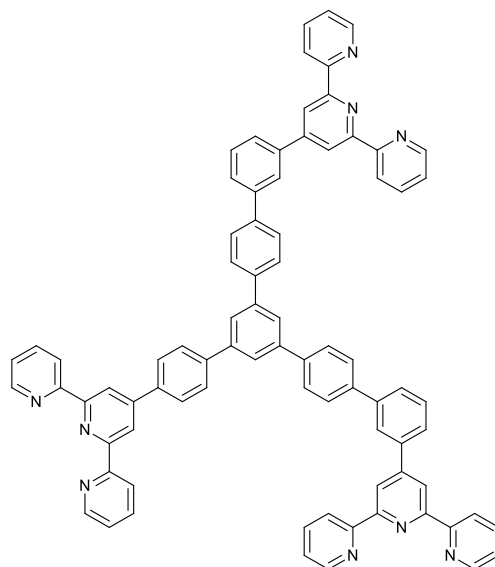


Figure 10 : The tristerpyridine ligand^[34c] used to assemble dimeric cages with Ru(II) ions.

Highly symmetric multidimensional arrays and networks in supramolecular chemistry can be achieved via interplay of coordinative, hydrogen bonding and π - π stacking interactions.^[35] Rigid polypyridine ligands are amongst the most interesting ligands used in building 3D metal coordination networks. If the network is only built via coordinate bonds, the final frame depends on the preferred coordination geometry of the metal ions and relative orientations of the donor groups of the ligands.

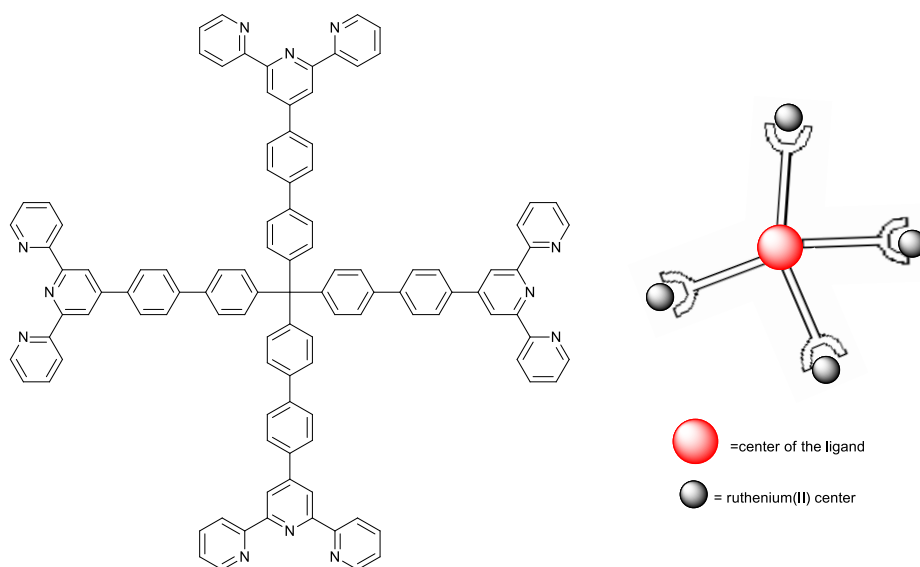


Figure 11 : Left: tetrakis[4-(4'-phenyl-2,2':6',2''-terpyridine)phenyl]methane ligand. Right: tetrahedral ligand coordinating to the ruthenium(II) center in the coordination network.^[36]

A diamonded coordination network has been reported based on the tetrahedral terpyridine-based ligand as a building block shown in Figure 11.^[36] High temperature (150 °C) or microwave conditions are used to force the reaction and the product precipitates from the solvent.^[36] Compared with single discrete $[\text{Ru}(\text{tpy})_2]^{2+}$ complex which has very weak room-temperature luminescence, the solid coordination network shows strong luminescence. After the ruthenium(II) centres in the network are excited, the rigid nature of the lattice limits the accessibility of the ^3MC state from the $^3\text{MLCT}$ state, which prevents loss of energy via non-radiative pathways and therefore improves the excited state lifetime.

A rhombododecahedral cage has been recently reported using tris(bidentate) metalloligands formed by functionalising phenanthroline ligands with a pendant pyridine group. This ligand selectively binds Ru(II) via the phenanthroline moiety, leaving the pendant pyridyl group free for complexation to additional metal ions (Figure 12).^[6c] Subsequent reaction with square planar Pd(II) ions leads to the self-assembly of a bimetallic cage structure consisting of six octahedral ruthenium(II) centres and eight square planar Pd(II) centres. One advantage of employing this metalloligand is the ligand is proposed to interact with electron rich aromatic guests via π - π interactions and the ligand can absorb the UV radiation. As edges of the cage system, it acts as a photoprotector to stabilize the photosensitive guests trapped inside over long time scales.

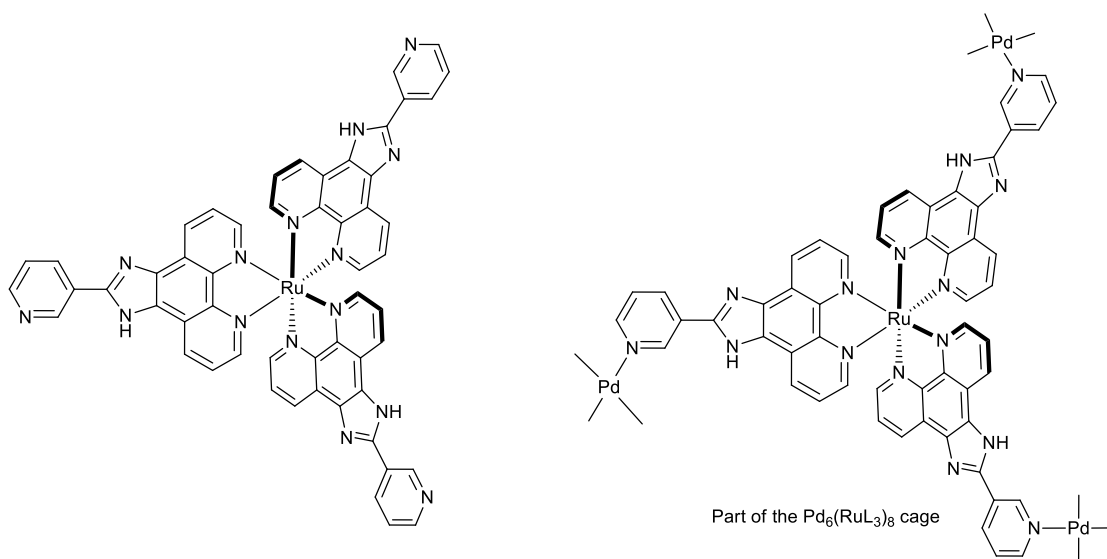


Figure 12 : Left: Tris(phenanthroline) Ru(II) derived metalloligand. Right: metalloligand in the rhombododecahedral metal-organic cage^[6c].

Other examples of the use of $[\text{Ru}(\text{tpy})_2]^{2+}$ units as expanded ligands include the incorporation of $[\text{Ru}(\text{pytpy})]^{2+}$ units into polymers via metal ion coordination to the pendant pyridyl groups.^[37] The bimetallic coordination polymer can be prepared by reaction of parent complexes with Ag(I) or Cu(II) ions to give 1D polymer chains (Figure 13).^[37-38]

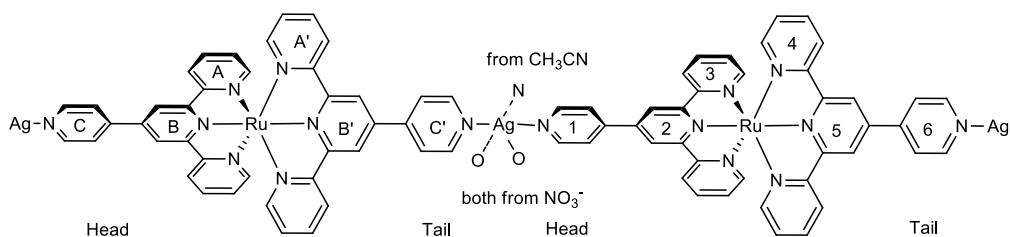


Figure 13 : Homoleptic $[\text{Ru}(\text{pytpy})]^{2+}$ one dimensional polymer linked by coordination bond from silver(I).

Another example is the homoleptic 4'-(hydrazones)tpy ruthenium(II) complex which can be assembled into 1D chains via coordination to Fe(II) centres which form heterometallomacrocycles. These chains are associated via π - π interactions to form 3D networks.^[39]

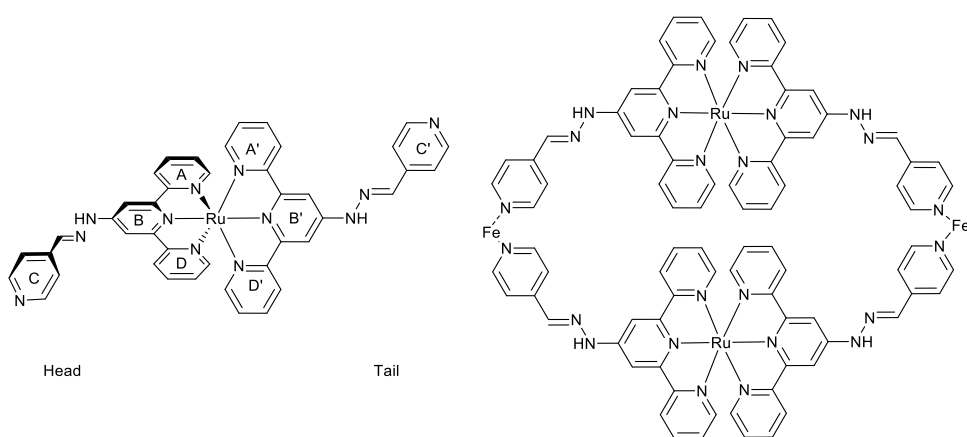


Figure 14 : Left: Homoleptic 4'-(2,2':6',2''-terpyridyl)hydrazones ruthenium(II) complex. Right: Banana shape heterometallomacrocycle which forms part of a 1D coordination polymer chain.

1.2. Chapter summary and conclusion

Ruthenium (II) polypyridyl complexes play important roles in supramolecular chemistry, principally as redox and photo-active structural elements, in addition to organic synthesis where their ability to act as photosensitisers and photoredox catalysts is proving to have versatile applications. Terpyridine-based ruthenium(II) complexes can be used for building large structures such as cages, polymers and networks via self-assembly with labile metal ions. The ruthenium(II) terpyridine complexes are substitutionally inert and labile metals therefore do not disturb the ruthenium(II) centre. Tridentate bipyridine-based ruthenium(II) complexes are applied in many organic chemistry. They have been shown to act as both electron donors *and* electron acceptors and can catalyse many organic reactions using visible solar energy. Introduction of ruthenium centres into large structures will have many applications in the future.

1.3. Project and its significance

In this project, the focus of interest is to introduce functionality to new heteroleptic ruthenium (II) complexes to enable these to be built into molecular cages and other extended structures.

Many different polypyridyl ruthenium(II) complexes have been synthesized and well-studied, especially homoleptic complexes. Relatively few contain ligands with pendant pyridyl groups and heteroleptic ruthenium(II) polypyridyl complexes contain pendant pyridyl groups. Additionally, to the best of our knowledge there are no examples of dimetallic Ru(II) complexes which can act as expanded ligands to form extended structures.

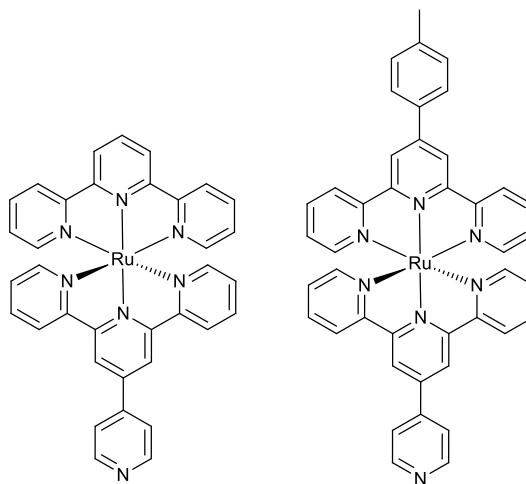


Figure 15 : Examples of known heteroleptic pyridyl terpyridine ruthenium(II) complexes^[30b, 31]

This thesis reports the synthesis of heteroleptic Ru(II) complexes featuring aryl bromide or boronic ester groups which are suitable for Pd(0)-catalysed cross-coupling reactions. These complexes are characterised in detail by ESI-MS, ¹H-NMR, ¹³C-NMR and several by elemental analysis. The reactivity and stability of these complexes is established allowing these to find applications as versatile building blocks for large metallocupramolecular structures. In particular their use as reagents for Suzuki coupling reactions are explored and reaction conditions and purification procedures are optimised. These complexes are then linked via Suzuki or Sonogashira coupling reaction to form very large dimetallic complexes. These dimetallic complexes feature pendant pyridyl groups and can therefore act as expanded analogues of the small bent organic molecules used by Fujita for forming large molecular cages with Pd(II) ions.^[40] A second goal is to prepare planar, tetrameric ruthenium(II) metalloligands which can act as molecular ‘panels’ to assemble large, box-like assemblies via self-assembly with palladium(II) ions.

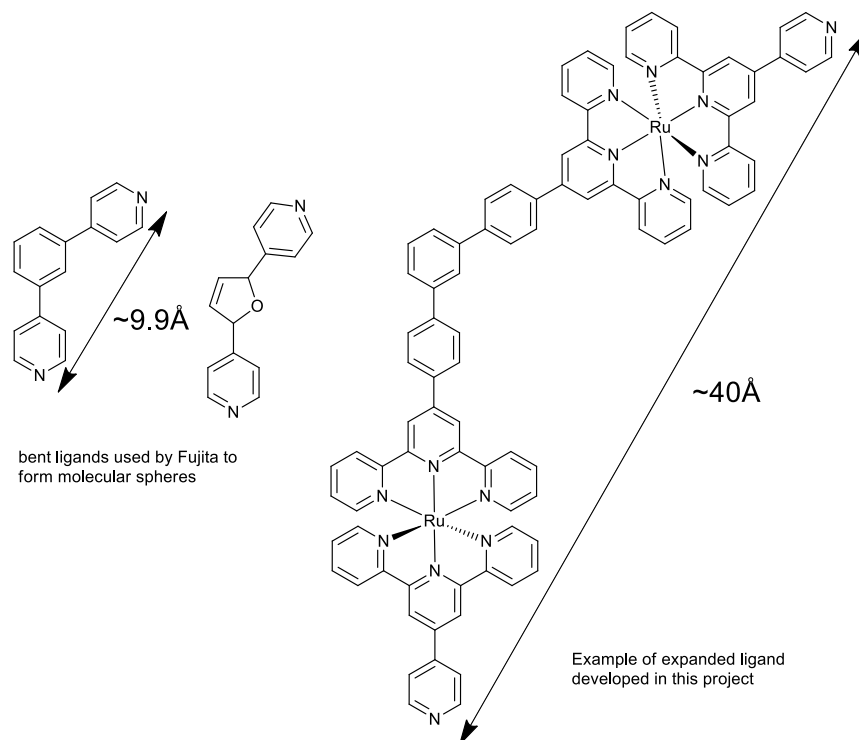


Figure 16 : Examples of dinuclear expanded ligand prepared in this project as a dimetallic analogue of small organic linkers used to self-assemble molecular spheres by Fujita^[7]

The mixed-metal cages which are targeted in this project could find applications as molecular photoreactors by combining the photophysical properties of the Ru(II) complexes with potential guest binding within the cavities of the cages.

2. Chapter 2

New ruthenium(II) complexes of 2,2':6',2''-terpyridine derivatives as supramolecular building blocks

This chapter is based on the published work

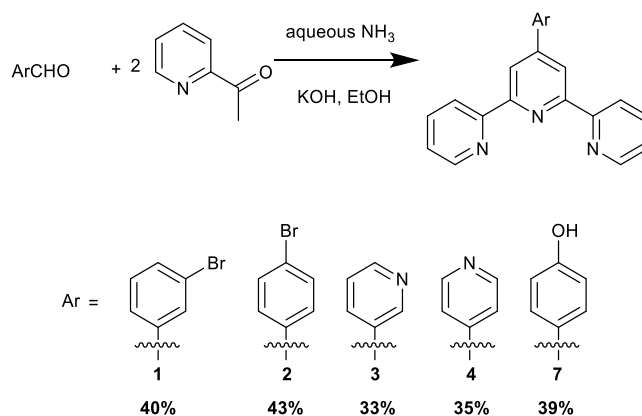
C. Shen, P. Wang, J. E. Beves, *Polyhedron*, 2015, *accepted*

2.1. Introduction

Ruthenium(II) complexes of 2,2':6',2''-terpyridine are substitution-inert complexes with redox- and photo-properties suitable for applications as photosensitizers.^[30] This class of complexes are also suitable building blocks^[41] for large supramolecular assemblies, such as coordination polymers,^[42] coordination networks,^[36] metallomacrocycles^[43] or large cage structures^[34a-c] and other metallosupramolecular structures.^[44] In order to assemble larger structures additional metal ion binding groups are appended to form 'expanded ligands'^[21] which can be combined with labile metal ions to self-assemble into the desired architectures. With this goal in mind, our approach was to use Pd(0)-mediated cross-coupling reactions on inert ruthenium(II) complexes^[45] to prepare large bridging units which feature metal ion binding groups on the periphery. Pyridyl donor groups are particularly appealing due to their ability to coordinate to a wide range of metal ions, including to square planar Pd(II) centres^[46] and are the basis of this work. In this chapter, eight new heteroleptic ruthenium(II) complexes of 4'-substituted 2,2':6',2''-terpyridine ligands featuring either pendant pyridyl units, aryl bromides or aryl boronic acids which can act as supramolecular building blocks.^[45, 47]

2.2. Ligand and ruthenium(II) complex Synthesis and Characterization

The 2,2':6',2'' terpyridine ligands (**1-4**) were prepared using the one-pot method of Hanan (Scheme 1).^[48] Specifically, reaction of 2-acetyl pyridine, the appropriate aryl aldehyde, aqueous ammonia and potassium hydroxide in ethanol gave ligands **1-4** as pure white microcrystalline solids in isolated yields of 33-43%.



Scheme 1 : Ligands **1-4** and **7** were prepared using the one-pot method by Hanan.^[48]

The boronic esters **5a** and **6a**^[47b] were prepared from the corresponding 3-bromophenyl (**1**) or 4-bromophenyl (**2**) functionalised terpyridine ligands following reported procedures.^[47b] Specifically, 3- or 4-bromophenyl terpyridine (ligands **1** or **2**) was treated with potassium acetate, bis(neopentyl glycolato)diboron and Pd(dppf)Cl₂ in DMSO at 80°C for 5.5 h under argon under argon to yield white solids in 55% and 60% respectively.^[47b] Bis(neopentyl-glycolato)diboron was used in preference to bis(pinacolato)diboron as it has been reported to readily hydrolyse to the boronic acid,^[47b] increasing the reactivity of this functional group. The ligands used in this study are shown in Figure 17, and have all been reported previously.^[49]

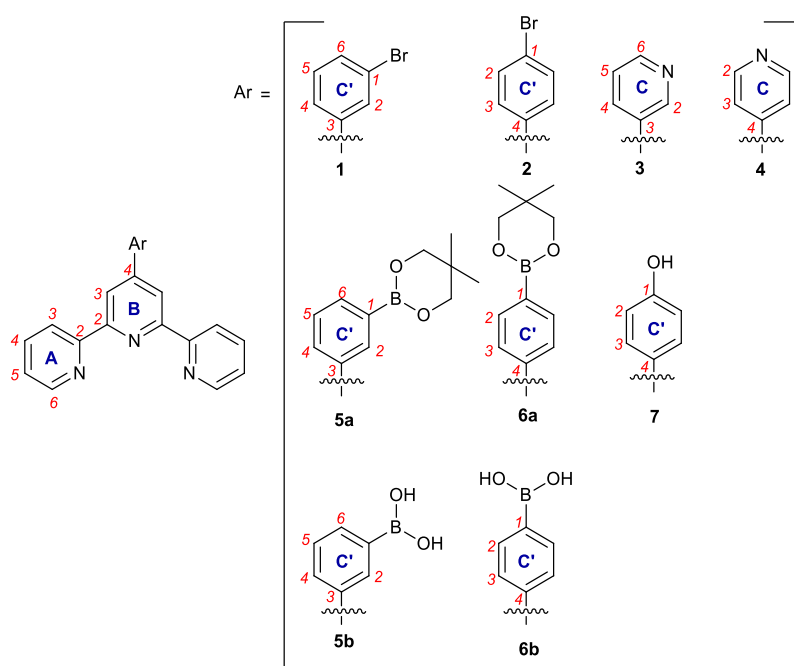


Figure 17 : Ligands used in this study and the numbering scheme adopted. Ligands **1**,^[50] **2**,^[51] **3**,^[52] **4**,^[53] **5a**,^[54] **5b**,^[34c] **6a**,^[47b] **6b**^[55] and **7**^[50] have been previously reported.

The reaction of “RuCl₃·3H₂O”, a starting material of ill-defined composition^[56] and one equivalent of a terpyridine ligand (Xtpy = a tpy derivative) in refluxing alcohols (ethanol, *n*-butanol etc.) typically results in complexes of the type Ru(Xtpy)Cl₃ as insoluble brown/black solids (Figure 18a). Characterization of these materials is difficult due to solubility problems, and therefore these are normally used in subsequent steps without further purification or analysis,^[31] as is the case in this study. The reaction of a suspension of Ru(Xtpy)Cl₃ and one equivalent of a second terpyridine derivative (Ytpy) in ethylene glycol at 150 °C for 2h gave intensely colored red solutions. Anion exchange with potassium hexafluorophosphate, followed by column chromatography and work up gave pure ruthenium complexes of the type [Ru(Xtpy)(Ytpy)](PF₆)₂ in yields of 20-33% over two steps (Figure 18b).

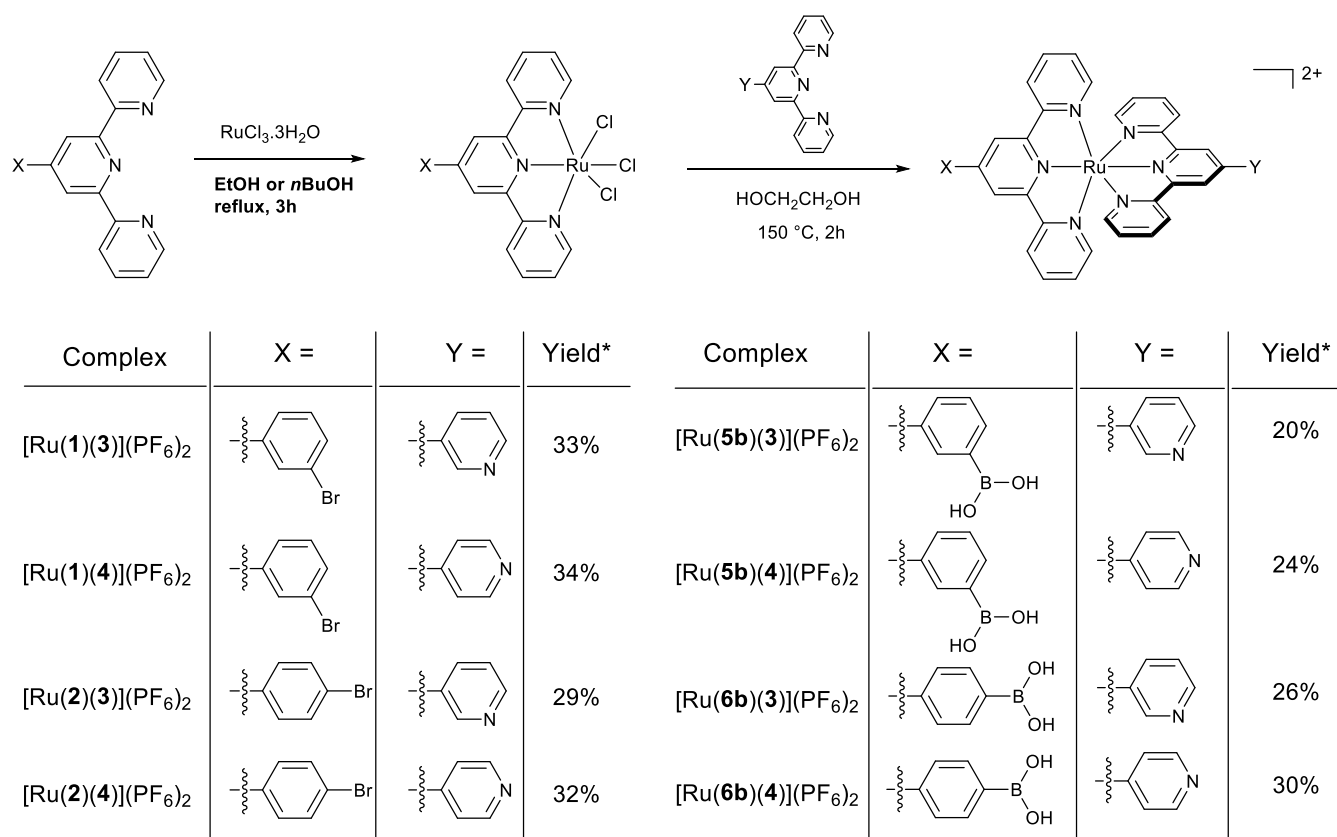


Figure 18 : Synthetic route to heteroleptic Ru(II) complexes prepared in this study. *Yields are given over 2 steps.

In the case of complexes prepared from ligands **5a** or **6a**, which feature boronic ester groups, ¹H NMR and electrospray ionization mass spectrometry (ESI-MS) confirmed the hydrolysis of the ester groups to form boronic acids. Similar behavior has been reported previously.^[57] The addition of the reducing agent 4-ethylmorpholine to the second complexation reaction, as is commonly performed,^[58] was found to result

poor yields in the cases of boronic ester substituted terpyridine ligands. In all cases short reaction times proved important for the isolation of the desired heteroleptic complexes. The ruthenium(II) complexes were characterized by ^1H and ^{13}C NMR, ESI-MS and elemental analysis.

2.3. Mass Spectrometry Characterization

Electrospray ionization mass spectrometry (ESI-MS) was used to identify charged ions for each complex. For complexes not containing boronic ester groups, peaks corresponding to $[\text{M}-\text{PF}_6]^+$ and $[\text{M}-2\text{PF}_6]^{2+}$ were observed when ionized from acetonitrile solutions, with isotope patterns matching that for the calculated ions. By comparison, complexes containing boronic acids were only found to show meaningful signals when methanol was used as the solvent for ESI-MS, with the adducts corresponding to $[\text{M}-\text{B}(\text{OMe})_2 + \text{PF}_6]^+$, $[\text{M}-\text{B}(\text{OH})(\text{OMe}) + \text{PF}_6]^+$, $[\text{M}-\text{B}(\text{OMe})_2]^{2+}$, $[\text{M}-\text{B}(\text{OH})(\text{OMe})]^{2+}$ being observed, where M = the complex in question. For example, for $[\text{Ru}(\mathbf{6b})(\mathbf{4})](\text{PF}_6)_2$ the series of peaks were observed (calc.) at m/z 938.12 (938.16), 924.16 (924.15), 396.72 (396.60) and 389.72 (389.59) m/z with isotope distributions and peak separations consistent with the theoretical values.

2.4. Nuclear Magnetic Resonance(NMR) Characterization

NMR spectra of all new compounds were assigned using ^1H NMR, ^{13}C NMR, COSY, HSQC, HMBC and NOESY techniques in CD_3CN . The ^1H NMR spectra of all complexes are shown in Figure 19. The proton NMR signals for the metal binding terpyridine units show a very similar pattern across all complexes studied. Due to closely overlapping multiplets, the assignment of signals corresponding to the terminal pyridyl rings of the terpyridine units (H^{A3} , H^{A4} , H^{A5} and H^{A6}) to each ligand was generally not feasible. The H^{B3} signals, which are expected to be more influenced by substituents in the B4 position, show greater variation and could be assigned for the 3-bromophenyl- or 4-bromophenyl- ligands (**1** and **2**). However for the boronic acid analogues (ligands **5b**, **6b**), these H^{B3} signals invariably occurred very close to the H^{B3} of the 3-pyridyl or 4-pyridyl functionalized terpyridine on the other side of the Ru(II) centre.

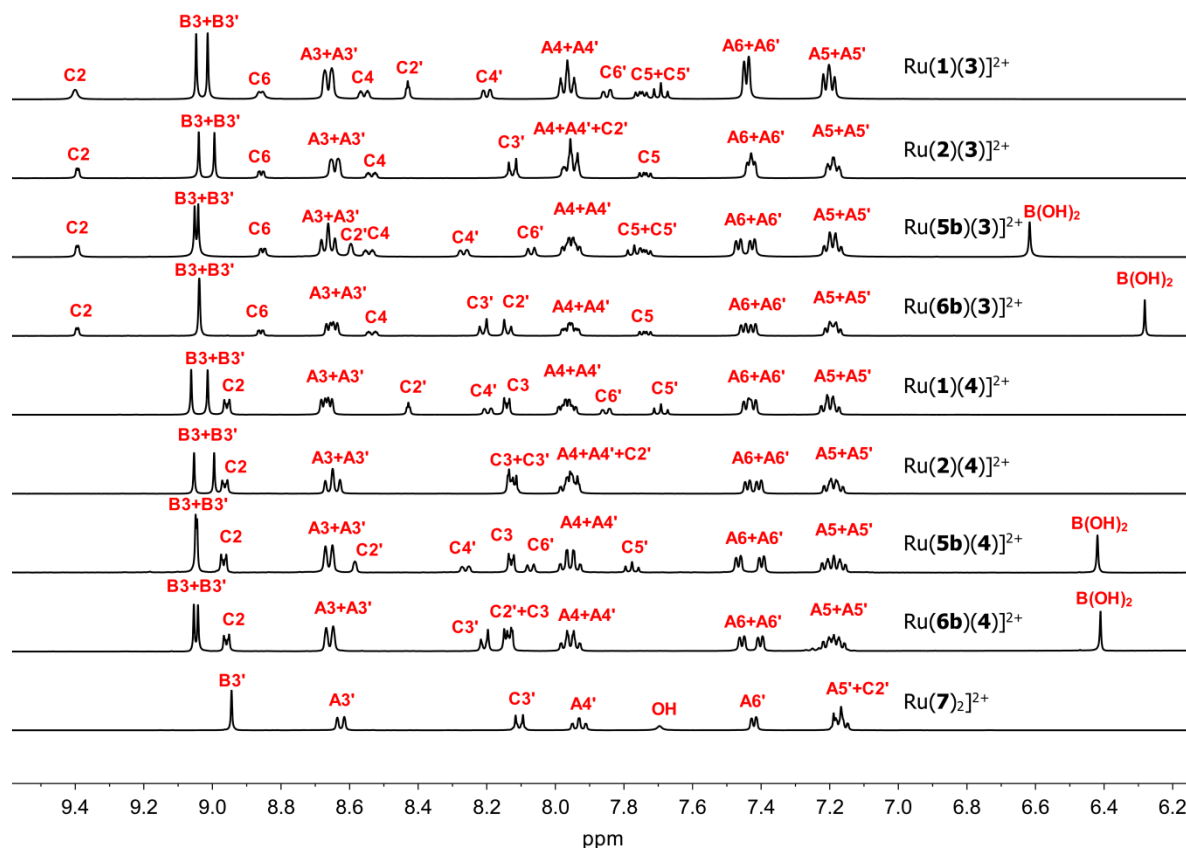


Figure 19 : ^1H NMR spectra (400 MHz, CD_3CN , 298K) for Ru(II) complexes synthesised in this study. Top to bottom: $[\text{Ru}(\mathbf{1})(\mathbf{3})](\text{PF}_6)_2$; $[\text{Ru}(\mathbf{2})(\mathbf{3})](\text{PF}_6)_2$; $[\text{Ru}(\mathbf{5b})(\mathbf{3})](\text{PF}_6)_2$; $[\text{Ru}(\mathbf{6b})(\mathbf{3})](\text{PF}_6)_2$; $[\text{Ru}(\mathbf{1})(\mathbf{4})](\text{PF}_6)_2$; $[\text{Ru}(\mathbf{2})(\mathbf{4})](\text{PF}_6)_2$; $[\text{Ru}(\mathbf{5b})(\mathbf{4})](\text{PF}_6)_2$; $[\text{Ru}(\mathbf{6b})(\mathbf{4})](\text{PF}_6)_2$ and $[\text{Ru}(\mathbf{7})_2](\text{PF}_6)_2$. See **Figure 17** for labelling scheme adopted.

Ligands **3** and ligand **4** both have two coordination domains: the pendant pyridyl group and the terpyridine domain. In each example containing the 3-pyridyl functionalised ligand **3** the ^1H NMR signals (δ /ppm: $\text{H}^{\text{C}2}$ 9.39; $\text{H}^{\text{C}6}$ 8.86; $\text{H}^{\text{C}4}$ 8.53; $\text{H}^{\text{C}5}$ 7.69) are effectively independent of the other terpyridine ligand coordinated to the Ru(II) centre. Similarly, the ^1H NMR signals corresponding to the pendant 4-pyridyl group of ligand **4** are constant for each complex containing this ligand (δ /ppm: $\text{H}^{\text{C}2}$ 8.97; $\text{H}^{\text{C}3}$ 8.13). ^{13}C NMR also confirmed both of these pyridyl units are independent of the other ligand coordinated to the metal centre. For complexes containing the 4-bromophenyl functionalized ligand **2**, signals corresponding to $\text{H}^{\text{C}2'}$ and $\text{H}^{\text{C}3'}$ were distinguished by the appearance in the NOESY spectrum of a cross peak between $\text{H}^{\text{B}3'}$ and $\text{H}^{\text{C}3'}$. Similar analysis can also distinguish the signals for $\text{H}^{\text{C}4'}$ and $\text{H}^{\text{C}6'}$ of the 3-bromophenyl functionalised ligand **1**, which appear at 8.19 ppm and 7.86 ppm. For the 3- or 4-boronic acid functionalized phenyl rings of ligands **5b** and **6b**, the signals around the phenyl ring were identified based on chemical shift and coupling patterns, and NOESY cross peaks similar to those

discussed above. The B(OH)₂ protons of this complexes, which are pH dependent, appear in the ¹H NMR as a sharp singlet in the range from 6.2 ppm and 6.6 ppm.

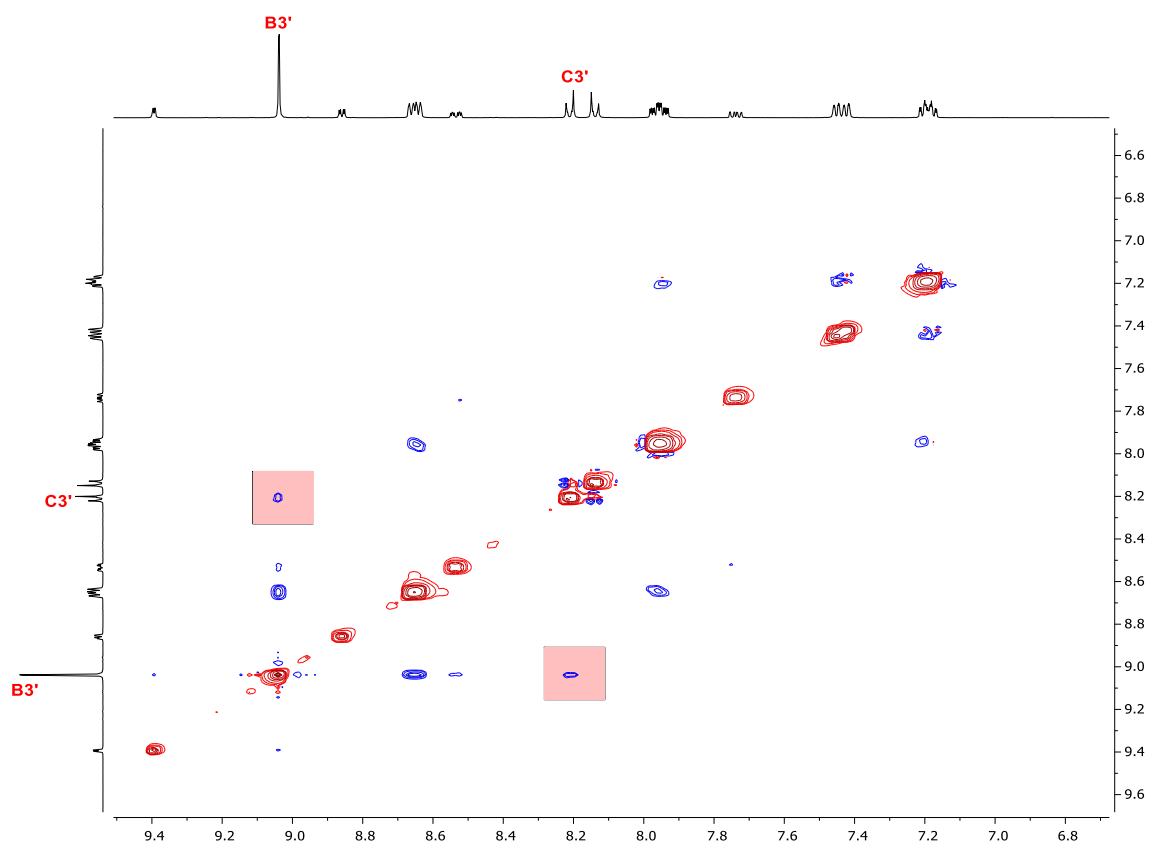


Figure 20 : NOESY(400 MHz, CD₃CN) spectrum of [Ru(**6b**)(**3**)](PF₆)₂

2.5. Stability of ruthenium(II) complexes

All new compounds were found to be stable during the workup (column chromatography with silica gel, washing with water, ethanol and ether) at room temperature. Aryl bromo functionalized complexes were stable in air, at room temperature for months. The synthesis of boronic acid functionalized ruthenium(II) complexes was repeated reliably many times. However, anion exchange using ammonium hexafluorophosphate was appeared to result in decomposition of the boronic acid groups, confirmed by the disappearance of the ¹H NMR signals for B(OH)₂ and the appearance of new aromatic signals, which do not correspond to the hydroxylated product (Figure 21), and were identified.

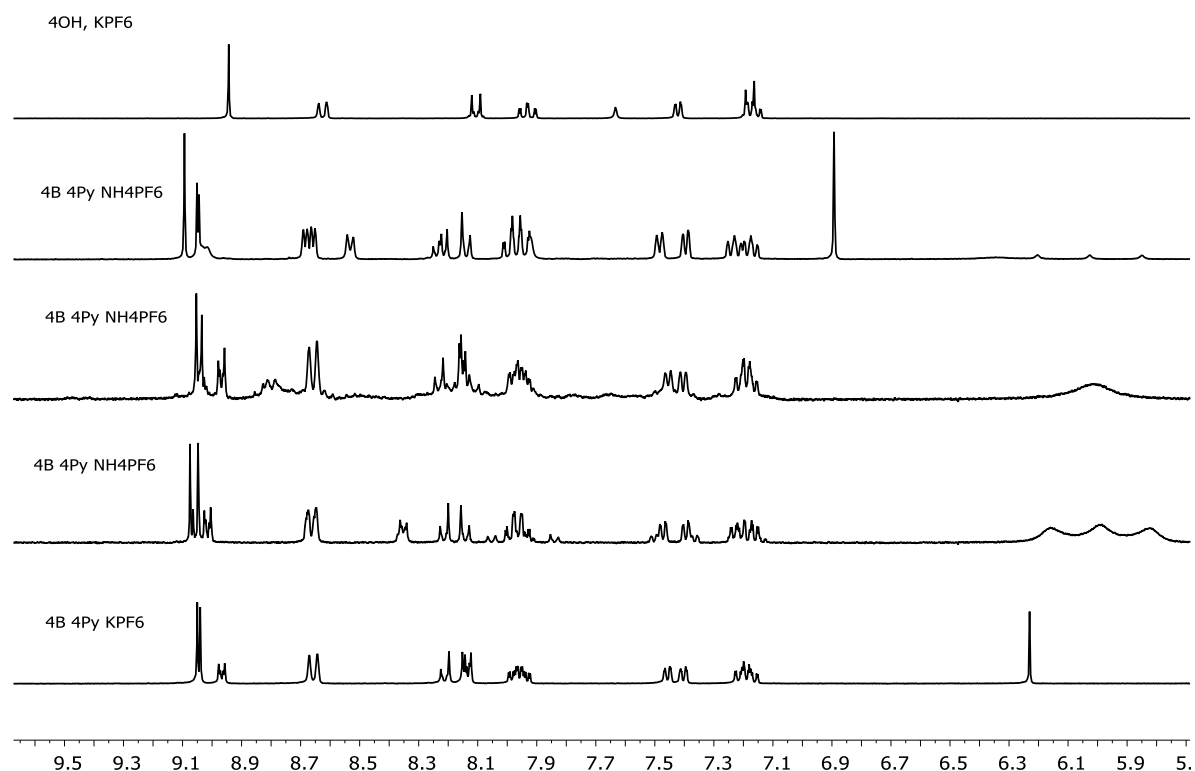


Figure 21 : ^1H NMR (CD_3CN , 400 MHz) of (top to bottom): $[\text{Ru}(\mathbf{7})_2]^{2+}$; $[\text{Ru}(\mathbf{6b})(\mathbf{4})]^{2+}$ precipitated with NH_4PF_6 ; $[\text{Ru}(\mathbf{5b})(\mathbf{4})]^{2+}$ precipitated with NH_4PF_6 (different sample) and (bottom) $[\text{Ru}(\mathbf{5b})(\mathbf{4})]^{2+}$ precipitated with KPF_6 . The large 1:1:1 triplet at 6.1 ppm is NH_4^+ .

No such decomposition products were observed when potassium hexafluorophosphate was used for anion exchange. Complexes with boronic acid groups were routinely collected as red solids which could not be redissolved in acetonitrile. Attempts to dissolve these materials by addition of dilute hydrochloric acid or trifluoroacetic acid also led to decomposition of the boronic acid group. Most importantly, the boronic acid functionalized complexes were found to be unstable when stored for weeks, even in the fridge. Previous reports show that the oxidative hydroxylation of aryl boronic acids to form phenols can be photocatalyzed by $\text{Ru}(\text{bpy})_3\text{Cl}_3$ (bpy = 2,2'-bipyridine) and visible light,^[59] as well as by CuCl_2 ,^[60] palladium(II) phosphine complexes,^[61] or non-metal oxidants such as hydrogen peroxide,^[62] peroxy sulfate,^[63] *N*-oxides^[64] or hydroxylamine.^[65] Similar reactions appear to occur to the Ru(II) complexes presented here which feature boronic acid groups, although the exact mechanism remains unclear. Due to the hydroxylation, the result of elemental analysis was not always satisfactory, but NMR spectra are consistent with the assigned structures.

To confirm isolated complexes are indeed the boronic acid derivatives, and not the phenol decomposition products, 4'-(4-phenol)-2,2':6',2''-terpyridine was synthesised and the homoleptic compound $[\text{Ru}(\mathbf{7})_2](\text{PF}_6)_2$ was prepared as a reference using the same method as for the other complexes reported here. The spectroscopic data was consistent with the literature,^[66] except the pH sensitive OH peak (Figure 19). The ^1H NMR signals of the $\text{H}^{\text{C}2'}$ protons of $[\text{Ru}(\mathbf{6b})(\mathbf{3})]^{2+}$ and $[\text{Ru}(\mathbf{6b})(\mathbf{4})]^{2+}$ both occur at 8.14 ppm, whereas the equivalent peak for $[\text{Ru}(\mathbf{7})_2]^{2+}$ appears at 7.17 ppm, overlapping with the signal of $\text{H}^{\text{A}5'}$. The broad peak which integrates as 1H at 7.70 ppm corresponding to the OH group is significantly different to the signal integrating as 2H for $\text{B}(\text{OH})_2$ which is observed between 6.6 – 6.2 ppm and provides additional evidence for the isolation of the boronic acid functionalised complexes.

2.6.Examples of protonation of bromo and boronic acid functionalized ruthenium (II) complex

$[\text{Ru}(\mathbf{1})(\mathbf{4})](\text{PF}_6)_2$ complex was used for protonation analysis to investigate the NMR peak shifts as a result of protonation state. As shown in the middle NMR spectrum in Figure 22, the pendant pyridyl group in the complex was protonated by trace acid in the solvent. The doublet of doublets peak of peak of $\text{H}^{\text{C}2}$ becomes a broad singlet peak which shifts from 8.96 ppm to 8.98 ppm. The $\text{H}^{\text{C}3}$ signal shifted downfield (δ/ppm : +0.07) as well. The complex was fully protonated by adding TFA until the $\text{H}^{\text{C}3}$ and $\text{H}^{\text{C}2}$ signals were constant which have chemical shifts of 8.76 ppm and 9.06 ppm.

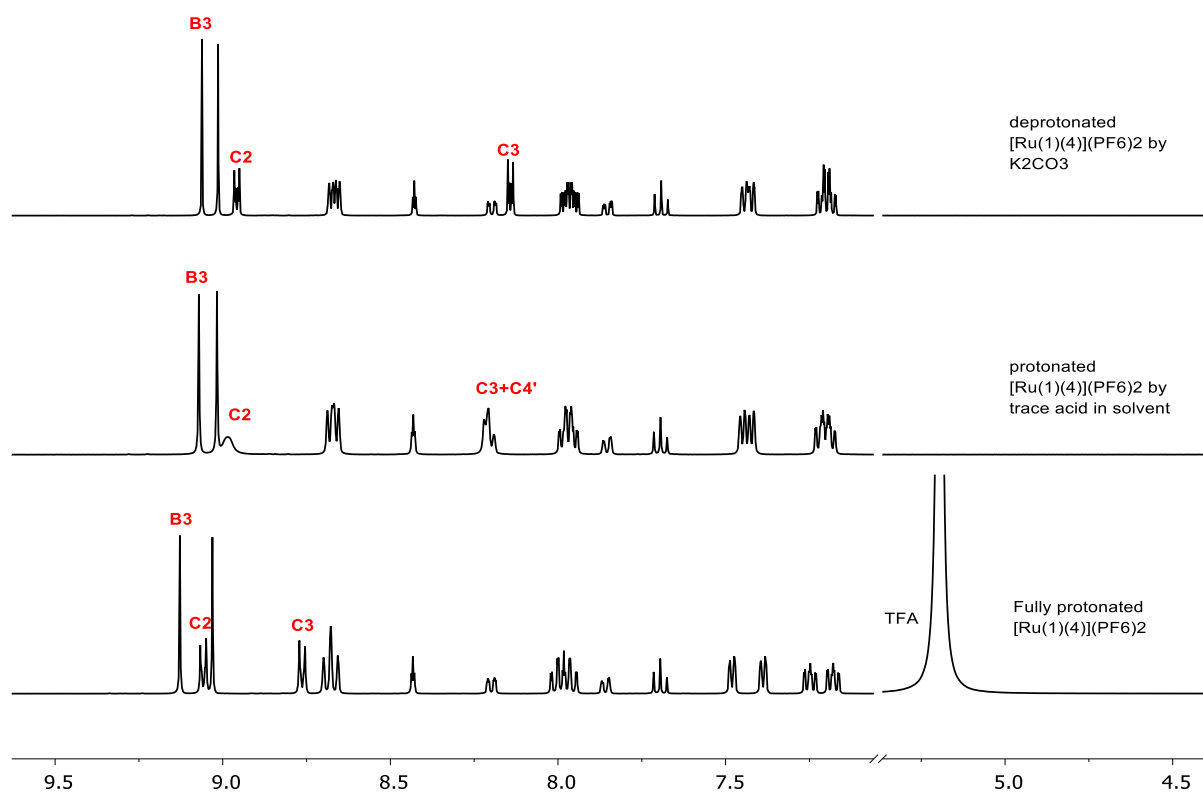


Figure 22 : ^1H NMR (CD_3CN , 400 MHz) of (top to bottom): deprotonated $[\text{Ru}(\mathbf{1})(\mathbf{4})](\text{PF}_6)_2$; protonated $[\text{Ru}(\mathbf{1})(\mathbf{4})](\text{PF}_6)_2$ by trace acid in solvent; Fully protonated $[\text{Ru}(\mathbf{1})(\mathbf{4})](\text{PF}_6)_2$ by TFA.

The protonation of boronic acid functionalized complex was investigated as well. Taken $\text{Ru}(\mathbf{6b})(\mathbf{4})(\text{PF}_6)_2$ as an example, the NMR spectrum in from the protonation by diluted trifluoroacetic acid in CD_3CN (See Figure 23). The boronic acid peak didn't exist which means this complex decomposed upon protonation. $\text{H}^{\text{C}2}$ peak overlapping with $\text{H}^{\text{B}3}$ peak shifted downfield by 0.96 ppm to 9.11 ppm. While the $\text{H}^{\text{C}3}$ signal shifted downfield from 8.52 ppm to 8.96 ppm

Protonation by trace amount of acid in the solvent made the $\text{H}^{\text{C}3}$ signal and $\text{H}^{\text{C}2}$ signal broader, both of which shifted upfield from 8.55 ppm to 8.13 ppm and 9.01 ppm to 8.96 ppm, respectively. In these two cases, the $\text{Ru}(\text{II})$ complex solution changed into dark red after protonation.

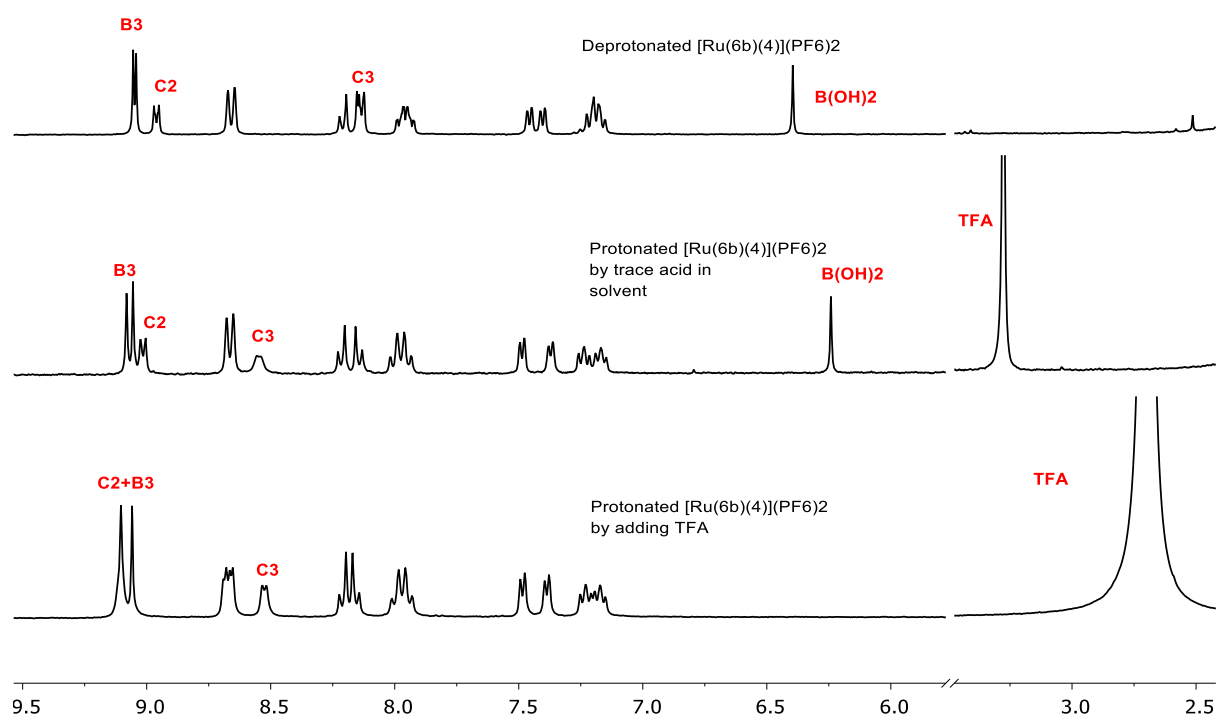


Figure 23 : ^1H NMR (CD_3CN , 300 MHz) of (top to bottom): deprotonated $[\text{Ru}(\mathbf{6b})(\mathbf{4})](\text{PF}_6)_2$; Protonated $[\text{Ru}(\mathbf{6b})(\mathbf{4})](\text{PF}_6)_2^+$ by trace amount of acid in the solvent; Protonated $[\text{Ru}(\mathbf{6b})(\mathbf{4})](\text{PF}_6)_2$ by adding TFA.

2.7. Chapter summary and conclusion

Eight new heteroleptic Ru(II) complexes of terpyridine ligands are reported. Those terpyridine ligands featuring boronic esters were hydrolysed to form boronic acids upon coordination to Ru(II) center. Furthermore, the resulting boronic acid functionalized complexes were unstable with respect to hydroxylation to form the corresponding phenols. Boronic acid functionalized Ru(II) complexes should be prepared from ethylene glycol. Anion exchange with NH_4PF_6 resulted in decomposition, but using KPF_6 anion exchange gave clean products. Protonation of boronic acid functionalized the new Ru(II) complexes resulted in decomposition. The complexes reported here are suitable for Suzuki cross coupling reactions to form dimetallic expanded ligands, provided they are reacted soon after preparation. The bromo functionalised complexes are stable and also suitable for other Pd(0) catalysed cross coupling reactions. The construction of large supramolecular structures from these building blocks is investigated in the next chapter.

2.8. Experimental Section

2.8.1. General procedure

2-Acetylpyridine (2.42 g, 20 mmol) was added into a solution of benzaldehyde (1.06 g, 10 mmol) in EtOH (50 mL). KOH pellets (1.54 g, 85%, 20 mmol) and aqueous NH₃ (29 mL, 25 mmol) were then added to the solution. The solution was stirred at room temperature for 4-12 hr. The pale green solid was collected by filtration and washed with EtOH (3 × 15 mL). Recrystallization for CH₃Cl-MeOH gave white solid.

The terpyridine ligands are synthesized and NMR data also agrees with literature.^[49]

2.8.2. Ligand 1: 4'-(3-bromophenyl)-2,2':6',2''-terpyridine

Yield: 27%. ¹H NMR (300 MHz, CDCl₃) δ 8.84 – 8.74 (m, 6H), 8.09 (t, *J* = 1.8 Hz, 1H), 8.05 – 7.92 (m, 3H), 7.60 (d, *J* = 7.8 Hz, 1H), 7.44 (dt, *J* = 15.8, 7.2 Hz, 3H)

2.8.3. Ligand 2: 4'-(4-bromophenyl)-2,2':6',2''-terpyridine

Yield: 43%. ¹H NMR (300 MHz, DMSO-*d*₆) δ 8.77 (ddd, *J* = 4.8, 1.8, 0.9 Hz, 2H), 8.71 (s, 2H), 8.68 (dt, *J* = 8.0, 1.1 Hz, 2H), 8.05 (td, *J* = 7.7, 1.8 Hz, 2H), 7.91 (d, *J* = 8.5 Hz, 2H), 7.79 (d, *J* = 8.4 Hz, 2H), 7.54 (dd, *J* = 7.4, 4.8 Hz, 2H).

2.8.4. Ligand 3: 4'-(3-pyridyl)-2,2':6',2''-terpyridine

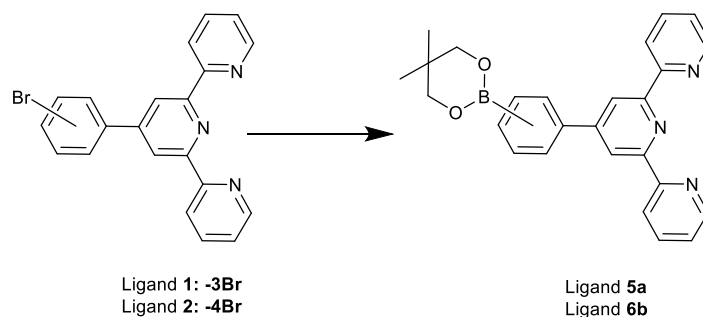
Yield: 33%. ¹H NMR (300 MHz, CDCl₃) δ 9.16 (dd, *J* = 2.4, 0.9 Hz, 1H), 8.81 (s, 2H), 8.76 (ddd, *J* = 4.8, 1.8, 0.9 Hz, 2H), 8.74 – 8.69 (m, 3H), 8.31 (d, *J* = 7.9 Hz, 1H), 7.94 (td, *J* = 7.7, 1.8 Hz, 2H), 7.53 (ddd, *J* = 7.9, 4.9, 0.9 Hz, 1H), 7.42 (ddd, *J* = 7.5, 4.8, 1.2 Hz, 2H).

2.8.5. Ligand 4: 4'-(4-pyridyl)-2,2':6',2''-terpyridine

Yield: 35%. ¹H NMR (300 MHz, CDCl₃) δ 8.81 (s, 2H), 8.78 (d, *J* = 1.3 Hz, 2H), 8.75 (ddd, *J* = 4.8, 1.8, 0.9 Hz, 2H), 8.70 (dt, *J* = 7.9, 1.1 Hz, 2H), 7.97 – 7.87 (m, 4H), 7.41 (ddd, *J* = 7.5, 4.8, 1.2 Hz, 2H).

2.8.6. Ligand 7: 4'-(4-hydroxyphenyl)-2,2':6',2''-terpyridine

Yield: 35%. ^1H NMR (300 MHz, Acetonitrile- d_3) δ 8.97 (s, 2H), 8.65 (d, $J = 8.1$ Hz, 2H), 8.13 (d, $J = 8.4$ Hz, 2H), 7.96 (t, $J = 7.8$ Hz, 2H), 7.72 (s, 1H), 7.45 (d, $J = 5.3$ Hz, 2H), 7.25 – 7.16 (m, 4H).



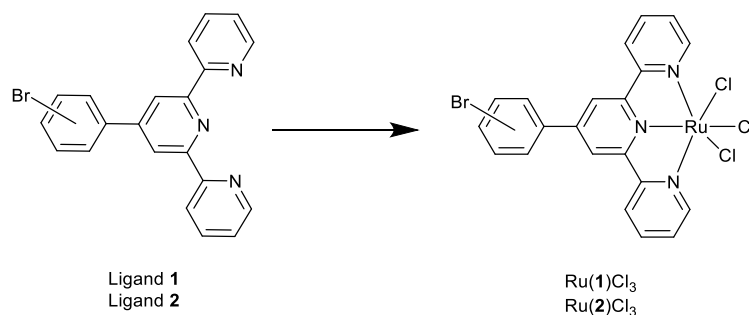
2.8.7. 4'-[3-(5,5-dimethyl-1,3,2-dioxaborinan-2-yl)phenyl]-2,2':6',2''-terpyridine

Ligand 5a: DMSO (20 mL) was added into dry Schlenk flask and degassed by three freeze-pump-thaw cycles before use. 4'-(3-bromophenyl)-2,2':6',2''-terpyridine (1.1 g, 3.0 mmol), dry potassium acetate (1.10 g, 11 mmol), neopentyl glycolato diboron (0.89 g, 4.0 mmol) and [(dppf)PdCl₂] (92 mg, 0.13 mmol) were added and the mixture stirred at 80°C for 5.5 h under an argon atmosphere. The reaction cooled to room temperature and the mixture was diluted with toluene (200 mL). The toluene layer was washed by H₂O (4 × 200 mL), and the organic layer was dried over Na₂SO₄. After filtration and removal of the solvent in vacuo, the grey solid was collected. DCM (30 mL) was added, followed by methanol (30 mL). DCM was removed in vacuo, and the solid was collected by filtration to yield 4'-[3-(5,5-dimethyl-1,3,2-dioxaborinan-2-yl)phenyl]-2,2':6',2''-terpyridine (0.80 g, 1.9 mmol, 63%) as a white solid. ^1H NMR (300 MHz, CDCl₃) δ 8.86 – 8.68 (m, 6H), 8.33 (s, 1H), 8.04 – 7.87 (m, 4H), 7.51 (t, $J = 7.5$ Hz, 1H), 7.39 (t, $J = 6.1$ Hz, 2H), 3.82 (s, 4H), 1.06 (s, 6H).

2.8.8. 4'-[4-(5,5-dimethyl-1,3,2-dioxaborinan-2-yl)phenyl]-2,2':6',2''-terpyridine

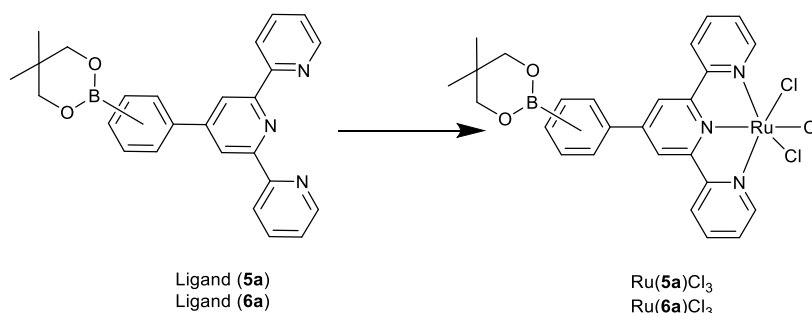
Ligand 6a: Same scale and conditions as for 4'-[3-(5,5-dimethyl-1,3,2-dioxaborinan-2-yl)phenyl]-2,2':6',2''-terpyridine: ^1H NMR (300 MHz, CDCl₃) δ 8.80 (s, 2H), 8.77 (ddd, $J = 4.9, 1.9, 0.9$ Hz, 2H), 8.71 (dt, $J = 8.0, 1.1$ Hz, 2H), 7.97 – 7.87 (m, 6H), 7.39 (ddd, $J = 7.5, 4.9, 1.2$ Hz, 2H), 3.81 (s, 4H), 1.06 (s, 6H).

2.8.9. $Ru(1)Cl_3$ and $Ru(2)Cl_3$



Ligand **1** (0.33 g, 0.85 mmol) and $RuCl_3 \cdot xH_2O$ (0.18 g, 0.85 mmol) was suspended in EtOH 95% (30 mL) and heated at reflux for 4h. After cooling to r.t., the precipitate was collected, washed with CH_3CN (2 x 5 mL), EtOH (5 mL) then Et_2O (5 mL) and dried in air to afford $Ru(1)Cl_3$ as a brown solid. Yield 0.42 g, 0.70 mmol, 82%.

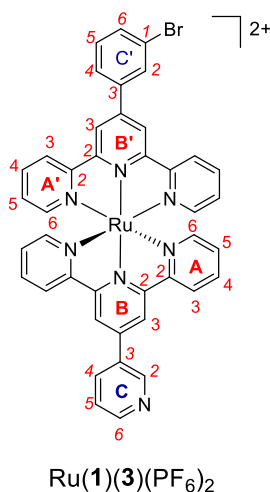
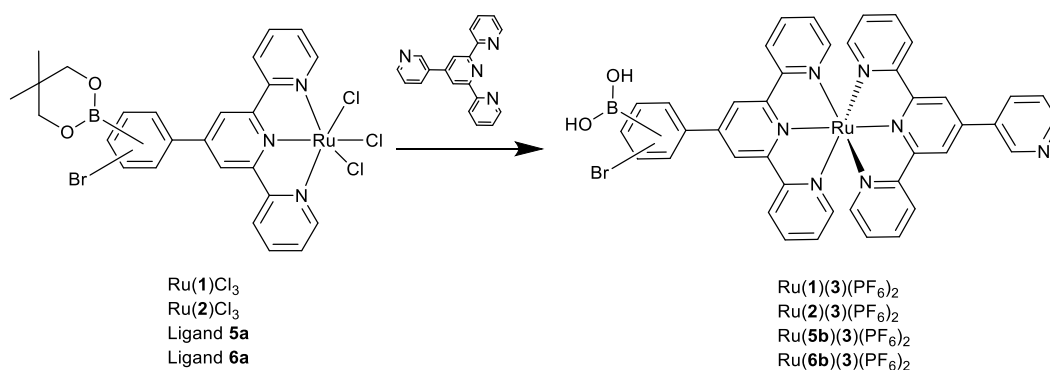
Same scale and conditions as for $Ru(2)Cl_3$. Yield: brown solid, 0.38 g, 0.64 mmol, 75%.



2.8.10. $Ru(5a)Cl_3$ and $Ru(6a)Cl_3$

Ligand **5a** (0.20 g, 0.47 mmol) and $RuCl_3 \cdot xH_2O$ (97 mg, 0.47 mmol) were suspended in *n*-butanol (15 mL) and heated at reflux for 6h. After cooling to r.t., the precipitate was collected, washed CH_3CN (2 x 5 mL), EtOH (5 mL) then Et_2O (5 mL) and dried in air to afford $Ru(5a)Cl_3$ as a brown solid. Yield 0.20 g, 0.32 mmol, 69%. Due to difficulties characterizing this intermediate, it is unclear whether the boronic ester remains intact, or is hydrolyzed to form the boronic acid.

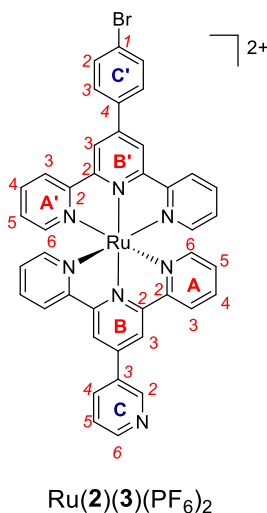
Same scale and conditions as for Ru(**6a**)Cl₃. Yield: brown solid, 0.21 g, 0.33 mmol, 71%. Due to difficulties characterizing this intermediate, it is unclear whether the boronic ester remains intact, or is hydrolysed to form the boronic acid.



Ru(**1**)Cl₃ (0.10 g, 0.17 mmol) and ligand **3** (0.05 g, 0.17 mmol) was suspended in ethane-1, 2-diol (8 cm³). The suspension heated at 150 °C for 2 h. The deep red solution was poured into excess aqueous KPF₆ (20 mL). A red precipitate formed and was collected on Celite, washed with H₂O (5 mL), EtOH (2 mL), Et₂O (5 mL), and dissolved in CH₃CN. The product was purified by chromatography (SiO₂, CH₃CN: H₂O: saturated aqueous KNO₃ 14: 1.2: 0.5). Addition of excess aqueous saturated KPF₆ solution and removal of CH₃CN under reduced pressure gave a red precipitate which was collected on Celite, washed with H₂O (5 mL), EtOH (2 mL), Et₂O (5 mL) and dissolved in CH₃CN. Removal of solvent gave [Ru(**1**)(**3**)](PF₆)₂ as a

red solid (74 mg, 68 μmol , 40%). ^1H NMR (400 MHz, CD_3CN) δ 9.39 (dd, $J = 2.5, 0.9$ Hz, 1H, $\text{H}^{\text{C}2}$), 9.04 (s, 2H, $\text{H}^{\text{B}3}$), 9.01 (s, 2H, $\text{H}^{\text{B}3'}$), 8.86 (dd, $J = 4.8, 1.6$ Hz, 1H, $\text{H}^{\text{C}6}$), 8.65 (m, 4H, $\text{H}^{\text{A}3+\text{A}3'}$), 8.53 (ddd, $J = 8.0, 2.5, 1.6$ Hz, 1H, $\text{H}^{\text{C}4}$), 8.43 (t, $J = 1.8$ Hz, 1H, $\text{H}^{\text{C}2'}$), 8.19 (ddd, $J = 7.8, 1.9, 1.0$ Hz, 1H, $\text{H}^{\text{C}4'}$), 8.02-7.94 (m, 4H, $\text{H}^{\text{A}4+\text{A}4'}$), 7.86 (ddd, $J = 8.0, 1.9, 0.9$ Hz, 1H, $\text{H}^{\text{C}6'}$), δ 7.75 (dd, $J = 8.0, 4.8$ Hz, 1H, $\text{H}^{\text{C}5}$), 7.69 (t, $J = 7.9$ Hz, 1H, $\text{H}^{\text{C}5'}$), 7.46 – 7.38 (m, 4H, $\text{H}^{\text{A}6+\text{A}6'}$), 7.25 – 7.14 (m, 4H, $\text{H}^{\text{A}5+\text{A}5'}$). ^{13}C NMR (101 MHz, CD_3CN) δ 159.0 ($\text{C}^{\text{A}2/\text{A}2'}$), 159.0 ($\text{C}^{\text{A}2/\text{A}2'}$), 156.6 ($\text{C}^{\text{B}2/\text{B}2'}$), 156.5 ($\text{C}^{\text{B}2/\text{B}2'}$), 153.5 ($\text{C}^{\text{A}6+\text{A}6'}$), 152.0 ($\text{C}^{\text{C}6}$), 149.6 ($\text{C}^{\text{C}2}$), 147.7 ($\text{C}^{\text{C}3'}$), 146.3 ($\text{C}^{\text{B}4}$), 140.0 ($\text{C}^{\text{B}4'}$), 139.15 ($\text{C}^{\text{A}4/\text{A}4'}$), 139.12 ($\text{C}^{\text{A}4/\text{A}4'}$), 136.4 ($\text{C}^{\text{C}4}$), 134.1 ($\text{C}^{\text{C}6'}$), 133.8 ($\text{C}^{\text{C}3}$), 132.5 ($\text{C}^{\text{C}5'}$), 131.7 ($\text{C}^{\text{C}2'}$), 128.6 ($\text{C}^{\text{A}5/\text{A}5'}$), 128.6 ($\text{C}^{\text{A}5/\text{A}5'}$), 127.7 ($\text{C}^{\text{C}4'}$), 125.64 ($\text{C}^{\text{A}3/\text{A}3'}$), 125.62 ($\text{C}^{\text{A}3/\text{A}3'}$), 125.4 ($\text{C}^{\text{C}5}$), 124.1 ($\text{C}^{\text{C}1'}$), 122.8 ($\text{C}^{\text{B}3/\text{B}3'}$), 122.8 ($\text{C}^{\text{B}3/\text{B}3'}$). LR-ESI-MS (in CH_3CN): m/z 945.98 $[\text{M}-\text{PF}_6]^+$ requires 946.03; 400.64 $[\text{M}-2\text{PF}_6]^{2+}$ requires 400.53. *Anal. Calc.* for $\text{C}_{41}\text{H}_{28}\text{F}_{12}\text{N}_7\text{P}_2\text{Ru}\cdot 4.5\text{H}_2\text{O}\cdot 1\text{CH}_3\text{CN}$: C, 45.63; H, 3.56; N, 9.90. Found: C, 45.51; H, 3.70; N, 9.95%.

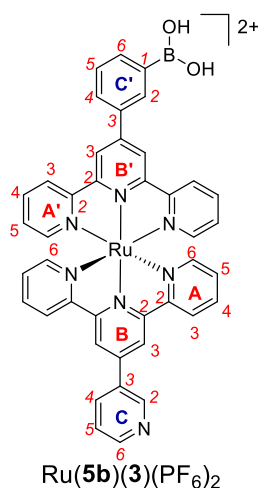
2.8.11. Synthesis of $[\text{Ru}(\mathbf{2})(\mathbf{3})](\text{PF}_6)_2$



The preparation of $[\text{Ru}(\mathbf{2})(\mathbf{3})](\text{PF}_6)_2$ was the same as for $[\text{Ru}(\mathbf{1})(\mathbf{3})](\text{PF}_6)_2$, starting with $\text{Ru}(\mathbf{2})\text{Cl}_3$ (0.10 g, 0.17 mmol) and ligand **3** (0.05 g, 0.17 mmol). $[\text{Ru}(\mathbf{2})(\mathbf{3})](\text{PF}_6)_2$ was isolated as a red solid (72 mg, 66 μmol , 39%). ^1H NMR (400 MHz, CD_3CN) δ 9.39 (dd, $J = 2.5, 0.9$ Hz, 1H, $\text{H}^{\text{C}2}$), 9.04 (s, 2H, $\text{H}^{\text{B}3}$), 8.99 (s, 2H, $\text{H}^{\text{B}3'}$), 8.86 (dd, $J = 4.8, 1.6$ Hz, 1H, $\text{H}^{\text{C}6}$), 8.64 (d, $J = 8.0$ Hz, 4H, $\text{H}^{\text{A}3+\text{A}3'}$), 8.53 (dt, $J = 8.1, 1.9$ Hz, 1H, $\text{H}^{\text{C}4}$), 8.12 (d, $J = 8.1$ Hz, 2H, $\text{H}^{\text{C}3'}$), 8.00 – 7.91 (m, 6H, $2\text{H}^{\text{C}2'} + 4\text{H}^{\text{A}4+\text{A}4'}$), 7.74 (dd, $J = 8.0, 4.8$ Hz, 1H, $\text{H}^{\text{C}5}$), 7.46 – 7.40 (m, 4H, $\text{H}^{\text{A}6+\text{A}6'}$), 7.23 – 7.17 (m, 4H, $\text{H}^{\text{A}5+\text{A}5'}$). ^{13}C NMR (101 MHz, CD_3CN) δ 159.1 ($\text{C}^{\text{A}2/\text{A}2'}$), 159.0 ($\text{C}^{\text{A}2/\text{A}2'}$), 156.6 ($\text{C}^{\text{B}2/\text{B}2'}$), 156.5 ($\text{C}^{\text{B}2/\text{B}2'}$), 153.5 ($\text{C}^{\text{A}6+\text{A}6'}$), 152.2 ($\text{C}^{\text{C}6}$), 149.7 ($\text{C}^{\text{C}2}$),

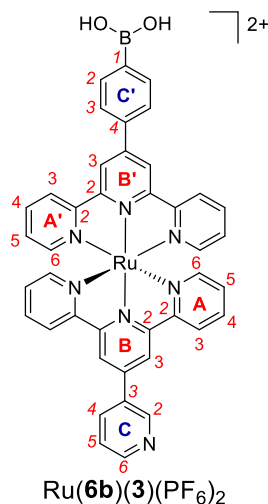
148.1 (C^{C4'}), 146.3 (C^{B4}), 139.14 (C^{A4/A4'}), 139.12 (C^{A4/A4'}), 137.0 (C^{B4'}), 136.2 (C^{C4}), 133.7 (C^{C2'}), 130.6 (C^{C3'}), 128.6 (C^{A5/A5'}), 128.5 (C^{A5/A5'}), 125.6 (C^{A3+A3'}), 125.4 (C^{C1'}), 125.3 (C^{C5}), 122.8 (C^{B3}), 122.6 (C^{B3'}). LR-ESI-MS (in CH₃CN): *m/z* 945.98 [M-PF₆]⁺ requires 946.03; *m/z* 400.64 [M-2PF₆]²⁺ requires 400.53. Calc. for C₄₁H₂₈F₁₂N₇P₂Ru·6.5H₂O: C, 43.70; H, 3.67; N, 8.70. Found: C, 43.19; H, 3.30; N, 8.65%.

2.8.12. Synthesis of [Ru(**5b**)(**3**)](PF₆)₂



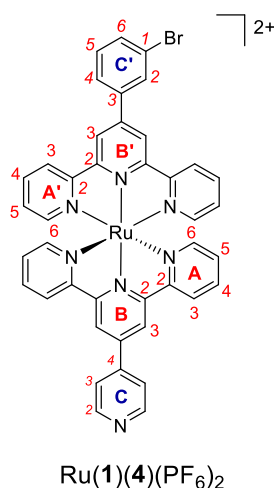
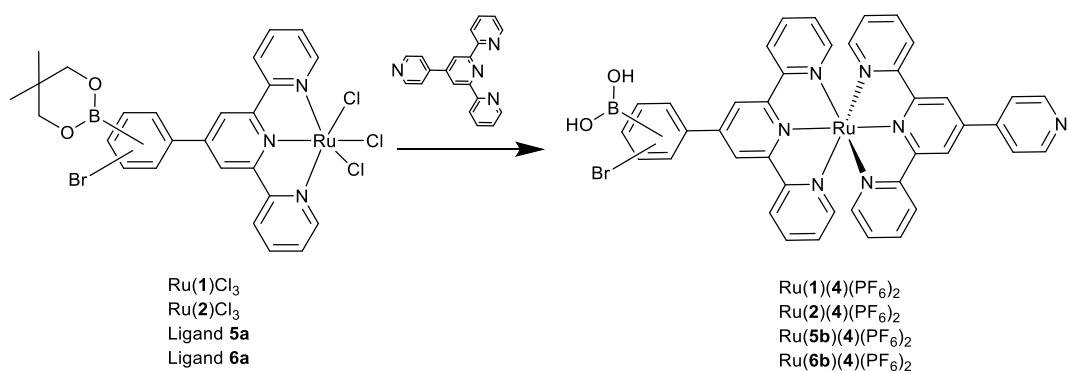
The preparation of [Ru(**5b**)(**3**)](PF₆)₂ was the same as for [Ru(**1**)(**3**)](PF₆)₂, starting with “Ru(**5a**)Cl₃” (0.10 g, 0.16 mmol) and ligand **3** (0.05 g, 0.17 mmol). [Ru(**5b**)(**3**)](PF₆)₂ was isolated as a red solid (50 mg, 46 μmol, 29%). ¹H NMR (400 MHz, CD₃CN) δ 9.39 (d, *J* = 2.1 Hz, 1H, H^{C2}), 9.06 (s, 2H, H^{B3}), 9.03 (s, 2H, H^{B3'}), 8.86 (dd, *J* = 4.8, 1.5 Hz, 1H, H^{C6}), 8.72 – 8.62 (m, 4H, H^{A3+A3'}), 8.59 (s, 1H, H^{C2'}), 8.53 (d, *J* = 8.1 Hz, 1H, H^{C4}), 8.26 (d, *J* = 8.1 Hz, 1H, H^{C4'}), 8.07 (d, *J* = 7.4 Hz, 1H, H^{C6'}), 8.00 – 7.90 (m, 4H, H^{A4+A4'}), 7.82 – 7.69 (m, 2H, H^{C5+C5'}), 7.51 – 7.39 (m, 4H, H^{A6+A6'}), 7.23 – 7.14 (m, 4H, H^{A5+A5'}), 6.42 (s, 2H, B(OH)₂). ¹³C NMR (75 MHz, CD₃CN) δ 159.2 (C^{A2/A2'}), 159.1 (C^{CA2/A2'}), 156.7 (C^{CB2/B2'}), 156.4 (C^{B2/B2'}), 153.50 (C^{A6/A6'}), 153.45 (C^{A6/A6'}), 152.1 (C^{C6}), 149.9 (C^{B4'}), 149.7 (C^{C2}), 146.2 (C^{B4}), 139.1 (C^{A4+CA4'}), 137.2 (C^{C3'}), 136.9 (C^{C6'}), 136.2 (C^{C4}), 134.5 (C^{C2'}), 133.8 (C^{C3}), 133.1 (C^{C1'}), 130.8 (C^{C4'}), 130.0 (C^{C5'}), 128.6 (C^{A5/A5'}), 128.4 (C^{A5/A5'}), 125.6 (C^{A3/A3'}), 125.3 (C^{C5}), 122.83 (C^{B3/B3'}), 122.78 (C^{B3/B3'}). LR-ESI-MS (in MeOH): *m/z* 938.10 [(MeOBOMe)PF₆ adduct]⁺ requires 938.16; 924.16 [(MeOBOH)PF₆ adduct]⁺ requires 924.15; 396.72 [(MeOBOMe) adduct]²⁺ requires 396.60; 389.74 [(MeOBOH) adduct]²⁺ requires 389.59.

2.8.13. Synthesis of $[Ru(\mathbf{6b})(\mathbf{3})](PF_6)_2$



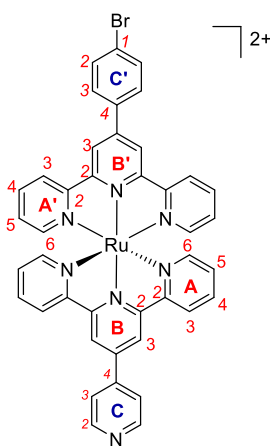
The preparation of $[Ru(\mathbf{6b})(\mathbf{3})](PF_6)_2$ was the same as for $[Ru(\mathbf{1})(\mathbf{3})](PF_6)_2$, starting with “ $Ru(\mathbf{6a})Cl_3$ ” (0.10 g, 0.16 mmol) and ligand **3** (0.05 g, 0.17 mmol). $[Ru(\mathbf{6b})(\mathbf{3})](PF_6)_2$ was isolated as a red solid (62 mg, 59 μ mol, 37%). 1H NMR (400 MHz, CD_3CN) δ 9.39 (d, $J = 2.6$ Hz, 1H, H^{C^2}), 9.04 (s, 2H, H^{B^3}), 9.04 (s, 2H, $H^{B^3'}$), 8.86 (dd, $J = 4.8, 1.6$ Hz, 1H, H^{C^6}), 8.70 – 8.60 (m, 4H, $H^{A^3+A^3'}$), 8.53 (ddd, $J = 8.0, 2.5, 1.6$ Hz, 1H, H^{C^4}), 8.21 (d, $J = 7.8$ Hz, 1H, $H^{C^3'}$), 8.14 (d, $J = 7.7$ Hz, 1H, $H^{C^2'}$), 8.00 – 7.91 (m, 4H, $H^{A^4+A^4'}$), 7.74 (dd, $J = 7.9, 4.8$ Hz, 1H, H^{C^5}), 7.50 – 7.37 (m, 4H, $H^{A^6+A^6'}$), 7.24 – 7.15 (m, 4H, $H^{A^5+A^5'}$), 6.52 (s, 2H, $B(OH)_2$). ^{13}C NMR (101 MHz, CD_3CN) δ 159.2 ($C^{A^2/A^2'}$), 159.0 ($C^{A^2/A^2'}$), 156.7 ($C^{B^2/B^2'}$), 156.4 ($C^{B^2/B^2'}$), 153.48 ($C^{A^6/A^6'}$), 153.45 ($C^{A^6/A^6'}$), 152.2 ($C^{C^1'}$), 149.7 (C^{C^2}), 149.3 ($C^{C^4'}$), 146.3 (C^{B^4}), 139.6 ($C^{B^4'}$), 139.1 ($C^{A^4/A^4'}$), 139.1 ($C^{A^4/A^4'}$), 136.2 ($C^{C^4/C^2'}$), 133.7 (C^{C^3}), 128.6 ($C^{A^5/A^5'}$), 128.5 ($C^{A^5/A^5'}$), 128.0 ($C^{C^3'}$), 125.6 ($C^{A^3+A^3'}$), 125.3 (C^{C^5}), 122.8 ($C^{B^3/B^3'}$), 122.7 ($C^{B^3/B^3'}$). LR-ESI-MS (in MeOH): m/z found 938.14 $[(MeOBOMe)PF_6 \text{ adduct}]^+$ requires 938.16; 924.14 $[(MeOBOH)PF_6 \text{ adduct}]^+$ requires 924.15; 396.72 $[(MeOBOMe) \text{ adduct}]^{2+}$ requires 396.60; 389.72 $[(MeOBOH) \text{ adduct}]^{2+}$ requires 389.59. *Anal. Calc.* for $C_{41}H_{30}F_{12}N_7O_2P_2Ru \cdot 2.5H_2O$: C, 45.23; H, 3.24; N, 9.01. Found: C, 45.55; H, 2.75; N, 9.11%.

2.8.14. Synthesis of $[Ru(\mathbf{1})(\mathbf{4})](PF_6)_2$



The preparation of [Ru(1)(4)](PF₆)₂ was the same as for [Ru(1)(3)](PF₆)₂, starting with Ru(1)Cl₃ (0.10 g, 0.17 mmol) and ligand 4 (0.05 g, 0.17 mmol). [Ru(1)(4)](PF₆)₂ was isolated as a red solid (76 mg, 70 μmol, 41%). ¹H NMR (400 MHz, CD₃CN) δ 9.05 (s, 2H, H^{B3}), 9.01 (s, 2H, H^{B3'}), 8.97 (d, *J* = 5.4 Hz, 2H, H^{C2}), 8.70 – 8.65 (d, *J* = 8.1 Hz, 4H, H^{A3+A3'}), 8.43 (t, *J* = 1.8 Hz, 1H, H^{C2'}), 8.19 (d, *J* = 8.2 Hz, 1H, H^{C4'}), 8.13 (d, *J* = 5.4 Hz, 2H, H^{C3}), 8.02 – 7.94 (m, 4H, H^{A4+A4'}), 7.86 (d, *J* = 6.5 Hz, 1H, H^{C6'}), 7.69 (t, *J* = 7.9 Hz, 1H, H^{C5'}), 7.48 – 7.42 (m, 4H, H^{A6+A6'}), 7.25 – 7.17 (m, 4H, H^{A5+A5'}). ¹³C NMR (101 MHz, CD₃CN) δ 159.0 (C^{A2/A2'}), 158.9 (C^{A2/A2'}), 156.9 (C^{B2/B2'}), 156.4 (C^{B2/B2'}), 153.5 (C^{A6/A6'}), 153.5 (C^{A6/A6'}), 151.1 (C^{C2}), 147.9 (C^{C3'}), 146.2 (C^{C4}), 145.9 (C^{B4}), 140.0 (C^{B4'}), 139.2 (C^{A4+A4'}), 134.1 (C^{C6'}), 132.5 (C^{C5'}), 131.7 (C^{C2'}), 128.7 (C^{A5/A5'}), 128.6 (C^{A5/A5'}), 127.74 (C^{C4}), 125.7 (C^{A4/A4'}), 125.6 (C^{A4/A4'}), 124.1 (C^{C1}), 123.4 (C^{C3}), 122.8 (C^{B3+B3'}). LR-ESI-MS (in CH₃CN): *m/z* 945.98 [M-PF₆]⁺ requires 946.03; 400.62 [M-2PF₆]²⁺ requires 400.53. *Anal. Calc.* for C₄₁H₂₈F₁₂N₇P₂Ru·1.5H₂O: C, 41.08; H, 4.12; N, 8.18. Found: C, 40.62; H, 3.7; N, 8.49%.

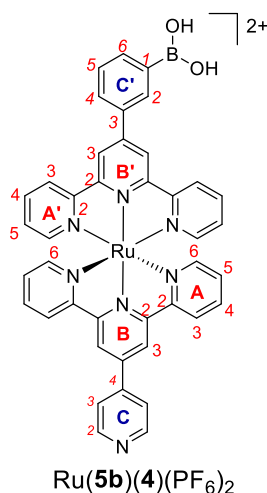
2.8.15. Synthesis of [Ru(2)(4)](PF₆)₂



Ru(2)(4)(PF₆)₂

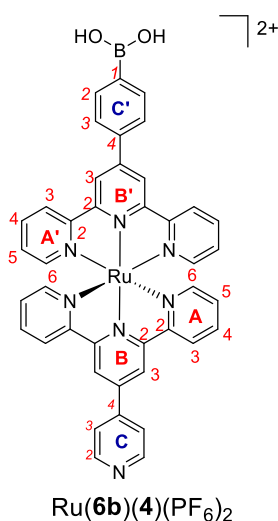
The preparation of [Ru(2)(4)](PF₆)₂ was the same as for [Ru(1)(3)](PF₆)₂, starting with Ru(2)Cl₃ (0.10 g, 0.17 mmol) and ligand 4 (0.05 g, 0.17 mmol) to give [Ru(2)(4)](PF₆)₂ as a red solid (76 mg, 73 μmol, 43%). ¹H NMR (400 MHz, CD₃CN) δ 9.05 (s, 2H, H^{B3}), 9.00 (s, 2H, H^{B3'}), 8.97 (d, *J* = 5.6 Hz, 2H, H^{C2}), 8.65 (m, 4H, H^{A3+A3'}), 8.18 – 8.07 (m, 4H, H^{C3+C3'}), 8.02 – 7.90 (m, 6H, 4H^{A4+A4'} + 2H^{C2'}), 7.49 – 7.36 (m, 4H, H^{A6+A6'}), 7.25 – 7.13 (m, 4H, H^{A5+A5'}). ¹³C NMR (101 MHz, CD₃CN) δ 159.0 (C^{A2/A2'}), 158.9 (C^{A2/A2}), 156.8 (C^{B2/B2'}), 156.4 (C^{B2/B2'}), 153.50 (C^{A6/A6'}), 153.46 (C^{A6/A6'}), 152.1 (C^{C2}), 148.3 (C^{C4'}), 146.3 (C^{C4}), 145.1 (C^{B4}), 139.2 (C^{A4+A4'}), 137.0 (C^{B4'}), 133.7 (C^{C2'}), 130.6 (C^{C3'}), 128.6 (C^{A5/A5'}), 128.5 (C^{A5/A5'}), 125.7 (C^{A3/A3'}), 125.6 (C^{A3/A3'}), 125.5 (C^{C1'}), 122.9 (C^{C3}), 122.8 (C^{B3}), 122.6 (C^{B3'}). LR-ESI-MS (in CH₃CN): *m/z* 945.98 [M-PF₆]⁺ requires 946.03; 400.62 [M-2PF₆]²⁺ requires 400.53. Calc. for C₄₁H₂₈F₁₂N₇P₂Ru·2H₂O: C, 47.09; H, 3.08; N, 9.38. Found: C, 46.79; H, 3.29; N, 9.67%.

2.8.16. Synthesis of $[Ru(\mathbf{5b})(\mathbf{4})](PF_6)_2$



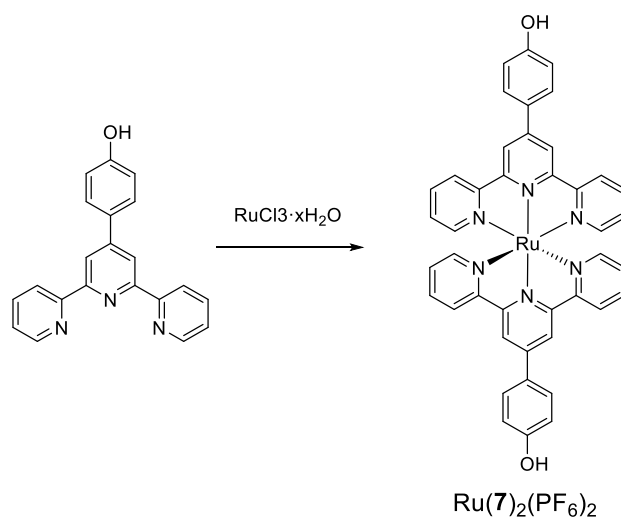
The preparation of $[Ru(\mathbf{5b})(\mathbf{4})](PF_6)_2$ was the same as for $[Ru(\mathbf{1})(\mathbf{3})](PF_6)_2$, starting with “ $Ru(\mathbf{5a})Cl_3$ ” (0.10 g, 0.16 mmol) and ligand **4** (0.05 g, 0.17 mmol). $[Ru(\mathbf{5b})(\mathbf{4})](PF_6)_2$ was isolated as a red solid (59 mg, 56 μ mol, 35%). 1H NMR (400 MHz, CD_3CN) δ 9.05 (s, 2H, H^{B3}), 9.04 (s, 2H, $H^{B3'}$), 8.97 (d, $J = 5.2$ Hz, 2H, H^{C2}), 8.70 – 8.62 (m, 4H, $H^{A3+A3'}$), 8.58 (s, 1H, $H^{C2'}$), 8.26 (d, $J = 7.8$ Hz, 1H, $H^{C4'}$), 8.13 (d, $J = 5.3$ Hz, 2H, H^{C3}), 8.07 (d, $J = 7.4$ Hz, 1H, $H^{C6'}$), 8.01 – 7.90 (m, 4H, $H^{A4+A4'}$), 7.78 (t, $J = 7.6$ Hz, 1H, $H^{C5'}$), 7.52 – 7.35 (m, 4H, $H^{A6+A6'}$), 7.25 – 7.14 (m, 4H, $H^{A5+A5'}$), 6.42 (s, 2H, $B(OH)_2$). ^{13}C NMR (75 MHz, CD_3CN) δ 159.2 ($C^{A2/A2'}$), 159.0 ($C^{A2/A2'}$), 156.9 ($C^{B2/B2'}$), 156.3 ($C^{B2/B2'}$), 153.5 ($C^{A6+A6'}$), 152.1 (C^{C2}), 150.0 ($C^{C3'}$), 146.2 (C^{C4}), 145.1 (C^{B4}), 139.2 ($C^{A4/A4'}$), 139.1 ($C^{A4/A4'}$), 137.2 ($C^{B4'}$), 136.9 ($C^{C6'}$), 134.5 ($C^{C2'}$), 132.9 ($C^{C1'}$), 130.8 ($C^{C4'}$), 130.0 ($C^{C5'}$), 128.6 ($C^{A5/A5'}$), 128.4 ($C^{A5/A5'}$), 125.7 ($C^{A3/A3'}$), 125.6 ($C^{A3/A3'}$), 122.9 (C^{C3}), 122.9 (C^{B3}), 122.8 ($C^{B3'}$). LR-ESI-MS (in MeOH): m/z 938.12 $[(MeOBOMe)PF_6 \text{ adduct}]^+$ requires 938.16; 924.16 $[(MeOBOH)PF_6 \text{ adduct}]^+$ requires 924.15; 396.70 $[(MeOBOMe) \text{ adduct}]^{2+}$ requires 396.60; 389.74 $[(MeOBOH) \text{ adduct}]^{2+}$ requires 389.59. *Anal. Calc.* for $C_{41}H_{30}F_{12}N_7O_2P_2Ru \cdot 2.4H_2O$: C, 45.30; H, 3.23; N, 9.02. Found: C, 44.81; H, 2.70; N, 8.84%.

2.8.17. Synthesis of $[Ru(\mathbf{6b})(\mathbf{4})](PF_6)_2$



The preparation of $[Ru(\mathbf{6b})(\mathbf{4})](PF_6)_2$ was the same as for $[Ru(\mathbf{1})(\mathbf{3})](PF_6)_2$, starting with “ $Ru(\mathbf{6a})Cl_3$ ” (0.10 g, 0.16 mmol) and ligand **4** (0.05 g, 0.17 mmol). $[Ru(\mathbf{6b})(\mathbf{4})](PF_6)_2$ was isolated as a red solid (71 mg, 67 μ mol, 42%). 1H NMR (400 MHz, CD_3CN) δ 9.05 (s, 2H, H^{B3}), 9.04 (s, 2H, $H^{B3'}$), 8.97 (d, $J = 5.2$ Hz, 2H, H^{C2}), 8.70 – 8.62 (m, 4H, $H^{A3+A3'}$), 8.24 – 8.10 (m, 6H, $2H^{C3} + 4H^{C2'+C3'}$), 8.01 – 7.91 (m, 4H, $H^{A4+A4'}$), 7.50 – 7.37 (m, 4H, $H^{A6+A6'}$), 7.24 – 7.14 (m, 4H, $H^{A5+A5'}$), 6.23 (s, 2H, $B(OH)_2$). ^{13}C NMR (151 MHz, CD_3CN) δ 159.1 ($C^{A2/A2'}$), 158.9 ($C^{A2/A2'}$), 156.9 ($C^{B2/B2'}$), 156.4 ($C^{B2/B2'}$), 154.3 ($C^{C1'}$), 153.5 ($C^{A6+A6'}$), 152.1 (C^{C2}), 149.5 ($C^{C4'}$), 146.2 (C^{C4}), 145.1 (C^{B4}), 139.5 ($C^{B4'}$), 139.2 ($C^{A4/A4'}$), 139.1 ($C^{A4/A4'}$), 136.2 ($C^{C2'}$), 128.6 ($C^{A5/A5'}$), 128.5 ($C^{A5/A5'}$), 128.0 (C^{C3}), 125.7 ($C^{A3/A3'}$), 125.6 ($C^{A3/A3'}$), 122.9 ($C^{B3/B3'}$), 122.8 ($C^{B3/B3'}$). LR-ESI-MS (in MeOH): m/z 938.12 [$(MeOBOMe)PF_6$ adduct] $^+$ requires 938.16; 924.16 [$(MeOBOH)PF_6$ adduct] $^+$ requires 924.15; 396.72 [$(MeOBOMe)$ adduct] $^{2+}$ requires 396.60; 389.72 [$(MeOBOH)$ adduct] $^{2+}$ requires 389.59.

2.8.18. Synthesis of $[Ru(\mathbf{7})_2](PF_6)_2$



Ligand **7** (0.20 g, 0.62 mmol) and $RuCl_3 \cdot xH_2O$ (64 mg, 0.31 mmol) was suspended in ethane-1, 2-diol (10 cm^3). The suspension heated at 150°C for 2 h. The deep red solution was poured into excess aqueous KPF_6 (10 mL). A red precipitate formed and was collected on Celite, washed with H_2O (10 mL), EtOH (5 mL), Et₂O (10 mL), and dissolved in CH_3CN . Removal of solvent gave $Ru(\mathbf{7})_2(PF_6)_2$ as a red solid (0.48 g, 0.46 mmol, 74%). ¹H NMR (400 MHz, CD_3CN) δ 8.94 (s, 4H), 8.63 (ddd, $J = 8.2, 1.4, 0.8$ Hz, 4H), 8.11 (d, $J = 8.2$ Hz, 4H), 7.93 (td, $J = 7.9, 1.5$ Hz, 4H), 7.70 (s, 2H), 7.42 (ddd, $J = 5.6, 1.5, 0.7$ Hz, 4H), 7.21 – 7.12 (m, 8H).

3. Chapter three: Dinuclear Ru(II) complexes as expanded ligands

3.1.Introduction

The dinuclear ruthenium(II) complex with one bridging ligand on the one side and one capping ligand on the other side were investigated two decades ago^[47a, 67] (Figure 24),but its capping ligand with no functionality limits its application in metallosupramolecular chemistry. Similar to the mononuclear complex, the disadvantage of $[\text{Ru}(\text{tpy})_2]^{2+}$ complex and its dinuclear $[(\text{tpy})\text{Ru}(\text{bridging ligand})\text{Ru}(\text{tpy})]^{4+}$ complex compared with the $[\text{Ru}(\text{bpy})_3]^{2+}$ analogues is its limitation as a photoactive unit due to the short excited lifetime and low quantum yield. However, the advantage of this motif is that it has well-defined molecular axes and no fac arrangements are found to give a single achiral complex.

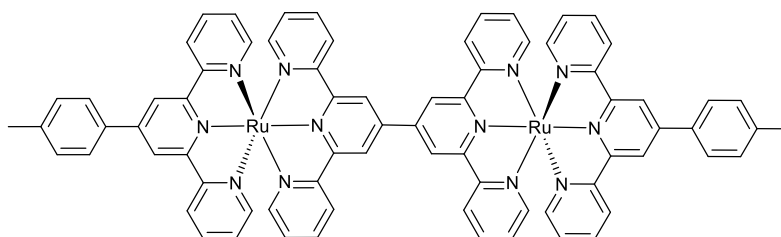


Figure 24 : Bridging ligand, 6',6''-di(pyridin-2-yl)-2,2':4',4'':2'',2'''-quaterpyridine and capping ligand, 4'-(4-methylphenyl)-2,2':6',2'''-terpyridine

The bridging ligand in supramolecular chemistry can be used for building large structures with pendent pyridines which act as donor sites. The spacer group plays an important role in the angular orientation of the building blocks, such as 60 angles for triangular structure,^[43b, 68] 180 angles for rodlike structure^[69], etc. The bridging ligand can also self-assemble into coordinating cage with labile metals such as palladium(II). The linkers and bending part composed of aromatic ring are the key to the formation of the different shaped cages,^[70] properties of coordination cages itself such as photoproperties^[70a, 71], electronic properties^[72] as well as the implementation of functionality of the coordination cages such as inclusion of guests,^[72b, 73] structural conversion of guests^[74] and drug delivery^[73a].

Banana shaped ligands such as 1,3-di(pyridin-4-yl)benzene and 1,3-bis(pyridin-3-ylethynyl)benzene which have a 60 bending angle can be self-assembled into a $\text{Pd}_{12}\text{L}_{24}$ spherical cage^[75] and Pd_2L_4 coordination cage (Figure 25), respectively.^[76] In the cage, each four donor sites of the each four bridging ligands share one naked palladium to form the Pd_nL_{2n} ($n=2, 3, 4, 5$). Anion of the Pd (II) precursor should have a weak coordination, such as BF_4^- or NO_3^- . Weak coordinating solvent such as CH_3CN , DMSO and acetone are employed.

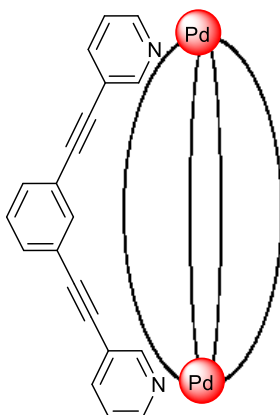


Figure 25: Coordination cage based on the banana shaped ligand, bis(pyridin-3-ylethynyl)benzene^[77]

In order to extend the utilization of the dinuclear complexes and introduction of pendent pyridyl sites, goals of this project were: 1) the expanded ligands contain two ruthenium(II) cores and 'back-to-back' 2,2' : 6',2"-terpyridine ligands and are the first expanded ligands to contain multiple Ru(II) centres; 2) use ruthenium(II) dinuclear angular expanded ligands for self-assembling of large structures. All compounds synthesized and characterized here have the same general structure via Sonogashira crossing coupling or Suzuki cross coupling reactions.

3.2.Synthesis of ruthenium(II) dinuclear complex

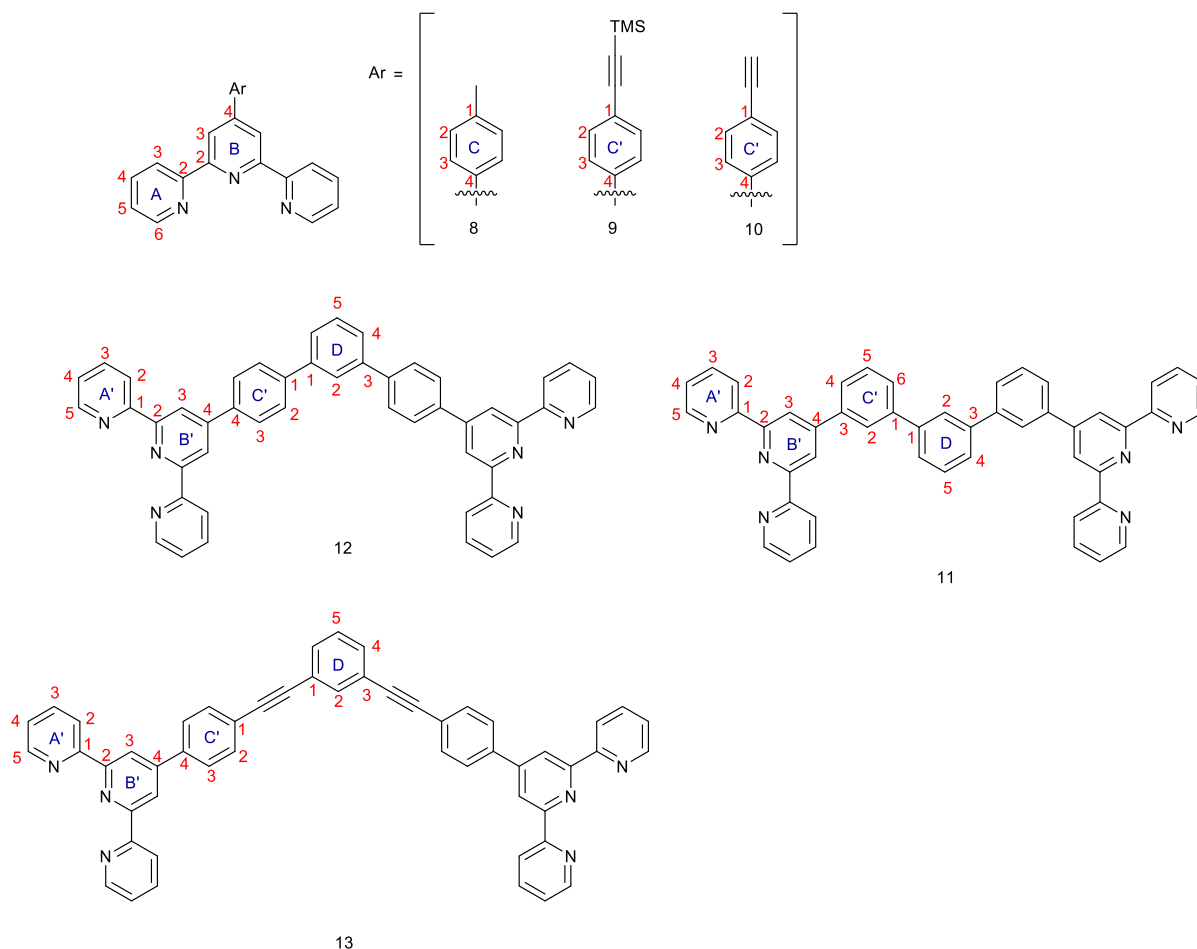
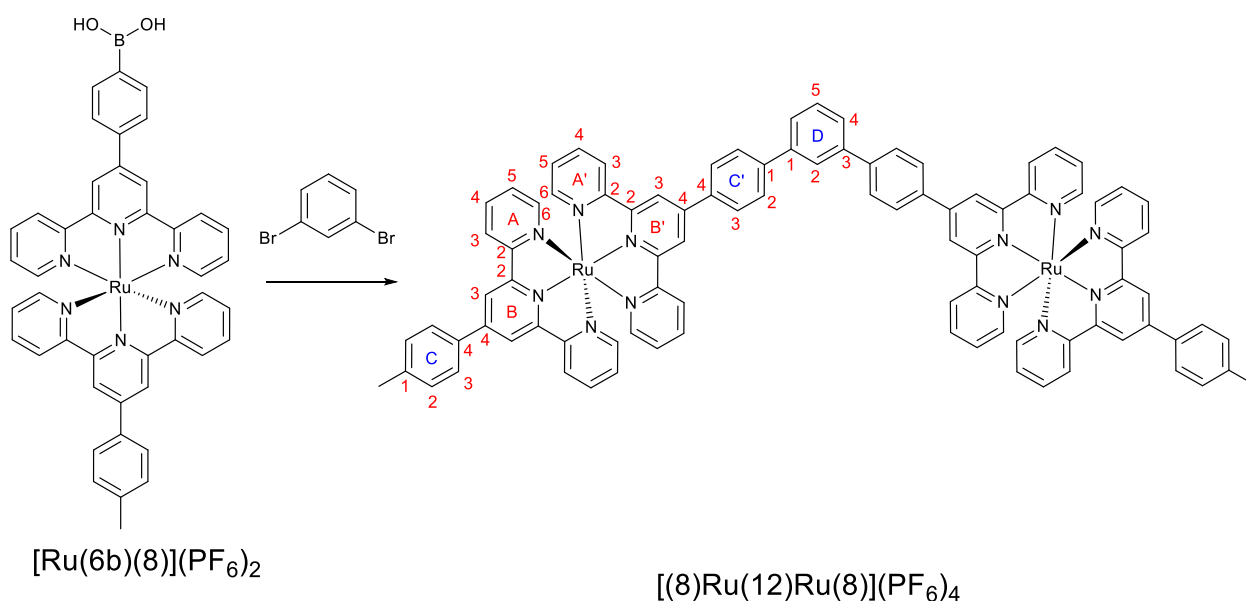


Figure 26 : Ligands used in this study and the numbering scheme adopted.

Prior to building dinuclear banana-shaped ruthenium(II) based expanded ligands with pendant pyridyl sites at the ends, the model compound $[(\mathbf{8})\text{Ru}(\mathbf{12})\text{Ru}(\mathbf{8})](\text{PF}_6)_4$ was prepared for optimization of the coupling reaction. 1,3-Dibromobenzene was chosen as a benzene ring spacer to introduce a 120 degree angle suitable to build large and intricate structures. With the help of methyl groups at the ends, all peaks in the NMR spectrum were not challenging to assign. Standard Suzuki coupling reaction conditions were used: 1,3-dibromobenzene (1 equivalent), DMF, CS_2CO_3 (20 equivalent), $\text{Pd}(\text{PPh}_3)_4$ (10% equivalent), $[\text{Ru}(\mathbf{6b})(\mathbf{8})](\text{PF}_6)_2$ (2 equivalent), 70°C and an argon atmosphere for two days. The reaction was followed by TLC plate after KPF_6 anion exchange and dissolving crude product in CH_3CN . TLC showed three spots: starting materials, decomposed starting materials (probably lost the boronic acid) and a very polar product. The compound was purified by chromatography (SiO_2 , $\text{CH}_3\text{CN}:\text{H}_2\text{O}:\text{saturated aqueous KNO}_3$ 5:

1: 1). The band of $[(\mathbf{8})\text{Ru}(\mathbf{12})\text{Ru}(\mathbf{8})](\text{PF}_6)_4$ on the TLC plate was found to have a long tail which contributes to the difficult purification by column. After the second purification by chromatography using the same concentration of eluent, anion exchange by PF_6 salt gave the red solid in 27% yield.



Scheme 2 : Suzuki cross coupling of $[\text{Ru}(\mathbf{6b})(\mathbf{8})](\text{PF}_6)_2$ with 1,3-dibromobenzene to give $[(\mathbf{8})\text{Ru}(\mathbf{12})\text{Ru}(\mathbf{8})](\text{PF}_6)_4$

After the Suzuki cross coupling reaction, the ^1H NMR signal of the proton corresponding to the boronic acid disappeared as expected. The most significant change is for the chemical shift of the protons in the C' ring. The $\text{H}^{\text{C}3'}$ peak was observed to shift upfield from 8.40 ppm to 8.21 ppm. While the $\text{H}^{\text{C}2'}$ was shifted upfield from 8.22 ppm to 8.12 ppm. The signals corresponding to ligand **8** are slightly dependent on the other side of the terpyridine units coordinated to the Ru(II) domain. But the phenyl ring part in the ligand **8** is independent of the other side of the complex which was supported by the observation that no significant changes in chemical shift were observed in comparison with the starting material $[\text{Ru}(\mathbf{6b})(\mathbf{8})](\text{PF}_6)_2$. Protons of the phenyl ring spacer (ring D) were assigned 8.30 ppm for $\text{H}^{\text{D}2}$, 7.97 ppm for $\text{H}^{\text{D}4}$ and 7.78 ppm for $\text{H}^{\text{D}5}$ with 2D NMR techniques (COSY, HSQC, NOESY).

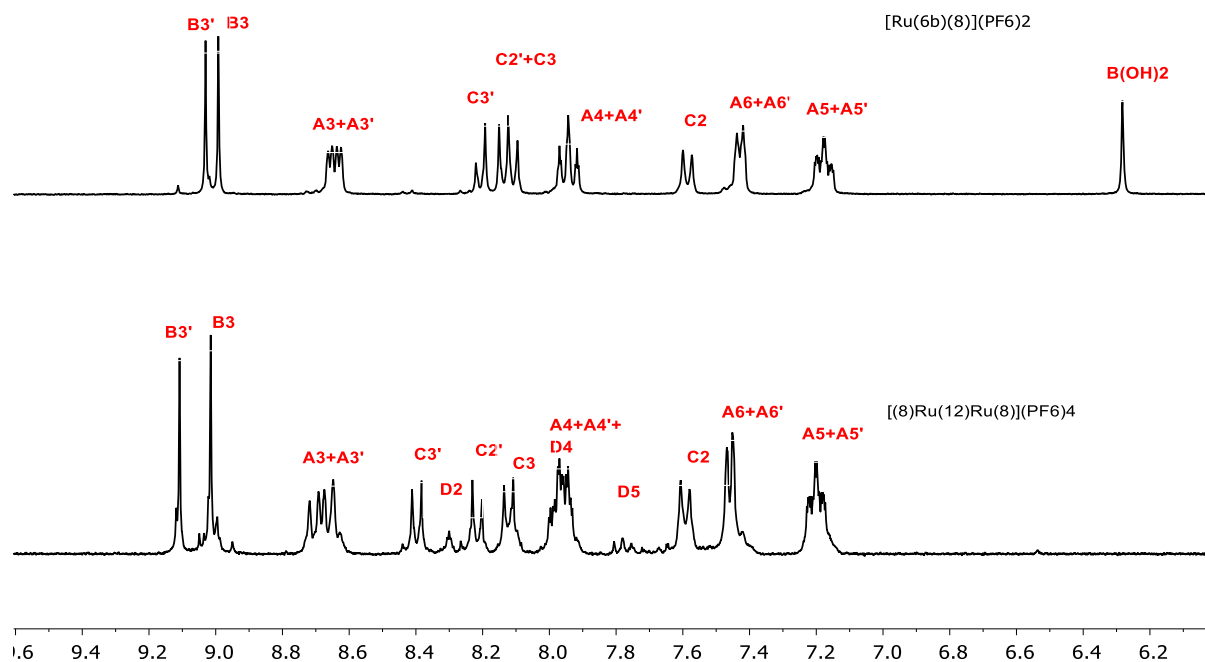
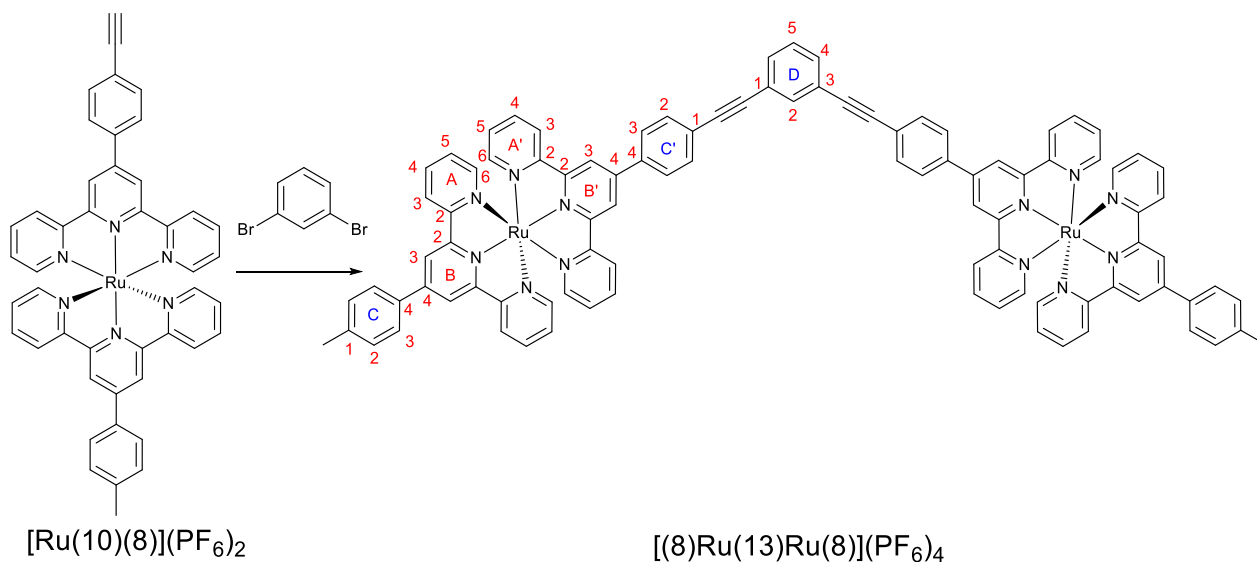


Figure 27 : NMR spectra of $[\text{Ru}(\mathbf{6b})(\mathbf{8})](\text{PF}_6)_2$ and $[(\mathbf{8})\text{Ru}(\mathbf{12})\text{Ru}(\mathbf{8})](\text{PF}_6)_4$

Increasing the distance between Ru(II) centres was achieved by introduction of a phenyl ring with alkyne spacers via Sonogashira cross coupling reactions: 1,3-dibromobenzene (1 equivalent), CH_3CN , THF, $\text{Pd}(\text{PPh}_3)_4$ (0.1 equivalent), CuI (0.1 equivalent), $[\text{Ru}(\mathbf{10})(\mathbf{8})](\text{PF}_6)_2$ (1.5 equivalent), 60°C , an argon atmosphere and for 2 days. After anion exchange with KPF_6 salt and redissolving in acetonitrile, the target complex $[(\mathbf{8})\text{Ru}(\mathbf{13})\text{Ru}(\mathbf{8})](\text{PF}_6)_4$ was observed. TLC revealed a red spot which had a similar R_f value using $\text{CH}_3\text{CN}:\text{H}_2\text{O}:\text{saturated aqueous KNO}_3$ 5: 1: 1 as the eluent. The reaction condition were optimized using DMF and DME as a solvent mixture and $[\text{Ru}(\mathbf{10})(\mathbf{8})](\text{PF}_6)_2$ (2.0 equivalent). The yield was improved up to 27% using the same workup.



Scheme 3: Sonogashira cross coupling of $[\text{Ru}(\mathbf{10})(\mathbf{8})](\text{PF}_6)_2$ with 1,3-dibromobenzene

Compared with the $[\text{Ru}(\mathbf{10})(\mathbf{8})](\text{PF}_6)_2$, many peaks shifted upfield in the $[(\mathbf{8})\text{Ru}(\mathbf{13})\text{Ru}(\mathbf{8})](\text{PF}_6)_4$ upon coupling. None of the signals of the terpyridine domain in the dinuclear complex shifted, except $\text{H}^{\text{B}3}$ and $\text{H}^{\text{B}3'}$. The dinuclear complex exhibited the expected upfield $\text{H}^{\text{C}3'}$ shifted signals (8.30 ppm to 8.21 ppm, see Figure 28). The $\text{H}^{\text{C}2'}$ peak also shifted upfield and overlapped with the multiple peaks of $\text{H}^{\text{A}4}$ and $\text{H}^{\text{A}4'}$. The signal of the alkyne proton disappeared as expected and the methyl group of the tolyl group still remains the same chemical shift. Protons of phenyl ring were assigned at 7.90 ppm for $\text{H}^{\text{D}2}$, 7.72 ppm for $\text{H}^{\text{D}4}$ and $\text{H}^{\text{D}5}$ 7.59 ppm which is quite different from the NMR environment of phenyl ring in $[(\mathbf{8})\text{Ru}(\mathbf{13})\text{Ru}(\mathbf{8})](\text{PF}_6)_4$ as expected gave the alkyne linkers.

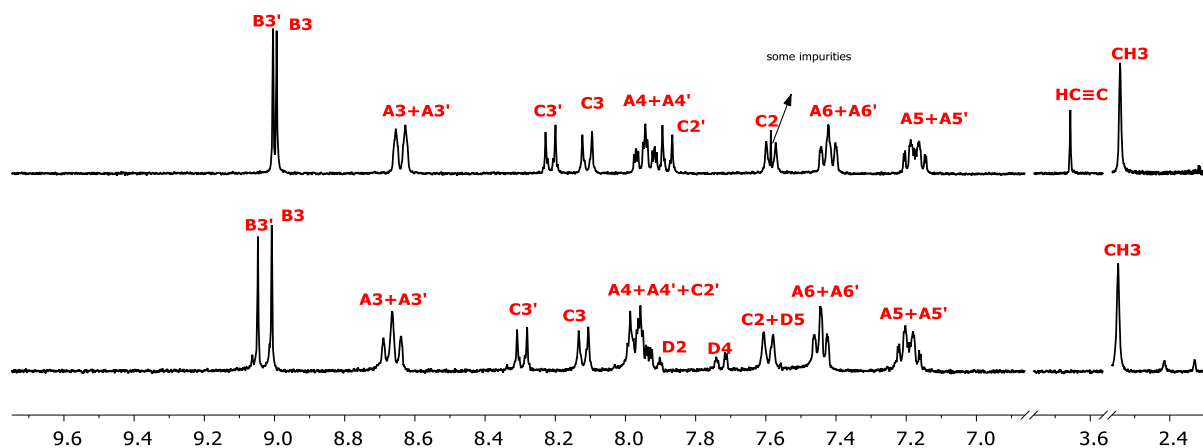


Figure 28 : NMR spectra of $[\text{Ru}(\mathbf{10})(\mathbf{8})](\text{PF}_6)_2$ and $[(\mathbf{8})\text{Ru}(\mathbf{13})\text{Ru}(\mathbf{8})](\text{PF}_6)_4$

Synthesis of dinuclear expanded ligands with pendent pyridines at the ends followed optimized conditions of synthesis of $[(\mathbf{8})\text{Ru}(\mathbf{12})\text{Ru}(\mathbf{8})](\text{PF}_6)_4$, 1,3-dibromobenzene (1 equivalent), DMF, CS_2CO_3 (20 equivalent), $\text{Pd}(\text{PPh}_3)_4$ (10% equivalent), $[\text{Ru}(\mathbf{6b})(\mathbf{8})](\text{PF}_6)_2$ (1.5 equivalent), 80°C and an argon atmosphere for two days. The compound was purified by chromatography (SiO_2 , $\text{CH}_3\text{CN}:\text{H}_2\text{O}:\text{TEA}:\text{saturated aqueous KNO}_3$ 5: 1: 1: 0.01%). The triethylamine was used for deprotonation of the pendent pyridine on the column. The analytical yield is higher than the isolated yield because some of the complexes, even the pure ruthenium(II) complex, remain stuck on the Celite. Attempt to completely wash off from the Celite by acidic CH_3CN failed. Palladium catalyst was also responsible for the decreased yield due to the coordination to the pendent pyridines.

The dinuclear ruthenium(II) $[(\text{Y})\text{Ru}(\text{X})\text{Ru}(\text{Y})](\text{PF}_6)_4$ complexes are separated into two parts for discussion: bridging ligand X = bis(tridentate) ligand **11** and **12**; terminal ligand Y = mono(tridentate) ligand, **3** and **4**.

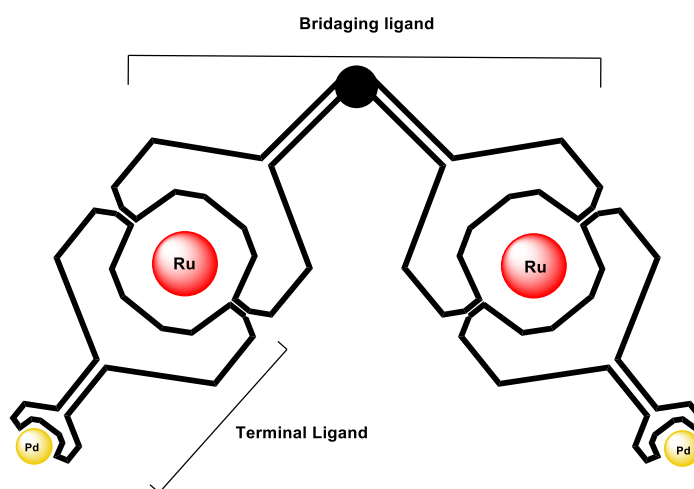


Figure 29 : Bridging ligand X and terminal ligand Y

3.3. Mass Spectrometry characterization

Electrospray ionization mass spectrometry (ESI-MS) was used to identify charged ions for each dinuclear complex. A small amount of each bimetallic complex was dissolved in acetonitrile and injected into ESI-MS. In each case, signals with isotope patterns matching that for the calculated ions were observed. Structural isomers of [(**3**)Ru(**11**)Ru(**3**)](PF₆)₄, [(**4**)Ru(**11**)Ru(**4**)](PF₆)₄, [(**3**)Ru(**12**)Ru(**3**)](PF₆)₄, and [(**4**)Ru(**12**)Ru(**4**)](PF₆)₄ each exhibited the expected peak and isotope pattern in the ESI-MS spectra corresponding to sequential loss of PF₆ counter ions. Specifically, [M-PF₆]⁺, [M-2PF₆]²⁺, [M-PF₆]³⁺ and [M-2PF₆]⁴⁺ ions were observed (calc) at *m/z*: 1951.40 (1951.22); 903.26 (903.13); 553.84 (553.76); 379.20 (379.08). Similar behavior was found for tolyl derivatives [(**8**)Ru(**12**)Ru(**8**)](PF₆)₄ and [(**8**)Ru(**13**)Ru(**8**)](PF₆)₄. For [(**8**)Ru(**12**)Ru(**8**)](PF₆)₄: 916.25 (916.15), [M - 2PF₆]²⁺; 562.48 (562.44), [M - 3PF₆]³⁺; 385.50 (385.59), [M - 4PF₆]⁴⁺. For [(**8**)Ru(**13**)Ru(**8**)](PF₆)₄: 939.67 (940.14), [M - 2PF₆]²⁺; 578.25 (578.44), [M - 3PF₆]³⁺; 397.75 (397.59), [M - 4PF₆]⁴⁺.

3.4. Nuclear Magnetic Resonance(NMR) characterization of dinuclear complex with two terminal pendent pyridines.

NMR spectra of [(**3**)Ru(**11**)Ru(**3**)](PF₆)₄, [(**4**)Ru(**11**)Ru(**4**)](PF₆)₄, [(**3**)Ru(**12**)Ru(**3**)](PF₆)₄, and [(**4**)Ru(**12**)Ru(**4**)](PF₆)₄ were assigned using ¹H NMR, ¹³C NMR, COSY, HSQC, HMBC and NOESY techniques in CD₃CN. The ¹H NMR spectra of all complexes are shown in Figure 30. Similar to the mononuclear complex described in Chapter 2, each terpyridine unit is independent of the other terpyridine coordinated to the ruthenium centre. More specifically, signals corresponding to H^{C2}, H^{C3} and H^{B3} peaks in the terminal terpyridine were constant in the dinuclear complexes of [(**4**)Ru(**11**)Ru(**4**)](PF₆)₄ and [(**4**)Ru(**12**)Ru(**4**)](PF₆)₄ (8.97 ppm, 8.15 ppm and 9.07 ppm). Signals corresponding to H^{C2}, H^{C6}, H^{C4} and H^{B3} peaks in the terminal terpyridine were also constant in the dinuclear complexes of [(**3**)Ru(**11**)Ru(**3**)](PF₆)₄ and [(**3**)Ru(**12**)Ru(**3**)](PF₆)₄ (9.41 ppm, 8.86 ppm, 8.56 ppm and 9.06 ppm). These three signals were shifted slightly upfield in comparison with their parent mononuclear complexes.

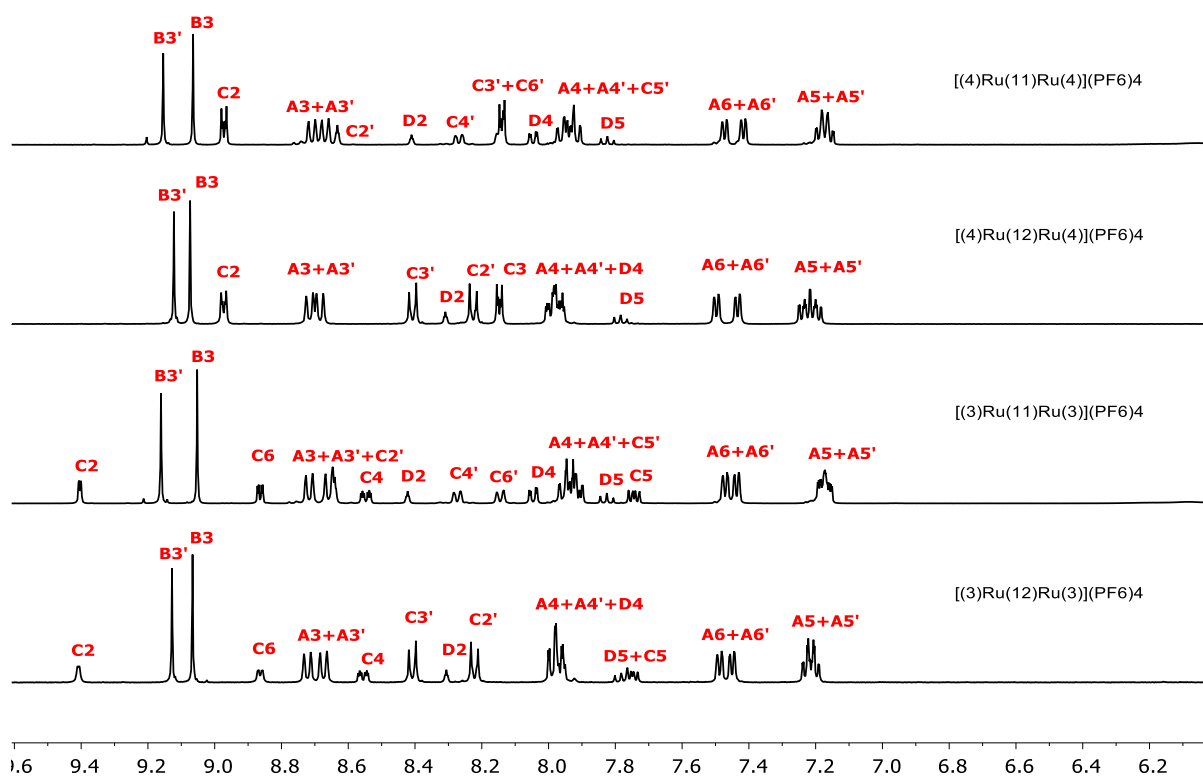


Figure 30 : ^1H NMR spectra (400 MHz, CD_3CN , 298K) for Ru(II) complexes synthesized in this study. Top to bottom: $[(4)\text{Ru}(11)\text{Ru}(4)](\text{PF}_6)_4$; $[(4)\text{Ru}(12)\text{Ru}(4)](\text{PF}_6)_4$; $[(3)\text{Ru}(11)\text{Ru}(3)](\text{PF}_6)_4$; $[(3)\text{Ru}(12)\text{Ru}(3)](\text{PF}_6)_4$; See Figure 26 for labelling scheme adopted.

Replacement of terminal terpyridine (ligand **4**) with another terminal terpyridine (Ligand **3**) did not result in changes in the signals corresponding to the bridging (ligand **11** and ligand **12**). Taking $[(4)\text{Ru}(11)\text{Ru}(4)](\text{PF}_6)_4$ as an example where the ligand **4** is replaced by ligand **3**, ^1H peaks corresponding to ligand **11** in the ring D' had the same chemical shift at 8.42 ppm for $\text{H}^{\text{D}2}$, 8.05 ppm for $\text{H}^{\text{D}4}$ and 7.82 ppm for $\text{H}^{\text{D}5}$. Similarly, the ^1H NMR signals corresponding to $\text{H}^{\text{D}2}$ (8.31 ppm), $\text{H}^{\text{D}4}$ (8.05 ppm) and $\text{H}^{\text{D}5}$ (7.78 ppm) had the same chemical shift in the cases of ligand **12** in the $[(4)\text{Ru}(12)\text{Ru}(4)](\text{PF}_6)_4$ and $[(3)\text{Ru}(12)\text{Ru}(3)](\text{PF}_6)_4$ (See Figure 30). The signals of protons of C' phenyl ring in $[(4)\text{Ru}(11)\text{Ru}(4)](\text{PF}_6)_4$ were slightly shifts upfield compared with the starting material $[\text{Ru}(\mathbf{5b})(\mathbf{4})_2](\text{PF}_6)_4$. In the case of $[(4)\text{Ru}(12)\text{Ru}(4)](\text{PF}_6)_4$ compared with its starting material $[\text{Ru}(\mathbf{6b})(\mathbf{4})](\text{PF}_6)_2$, the signal corresponding to boronic acid at 6.41 ppm disappeared as expected. Phenyl $\text{H}^{\text{C}3'}$ signal had a significant upfield chemical shift from 8.41 ppm to 8.21 ppm. The signal of $\text{H}^{\text{C}2'}$ was shifted upfield from 8.23 ppm to 8.14 ppm (See Figure 31).

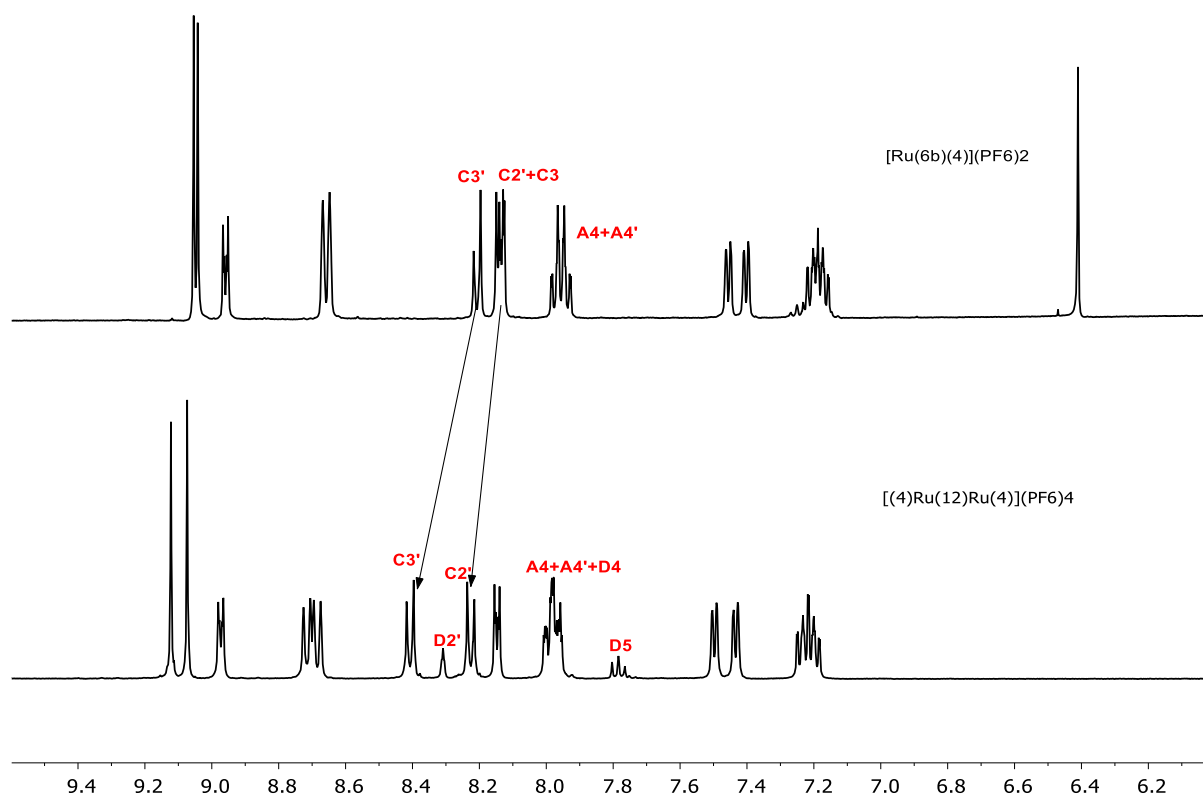


Figure 31 : new signals appear in the [(4)Ru(12)Ru(4)] (PF₆)₄ and protons of ring C' shift upfield after Suzuki cross coupling reaction.

The H^{B3'} and H^{B3} signals of [(4)Ru(11)Ru(4)](PF₆)₄ were distinguished by the appearance in the NOESY spectrum of a cross peak between H^{B3'} and H^{C2'} and H^{B3'} and H^{C4'} (See Figure 32). H^{D2} peak was assigned at 8.31 ppm as a singlet peak and integrated as one proton. The signal of H^{D5} which was identified as a triplet peak had a chemical shift at 7.82 ppm. The central phenyl signals of H^{D4} were assigned at 8.13 ppm by the NOESY cross peak between H^{D4} and H^{D5}.

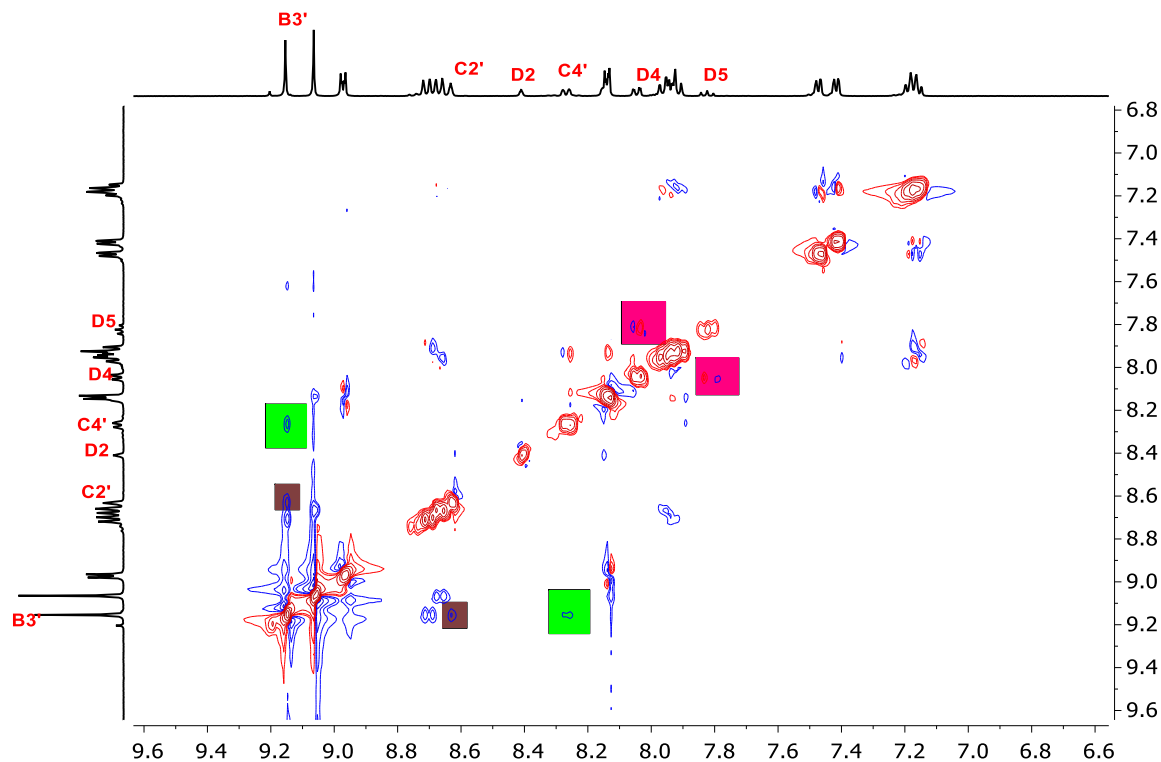


Figure 32 : NOESY spectrum of [(4)Ru(11)Ru(4)](PF₆)₄

3.5. Stability of ruthenium(II) dinuclear complex

Dinuclear complexes were found to be more stable than the starting material (functionalized mononuclear complex). During the workup, cation in the PF₆⁻ salt had no side effect on the compound. Purification by column twice didn't cause the decomposition which is significantly different from stability of boronic acid in the column. Exposed to the air and stored at room temperature, the dinuclear complexes were not observed to decompose.

3.6. Example of protonation of dinuclear complex

[(4)Ru(11)Ru(4)](PF₆)₄ was used for protonation analysis as ¹H NMR peak shifts of the signals corresponding to the pendant pyridyl rings were found to have differ from sample to sample. The top spectrum in the Figure 33 showed the deprotonated [(4)Ru(11)(4)](PF₆)₄ complex by K₂CO₃. Protonation was apparent from peaks of the pendent pyridine ring as shown in Figure 33. Addition of 5 μL TFA by micro syringe into the NMR tube showed the H^{C2} shifted downfield from 8.97 ppm to 9.10 ppm and

H^{C3} shifted from 8.14 ppm to 8.62 ppm. Addition of another 5 μ L TFA fully protonated the pyridine ring supported by the downfield shifted H^{C3} peak to 8.76 ppm. While the H^{C2} peak had a signal at 9.07 ppm. Further addition of 5 μ L TFA didn't result in any further changes in chemical shifts of all peaks. The results agree with the protonation analysis of mononuclear complex.

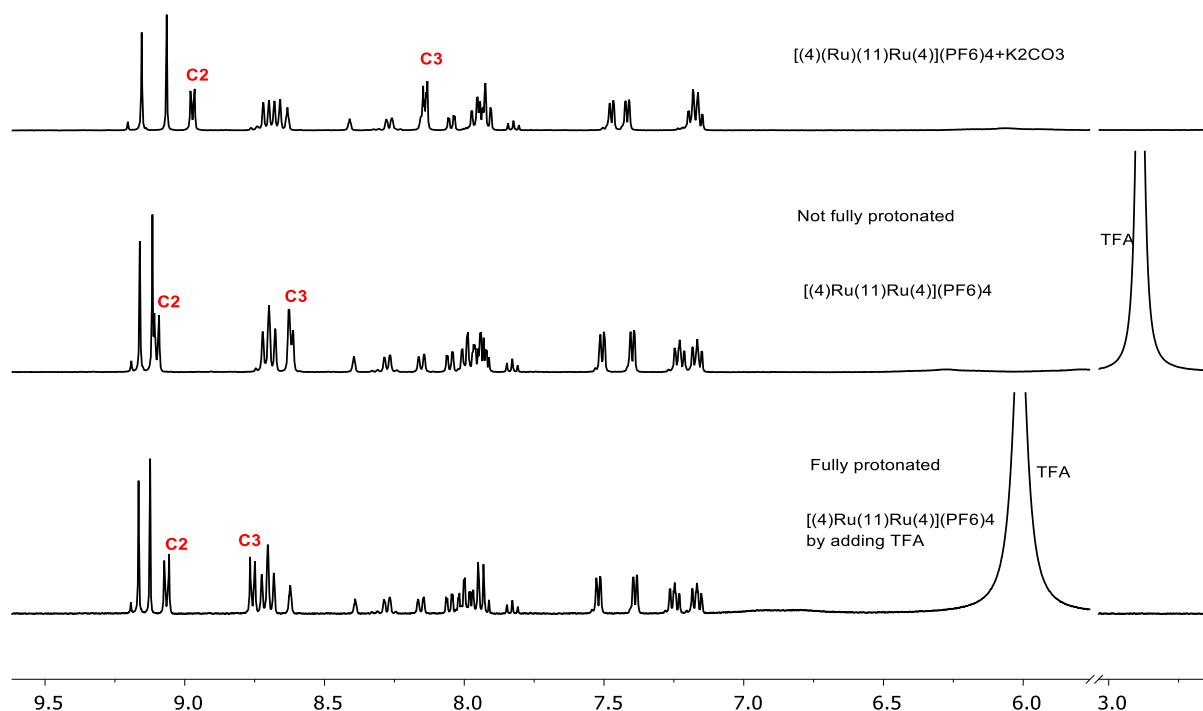


Figure 33 : 1H NMR (CD_3CN , 400 MHz) of (top to bottom): non-protonated $[(4)Ru(11)Ru(4)](PF_6)_4$ complex; Not fully protonated $[(4)Ru(11)Ru(4)](PF_6)_4$ complex; Fully protonated $[(4)Ru(11)Ru(4)](PF_6)_4$ complex.

3.7. Attempts to build large molecular cages

The spherical cage has been well studied by Fujita and co-workers.^[40] The bent bidentate ligand with two pendent pyridyl sites (two equivalents) was treated with $Pd(NO_3)_2$ or $Pd(MeCN)_4(BF_4)_2$ or $Pd(TfO)_2$ (one equivalent) at 70~80°C in DMSO for six hours. All of these employed counter anion have a very weak coordinating bond to the naked palladium(II). Addition or slow diffusion by diethyl ether resulted in precipitation of the cage^[7, 78]. DMSO- d_6 was used for tracking the reaction progress.

In this study, the ruthenium(II) terpyridine ligands were introduced instead of traditional organic spacers, following the literature procedure described above. The reaction was first tried using $[(4)\text{Ru}(12)\text{Ru}(4)](\text{PF}_6)_4$ (two equivalents) and $\text{Pd}(\text{NO}_3)_2$ (one equivalent) to build $\text{M}_{12}\text{L}_{24}$ sphere in DMSO-d_6 at 80°C for 6 h. The mixture was cooled to room temperature and analysed by ^1H NMR (Figure 34). From the NMR spectra, it was obvious that the pendent pyridyl coordination sites bind to the palladium(II) ions. Both of $\text{H}^{\text{C}2}$ and $\text{H}^{\text{C}3}$ signals shifted only slightly downfield and became broader than that in the free ligand. Using $\text{Pd}(\text{CH}_3\text{CN})_4(\text{BF}_4)_2$ instead of $\text{Pd}(\text{NO}_3)_2$ gave similar spectra. However, much larger upfield shifts would be expected upon cage formation, due to the highly shielding environment within a molecular cage.^[79]

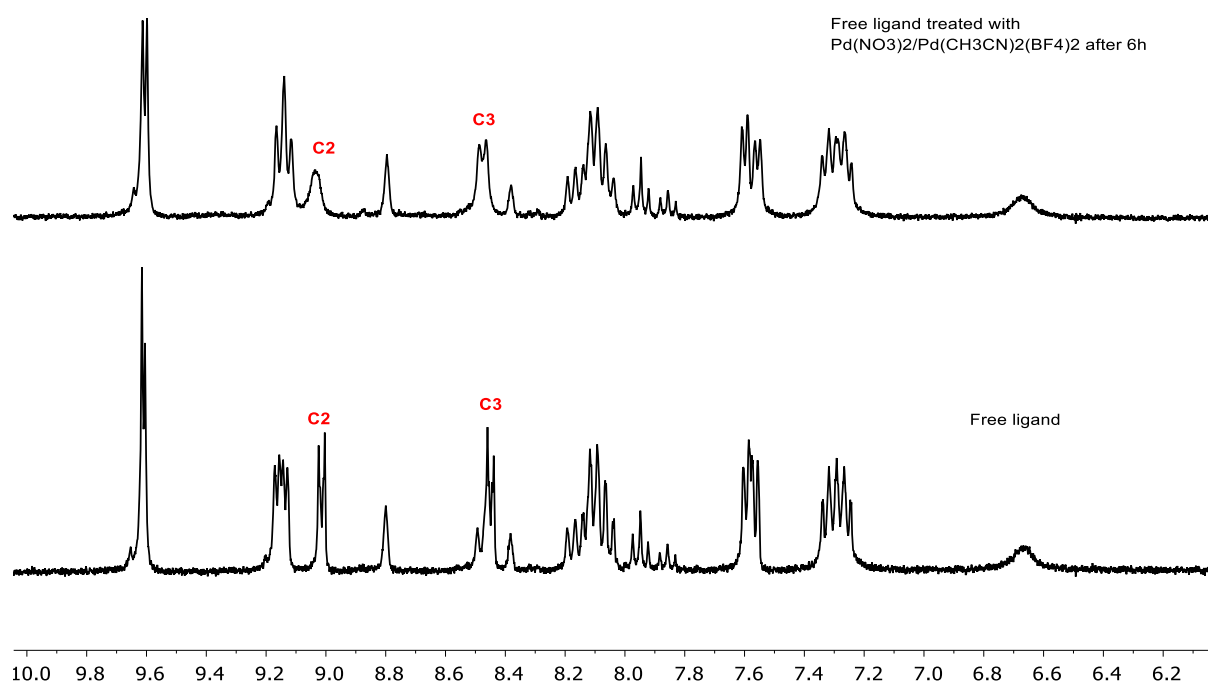


Figure 34 : Top, $[(4)\text{Ru}(12)\text{Ru}(4)](\text{PF}_6)_4$ in DMSO-d_6 after treated with $\text{Pd}(\text{NO}_3)_2/\text{Pd}(\text{CH}_3\text{CN})_4(\text{BF}_4)_2$ at 80°C for 6 h. Bottom, free ligand in DMSO-d_6 , $[(4)\text{Ru}(12)\text{Ru}(4)](\text{PF}_6)_4$.

Deuterated acetonitrile was employed although literature showed the acetonitrile can compete effectively with *t* pyridine for $\text{Pd}(\text{II})$ centres to contributes to the disassembly the cage at low concentrations.^[79] The reaction conditions was the same as stated above: $[(4)\text{Ru}(12)\text{Ru}(4)](\text{PF}_6)_4$ (two equivalents) and

$\text{Pd}(\text{CH}_3\text{CN})_4(\text{BF}_4)_2$ (one equivalent), CD_3CN at 80°C for 6 h. The NMR spectra showed significant chemical shift for most of signals (Figure 35). The NMR shifts which were observed were strongly indicative of the formation of a supramolecular structure, such as a Pd_2L_4 dimer, analogous to that reported by Clever^[76] and shown in Figure 25. Although ESI-MS was unable to provide evidence to support this assignment, the high molecular weight potentially over 50000 is perhaps a contributing factor as the ESI-MS instrument is less sensitive as m/z over 2000 m/z and highly charged ions may be unstable and fragment.

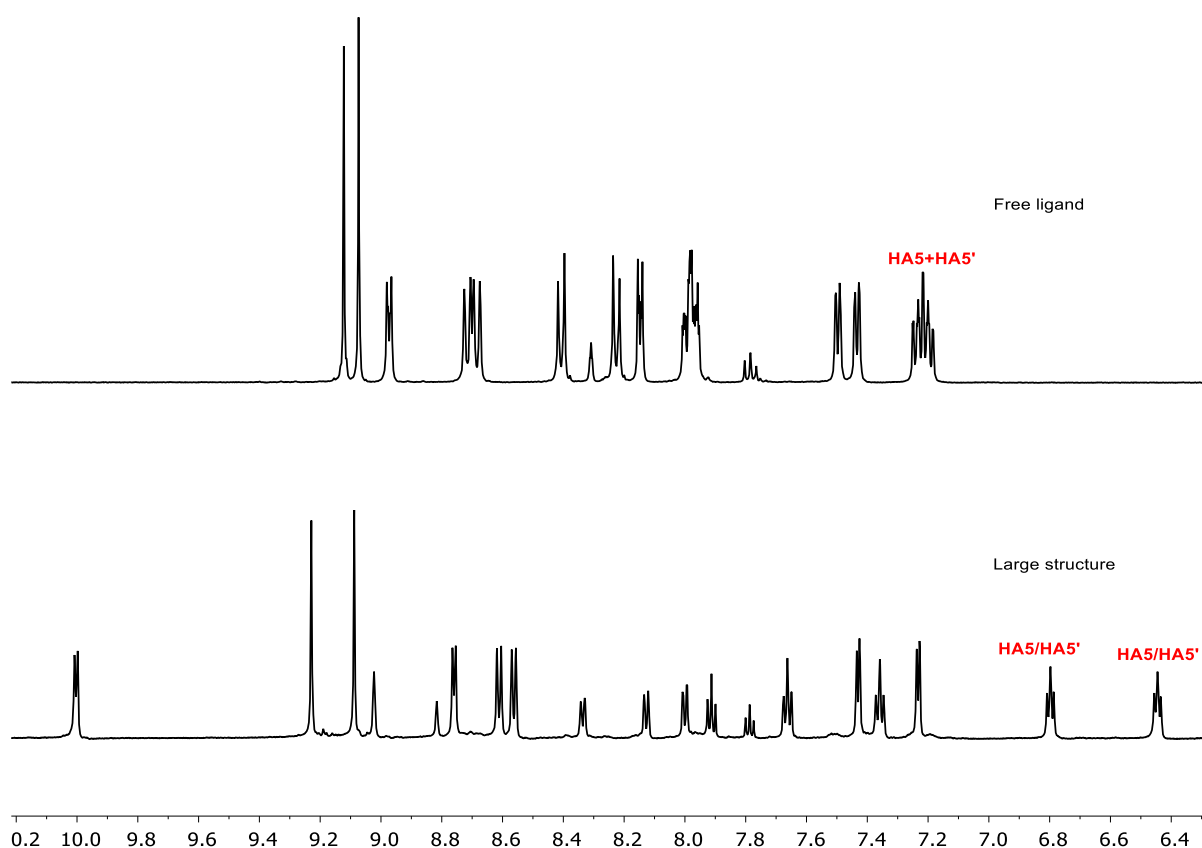


Figure 35 : Top, free ligand in CD_3CN , $[(4)\text{Ru}(12)\text{Ru}(4)](\text{PF}_6)_4$. Bottom, free ligand, $[(4)\text{Ru}(12)\text{Ru}(4)](\text{PF}_6)_4$ in CD_3CN after treatment with $\text{Pd}(\text{NO}_3)_2/\text{Pd}(\text{CH}_3\text{CN})_4(\text{BF}_4)_2$ at 80°C for 6 h.

2D COSY, NOESY and HSQC spectra were shown in Figure 36 to Figure 38 and confirmed the presence of a single species in solution, consistent with a $\text{Pd}_2[(4)\text{Ru}(12)\text{Ru}(4)]$ structure. The presence of signals ($\text{H}^{\text{A}5}$ and $\text{H}^{\text{A}5'}$) shifted strongly upfield, to 6.4 and 6.8 ppm from 7.20 ppm in the free ligand, is consistent with these groups being inside a molecular cavity, as observed for related cages.^[79] ESI-MS did not show peaks corresponding to $[(4)\text{Ru}(12)\text{Ru}(4)]^{2+}$, with some evidence for Pd(II) containing species. However,

no ions to confirm the structure of the cage could be detected. This is potentially due to the fact that the cage likely has a very high molecular weight. For example the relatively small tetramer (i.e. $\{[(4)\text{Ru}(12)\text{Ru}(4)]\text{Pd}_4\}_4(\text{PF}_6)_{32}$) would have a neutral molecular weight of 14718 mass units. In order to be observed in the range commonly available on ESI-MS instruments (100-4000 m/z) the ions would require very high charge, which would be potentially unstable. Therefore, the fact that these peaks were not observed does not eliminate the possibility of large cage formation but prevents unambiguous assignment of its structure. Ultimately a single crystal X-ray structure will be required to determine the exact structure of this assembly.

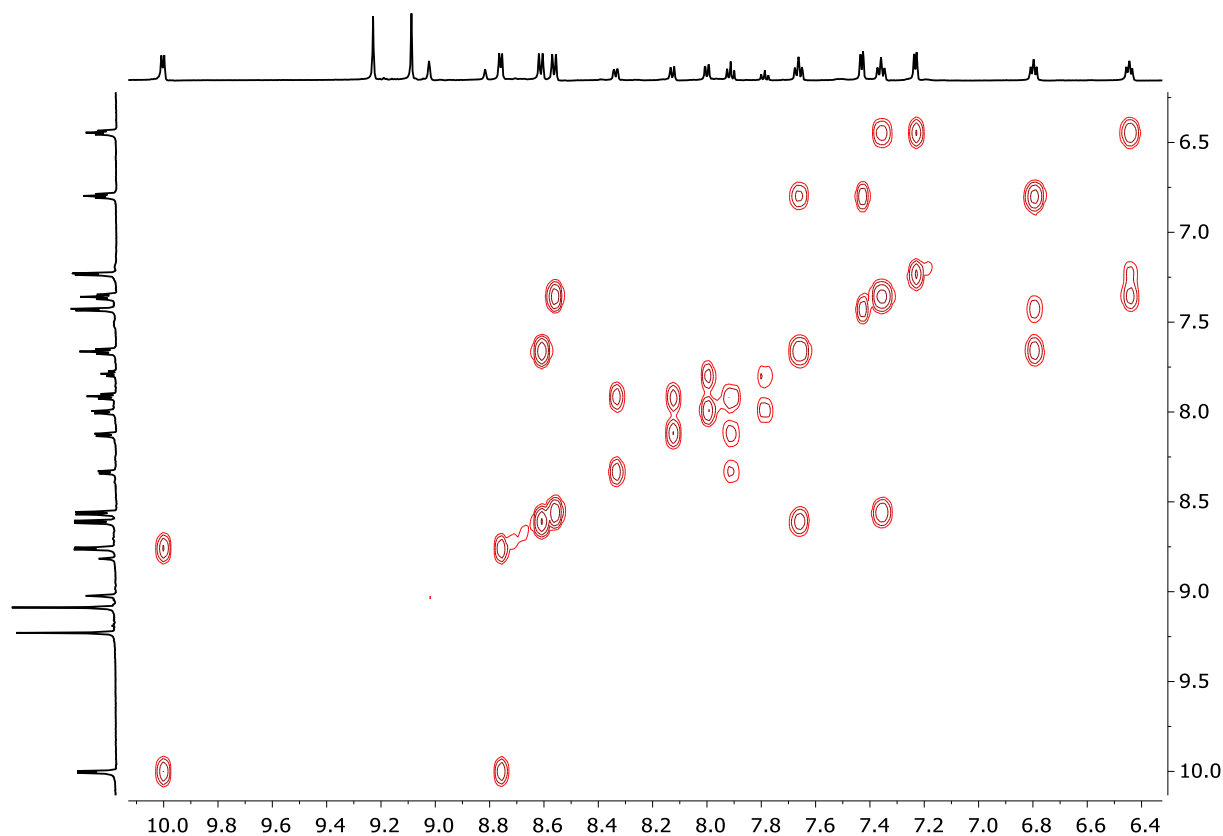


Figure 36 : COSY Spectrum of the supramolecular structure

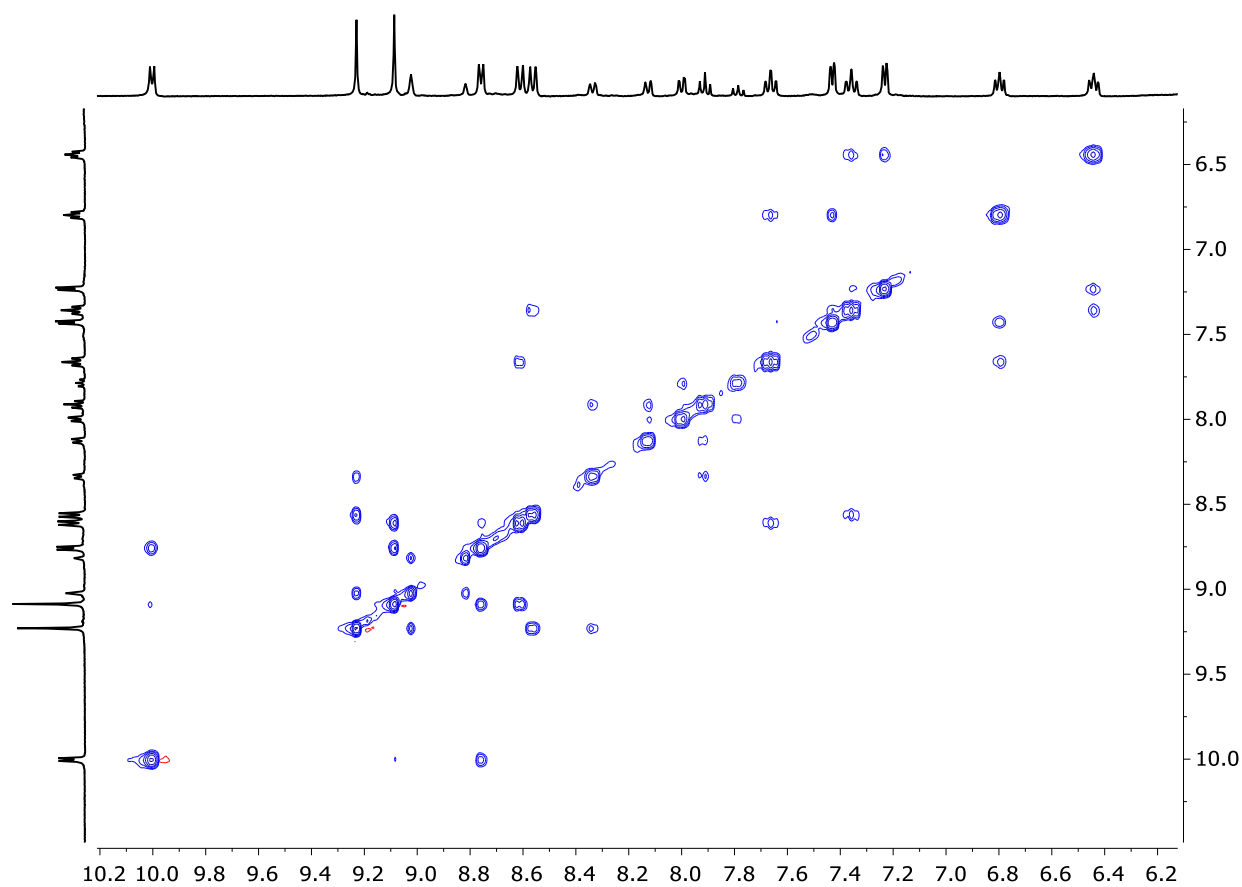


Figure 37 : NOESY Spectrum of the supramolecular structure

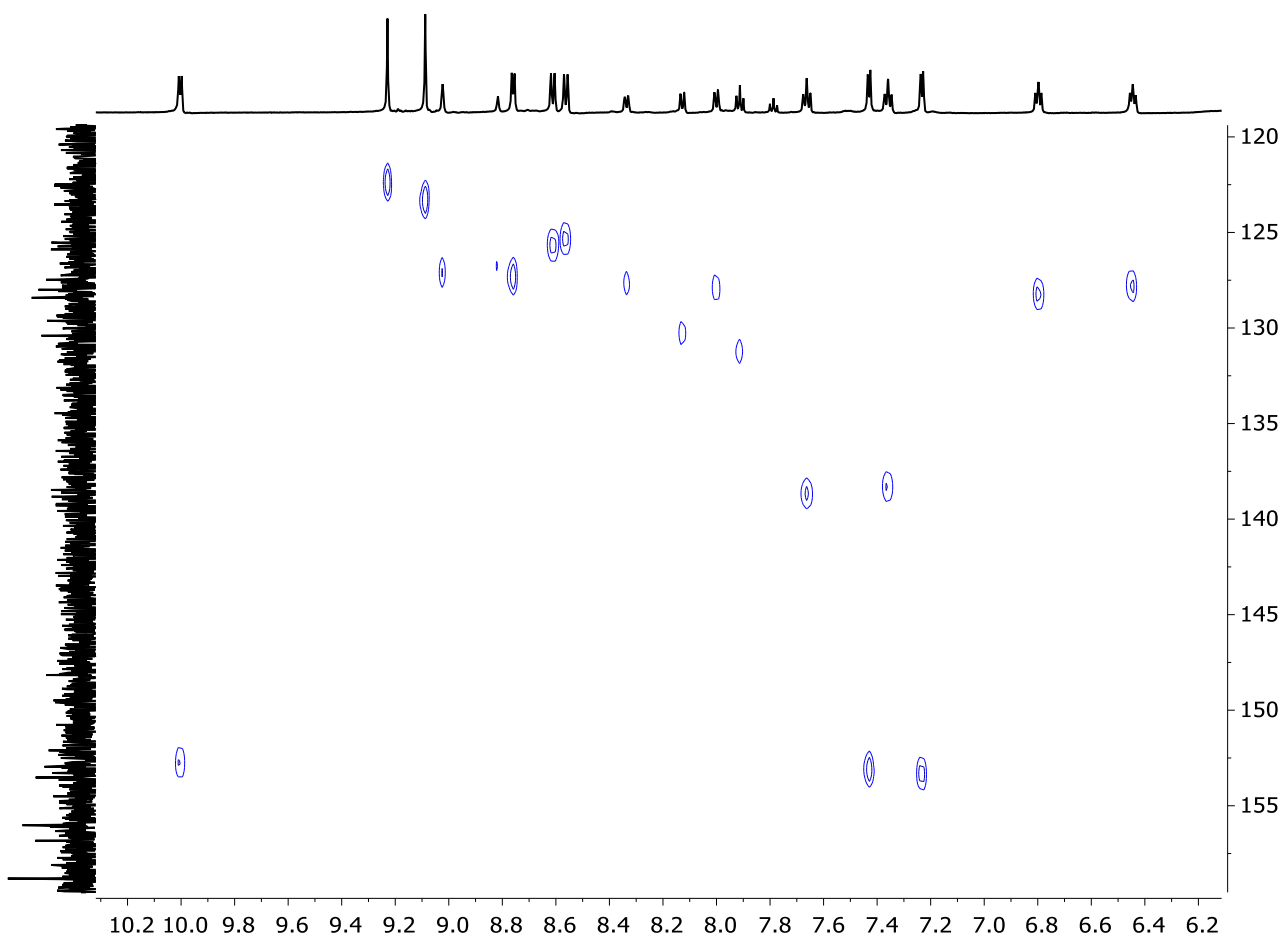


Figure 38 : ^1H - ^{13}C HSQC (600 MHz, CD_3CN) spectrum of the supramolecular structure.

3.8. Chapter summary and conclusion

Conditions for Pd(0) crossing coupling reactions have been optimized using toly group capped ligand, with the choice of solvent, base and reaction time examined. The optimized conditions for synthesizing the first expanded ligand with two ruthenium(II) core and two pendent pyridyl sites was successful. These dinuclear complexes were found to be more stable than the boronic acid functionalized mononuclear complexes at room temperature. Protonation of dinuclear complexes resulted in signals shifting to the downfield around pyridine rings. The first metallocupramolecular cage containing dinuclear Ru(II) complexes has been prepared, and future work to unambiguously identify the structure of this molecule is ongoing.

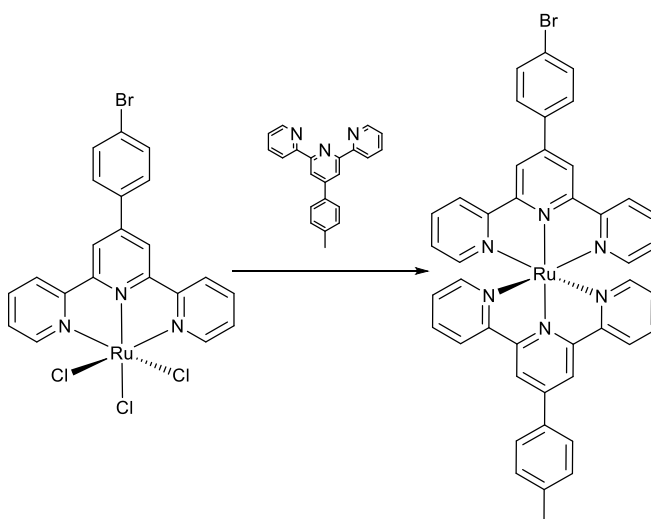
3.9. Experimental Section

3.9.1. Ligand 8: 4'-(4-methylphenyl)-2,2':6',2''-terpyridine

Following general procedure outlined in Chapter 2. The NMR data agrees with literature.^[49]

Yield: 35%. ^1H NMR (300 MHz, CDCl_3) δ 8.86 (s, 2H), 8.83 – 8.75 (m, 4H), 8.00 (td, $J = 7.7, 1.8$ Hz, 2H), 7.91 (d, $J = 7.9$ Hz, 2H), 7.46 (dd, $J = 7.5, 5.0$ Hz, 2H), 7.35 (d, $J = 7.9$ Hz, 2H), 2.46 (s, 3H).

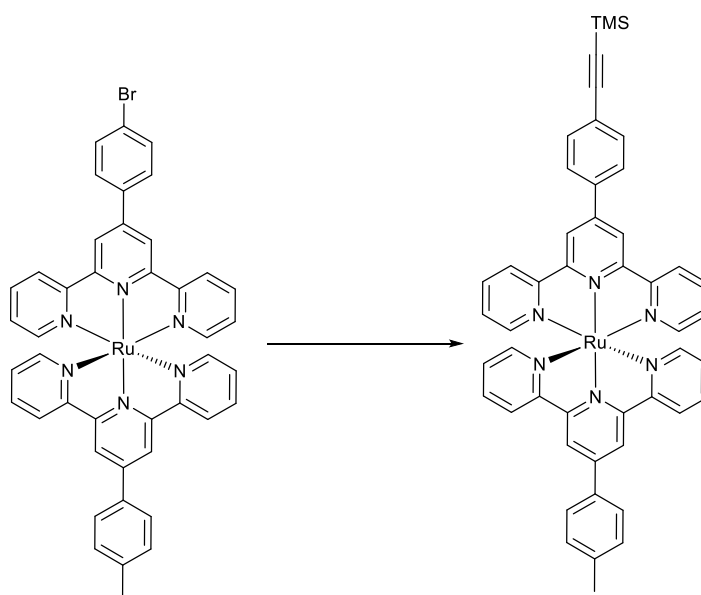
3.9.2. $[\text{Ru}(2)(8)](\text{PF}_6)_2$



The Ru(2)Cl₃ (0.3 g, 0.50 mmol) was suspended in ethanol (10mL). 4-methyl phenyl terpyridine (0.16 g, 0.50 mmol) was added to the suspension and the mixture was refluxing for 12h. The saturated aqueous KPF₆ solution was poured into the solution after filtration. The red precipitate was collected on the Celite, followed by washing with H₂O (5 mL), EtOH (2 mL) and ether (5 mL). The red solid was redissolved in acetonitrile. After removal of the solvent, the red precipitate [Ru(2)(8)](PF₆)₂ (0.44 g, 0.40 mmol, 80%) was used for the Sonogashira reaction without further purification. ¹H NMR (300 MHz, CD₃CN) δ 9.03 (s, 2H), 9.02 (s, 2H), 8.69 – 8.64 (m, 4H), 8.19 – 8.11 (m, 4H), 8.02 – 7.93 (m, 6H), 7.61 (d, *J* = 8.0 Hz, 2H), 7.51 – 7.39 (m, 4H), 7.27 – 7.14 (m, 4H), 2.57 (s, 3H).

The NMR data agrees with literature.^[57]

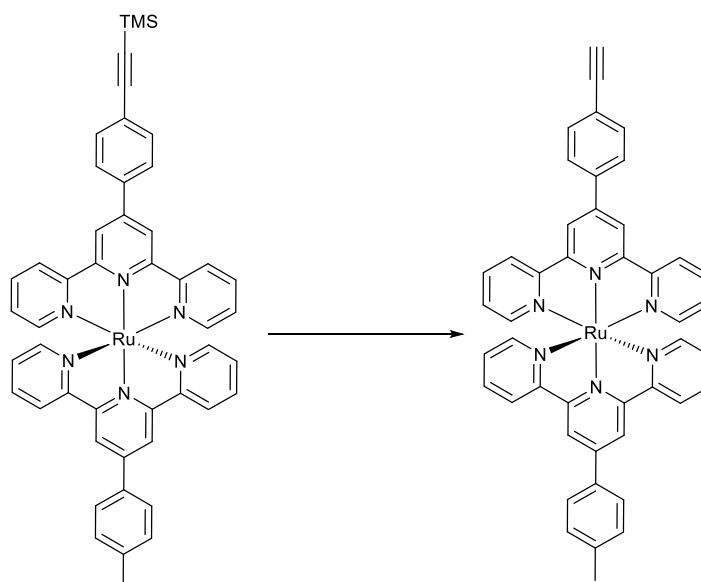
3.9.3. [Ru(9)(8)](PF₆)₂



The [Ru(2)(8)](PF₆)₂ complex (0.44 g, 0.40 mmol) was dissolved in CH₃CN (10 mL), THF (5 mL) and diisopropylamine (5 mL). After the mixture solution was degassed via three freezing-pump-thaw cycles, Pd(PPh₃)₄ (51 mg, 0.040 mmol) and CuI (7.6 mg, 0.040 mmol) were quickly added under an argon atmosphere. Trimethylsilylacetylene (1.12 mL, 8.0 mmol) was added through a syringe. The resulting mixture was stirred at 60°C for 18hr. The mixture solution was cooled to the room temperature. The solvent mixture was reduced to 3 mL and the product was purified (SiO₂, CH₃CN: H₂O: saturated aqueous KNO₃ 10: 1: 0.1). Addition of excess aqueous saturated KPF₆ solution and removal of CH₃CN

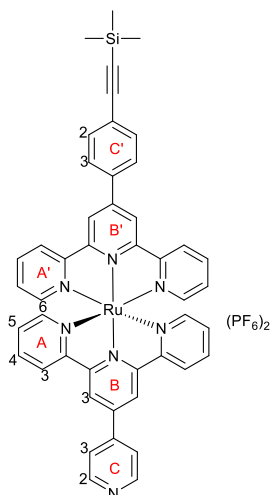
under reduced pressure gave a red precipitate which was collected on Celite, washed with H₂O (5 mL), EtOH (2 mL), Et₂O (5 mL) and dissolved in CH₃CN. Removal of solvent gave product as a red solid (0.33 g, 0.29 mmol, 73%). ¹H NMR (300 MHz, CD₃CN) δ 9.03 (s, 2H), 9.02 (s, 2H), 8.72 – 8.53 (m, 4H), 8.23 (d, *J* = 8.1 Hz, 2H), 8.14 (d, *J* = 7.9 Hz, 2H), 8.04 – 7.91 (m, 4H), 7.84 (d, *J* = 8.1 Hz, 2H), 7.61 (d, *J* = 8.1 Hz, 2H), 7.51 – 7.40 (m, 4H), 7.27 – 7.14 (m, 4H), 2.57 (s, 3H), 0.34 (s, 9H)

3.9.4. [Ru(**10**)(**8**)](PF₆)₂



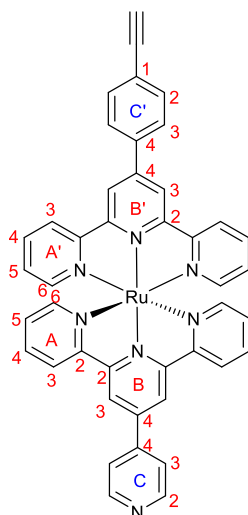
[Ru(**9**)(**8**)](PF₆)₂ (0.33 g, 0.29 mmol) was dissolved in acetonitrile (10 mL). The KF was dissolved in the methanol (3 mL) and added into the solution. The solution was stirred for 3 hr at room temperature. The saturated aqueous KPF₆ solution was poured into the solution. The red precipitate was collected on the Celite, followed by washing with H₂O (5 mL), EtOH (2 mL) and ether (5 mL). The red solid was redissolved in the acetonitrile. Removal of solvent gave the product as a red solid (0.29 g, 0.28 mmol, 95%). ¹H NMR (300 MHz, CD₃CN) δ 9.03 (s, 2H), 9.02 (s, 2H), 8.69 – 8.63 (m, 4H), 8.27 – 8.21 (m, 4H), 8.14 (d, *J* = 8.2 Hz, 2H), 8.04 – 7.87 (m, 6H), 7.61 (d, *J* = 7.9 Hz, 2H), 7.49 – 7.42 (m, 4H), 7.27 – 7.14 (m, 4H), 3.68 (s, 1H), 2.57 (s, 3H).

3.9.5. $[Ru(\mathbf{9})(\mathbf{4})](PF_6)_2$



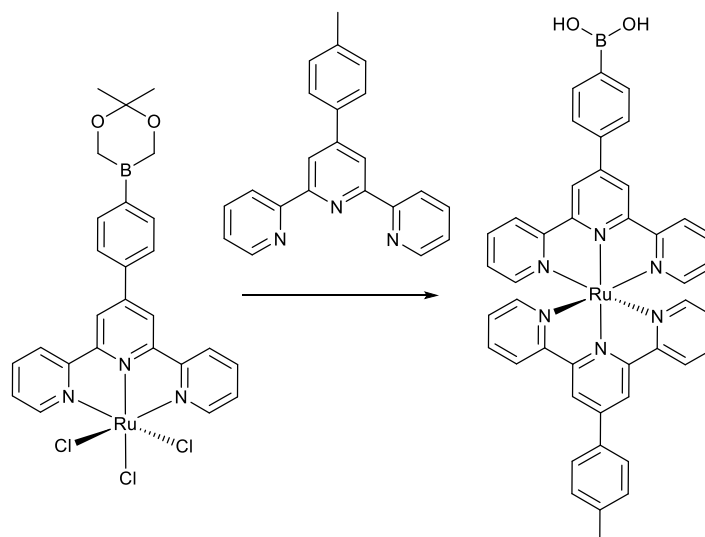
$[Ru(\mathbf{1})(\mathbf{5})][PF_6]_2$ (0.12 g, 0.11 mmol), trimethylsilylacetylene (0.30 mL, 2.2 mmol), diisopropylamine (0.80 mL), acetonitrile (5.0 mL) and THF (2.0 mL) were placed in a dry Schlenk flask. The solution was degassed via three freeze-pump-thaw cycles, following which $Pd(PPh_3)_4$ (19 mg, 17 μ mol) and CuI (2.9 mg, 15 μ mol) were added. The reaction was stirred under an argon atmosphere at 50°C for 20 h. The deep red solution was poured into aqueous NH_4PF_6 (20 mL). A red precipitate formed and was collected on Celite, washed with H_2O , EtOH, Et_2O , and redissolved in CH_3CN . The product was purified by chromatography (SiO_2 , CH_3CN : H_2O : saturated aqueous KNO_3 14: 1: 0.5). Addition of aqueous NH_4PF_6 and removal of CH_3CN gave a red precipitate which was collected on Celite, washed with H_2O , EtOH and Et_2O and redissolved in CH_3CN . Recrystallization from CH_3CN /toluene gave the pure product as a red solid (95 mg, 86 μ mol, 78%). 1H NMR (600 MHz, CD_3CN) δ 9.06 (s, 2H, H^{B3}), 9.01 (s, 2H, $H^{B3'}$), 8.96 (d, $J = 5.1$ Hz, 2H, H^{C2}), 8.65 (d, $J = 8.1$ Hz, 4H, $H^{A3+A3'}$), 8.25 – 8.10 (m, 4H, $H^{C3+C3'}$), 8.00 – 7.90 (m, 4H, $H^{A4+A4'}$), 7.82 (d, $J = 8.2$ Hz, 2H, $H^{C2'}$), 7.42 (dd, $J = 11.6, 5.5$ Hz, 4H, $H^{A6+A6'}$), 7.24 – 7.12 (m, 4H, $H^{A5+A5'}$), 0.30 (s, 9H, $Si(CH_3)_3$). ^{13}C NMR (151 MHz, CD_3CN) δ 159.04 ($C^{A2/A2'}$), 158.91 ($C^{A2/A2'}$), 156.82 ($C^{B2/B2'}$), 156.41 ($C^{B2/B2'}$), 153.49 ($C^{A6+A6'}$), 152.10 (C^{C2}), 148.31 ($C^{C4'}$), 146.29 (C^{C4}), 145.06 (C^{B4}), 139.17 ($C^{A4+A4'}$), 137.81 ($C^{B4'}$), 135.76 ($C^{C1'}$), 133.82 ($C^{C2'}$), 128.94 ($C^{C3'}$), 128.62 ($C^{A3/A3'}$), 128.50 ($C^{CA3/A3'}$), 125.67 ($C^{A5/A5'}$), 125.63 ($C^{A5/A5'}$), 122.89 (C^{C3}), 122.77 (C^{B3}), 122.54 ($C^{B3'}$), 104.27 ($C^{C=C}$), 97.59 ($C^{C=C}$), -0.13 (C^{TMS}). LR-ESI-MS (in CH_3CN): m/z 962.08 $[M - PF_6]^+$ requires 962.16; m/z 408.75 $[M - 2PF_6]^{2+}$ requires 408.60. *Anal.* Calc. for $C_{46}H_{37}F_{12}N_7P_2RuSi \cdot 3.5H_2O$: C, 47.27; H, 3.79; N, 8.39. Found: C, 47.02; H, 3.42; N, 8.20%.

3.9.6. $[Ru(\mathbf{10})(\mathbf{4})](PF_6)_2$



$[Ru(\mathbf{9})(\mathbf{4})](PF_6)_2$ (76 mg, 69 μ mol) was dissolved in the CH_3CN (10 mL). Potassium fluoride (0.10 g, 1.7 mmol) was dissolved in the methanol (2 mL) and added to the acetonitrile solution. The mixture solution was stirred at room temperature for 3h. The solution was poured in to saturated aqueous KPF_6 solution. The red precipitate was collected on Celite, washed with H_2O (2×3 mL), EtOH (2 mL) and Et_2O (4 mL) and redissolved in CH_3CN . Removal of solvent gave the product as a red solid (71 mg, 68 μ mol, 99%). 1H NMR (400 MHz, CD_3CN) δ 9.05 (s, 2H, H^{B3}), 9.01 (s, 2H, $H^{B3'}$), 8.97 (d, $J = 5.4$ Hz, 2H, H^{C2}), 8.69 – 8.61 (m, 4H, $H^{A3+A3'}$), 8.22 (d, $J = 7.9$ Hz, 2H, $H^{C3'}$), 8.13 (d, $J = 5.0$ Hz, 2H, H^{C3}), 8.01 – 7.91 (m, 4H, $H^{A4+A4'}$), 7.88 (d, $J = 7.9$ Hz, 2H, $H^{C2'}$), 7.47 – 7.38 (m, 4H, $H^{A6+A6'}$), 7.24 – 7.14 (m, 4H, $H^{A5+A5'}$), 3.66 (s, 1H, $H^{C=C}$). ^{13}C NMR (151 MHz, CD_3CN) δ 159.04 ($C^{A2/A2'}$), 158.92 ($C^{A2/A2'}$), 156.82 ($C^{B2/B2'}$), 156.41 ($C^{B2/B2'}$), 153.50 ($C^{A6/A6'}$), 153.47 ($C^{A6/A6'}$), 152.12 (C^{C2}), 148.36 ($C^{C4'}$), 146.32 (C^{C4}), 145.05 (C^{B4}), 139.17 ($C^{A4+A4'}$), 138.10 ($C^{B4'}$), 134.13 ($C^{C2'}$), 128.95 94 ($C^{C3'}$), 128.63 ($C^{A3/A3'}$), 128.51 ($C^{CA3/A3'}$), 125.67 ($C^{A5/A5'}$), 125.63 ($C^{A5/A5'}$), 122.88 (C^{C3}), 122.78 (C^{B3}), 122.64 ($C^{B3'}$), 83.52 ($C^{C=C}$), 81.41 ($C^{C=C}$), ($C1'$ peak missing). LR-ESI-MS (in CH_3CN): m/z 890.06 [$M - PF_6$] $^+$ requires 890.12; m/z 372.69 [$M - 2PF_6$] $^{2+}$ requires 372.58.

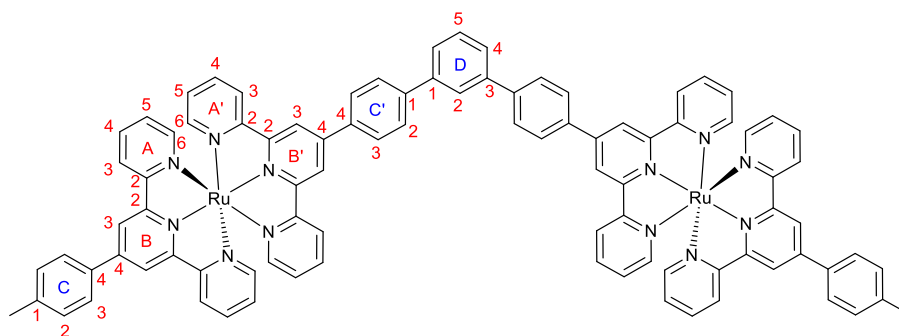
3.9.7. $[Ru(\mathbf{6b})(\mathbf{9})](PF_6)_2$



The $Ru(\mathbf{6a})Cl_3$ (0.30 g, 0.48 mmol) was suspended in ethanol (10mL). 4-methyl phenyl terpyridine (0.16 g, 0.48 mmol) was added to the suspension and the mixture was refluxing for 12h. The saturated aqueous KPF_6 solution was poured into the solution after filtration. The red precipitate was collected on the Celite, followed by washing with H_2O (5 mL), EtOH (2 mL) and ether (5 mL). The red solid was redissolved in the acetonitrile. Removal of the solvent gave the red precipitate $[Ru(\mathbf{6b})(\mathbf{8})](PF_6)_2$ (0.37 g, 0.35 mmol, 72%). 1H NMR (300 MHz, CD_3CN) δ 9.03 (s, 2H), 8.99 (s, 2H), 8.68 – 8.61 (m, 4H), 8.23 – 8.09 (m, 6H), 7.94 (m, 4H), 7.61 – 7.56 (m, 2H), 7.46 – 7.41 (m, 4H), 7.24 – 7.12 (m, 4H), 6.26 (s, 2H), 2.54 (s, 3H).

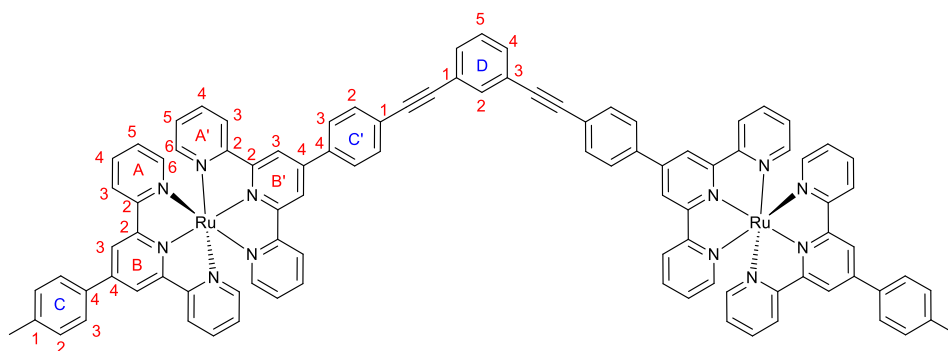
The NMR data agrees with literature.^[57]

3.9.8. [(8)Ru(12)Ru(8)](PF₆)₄



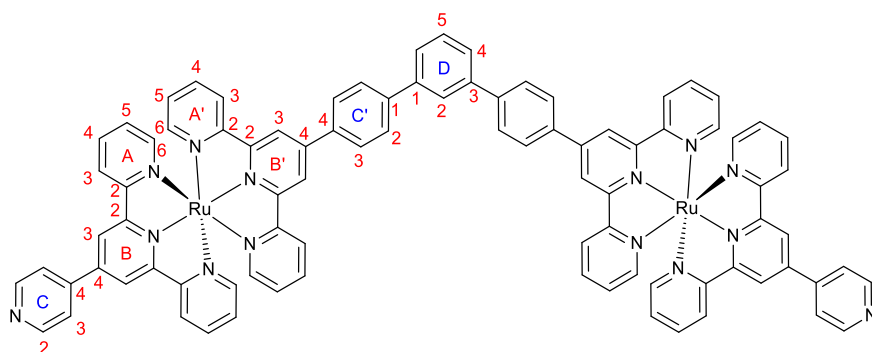
[Ru(**6b**)(**8**)](PF₆)₂ (0.05 g, 47 μmol), Cs₂CO₃ (0.36 g, 1.1 mmol), DMF (5.5 mL), 1,3-dibromobenzene (2.8 mg, 12 μmol) were placed in a dry Schlenk flask. The solution was degassed via argon for 10 min, following which Pd(PPh₃)₄ (3.0 mg, 2.6 μmol) were added. The reaction was stirred under Ar at 80°C for 2 days. The deep red solution was poured into aqueous NH₄PF₆ (10 mL). A red precipitate formed and was collected on Celite, washed with H₂O (2 × 5 mL), EtOH (3 mL), Et₂O (5 mL), and redissolved in CH₃CN. The product was purified by chromatography (SiO₂, CH₃CN: H₂O: saturated aqueous KNO₃ 10: 1: 0.5). Addition of aqueous KPF₆ and removal of CH₃CN gave a red precipitate which was collected on Celite, washed with H₂O (2 × 5 mL), EtOH (3 mL) and Et₂O (5 mL) and redissolved in CH₃CN. Removal of solvent gave the product as a red solid (6.9 mg, 3.2 μmol, 27%). ¹H NMR (300 MHz, CD₃CN) δ 9.11 (s, 4H, H^{B3}), 9.02 (s, 4H, H^{B3'}), 8.73 – 8.63 (m, 8H, H^{A3+A3'}), 8.40 (d, *J* = 8.1 Hz, 4H, H^{C3'}), 8.30 (t, *J* = 1.8 Hz, 1H, H^{D2}), 8.22 (d, *J* = 8.2 Hz, 4H, H^{C2'}), 8.12 (d, *J* = 7.8 Hz, 2H, H^{C3}), 8.03 – 7.90 (m, 3H, H^{A4+A4'+D4}), 7.78 (t, *J* = 7.7 Hz, 1H, H^{D5}), 7.59 (d, *J* = 7.9 Hz, H^{C2}), 7.46 (d, *J* = 5.6 Hz, 8H, H^{A6+A6'}), 7.25 – 7.14 (m, 8H, H^{A5+A5'}), 2.5 (s, 3H, H^{CH3}). LR-ESI-MS (in CH₃CN): *m/z* 916.25 [M - 2PF₆]⁺ requires 916.15; *m/z* 562.48 [M - 3PF₆]³⁺ requires 562.44; *m/z* 385.50 [M - 4PF₆]⁴⁺ requires 385.59. *Anal. Calc.* for C₉₂H₆₆F₂₄N₁₂P₄Ru₂·1H₂O·0.4CH₃CN: C, 50.07; H, 3.63; N, 8.52. Found: C, 49.71; H, 3.63; N, 8.97%. [M - 1PF₆]⁺ missed.

3.9.9. $[(\mathbf{8})Ru(\mathbf{13})(\mathbf{8})](PF_6)_4$



$[Ru(\mathbf{10})(\mathbf{8})](PF_6)_2$ (23 mg, 24 μmol) was dissolved in CH_3CN (10 mL), THF (5 mL) and diisopropylamine (5 mL). After the mixture solution was degassed via argon for 10 min, 1,3-dibromobenzene (2.8 mg, 12 μmol) (2.8 mg, 5.5 μmol), $Pd(PPh_3)_4$ (2.8 mg, 2.4 μmol) and CuI (0.46 mg, 2.4 μmol) were quickly added under an argon atmosphere. The resulting mixture was stirred at 60°C for 2 days. The mixture was cooled to the room temperature. Saturated KPF_6 aqueous solution was poured into the slurry. The precipitate was collected on Celite, following by washing with H_2O (5 mL), EtOH (2 mL) and ether (5 mL). The product was purified by chromatography (SiO_2 , CH_3CN : H_2O : saturated aqueous KNO_3 10: 1: 0.5). A second anion exchange with KPF_6 gave the product as a red solid (6.5 mg, 3 μmol , 25%). 1H NMR (300 MHz, CD_3CN) δ 9.05 (s, 4H, H^{B^3}), 9.01 (s, 4H, $H^{B^{3'}}$), 8.66 (m, 8H, $H^{A^3+A^{3'}}$), 8.29 (d, $J = 8.5$ Hz, 4H, $H^{C^3'}$), 8.12 (d, $J = 8.2$ Hz, 4H, H^{C^3}), 8.02 – 7.91 (m, 12H, $8H^{A^4+A^{4'}+C^2'}$), 7.90 (s, 1H, H^{D^2}), 7.73 (d, $J = 7.9$ Hz, 2H, H^{D^4}), 7.59 (d, $J = 7.9$ Hz, 4H, H^{C^2}), 7.50 – 7.39 (m, 8H, $H^{A^6+A^{6'}}$), 7.26 – 7.13 (m, 3H, $H^{A^5+A^{5'}}$), 2.5 (s, 3H, H^{CH_3}). LR-ESI-MS (in CH_3CN): m/z 939.67 $[M - 2PF_6]^{2+}$ requires 940.14; m/z 578.25 $[M - 3PF_6]^{3+}$ requires 578.44; m/z 397.75 $[M - 4PF_6]^{4+}$ requires 397.59. *Anal.* Calc. for $C_{96}H_{66}F_{24}N_{12}P_4Ru_2 \cdot 3.5H_2O \cdot 2CH_3CN$: C, 41.91; H, 5.20; N, 9.40. Found: C, 42.38; H, 5.67; N, 9.84%. m/z of $[M - 1PF_6]^+$ over 2000, so missed

3.9.10. [(4)Ru(12)Ru(4)](PF₆)₄

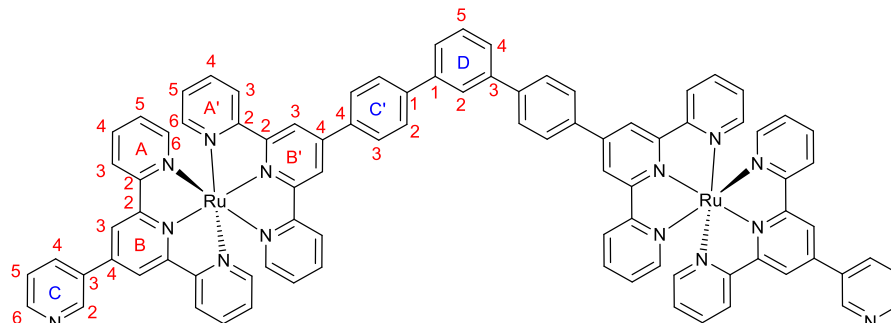


[Ru(6b)(4)](PF₆)₂ (50 mg, 47 μmol), Cs₂CO₃ (0.31 g, 0.95 mmol), DMF (5.0 mL), 1,3-dibromobenzene (2.8 mg, 12 μmol) were placed in a dry Schlenk flask. The solution was degassed via three freeze-pump-thaw cycles, following which Pd(PPh₃)₄ (11 mg, 9.4 μmol) was added. The reaction was stirred under Ar at 80°C for 2 days. The deep red solution was poured into aqueous NH₄PF₆ (10 mL). A red precipitate formed and was collected on Celite, washed with H₂O (2 × 5 mL), EtOH (3 mL), Et₂O (5 mL), and redissolved in CH₃CN. The product was purified by chromatography (SiO₂, CH₃CN: H₂O: saturated aqueous KNO₃: TEA 7: 1: 0.5: 0.01%). Addition of aqueous NH₄PF₆ and removal of CH₃CN gave a red precipitate which was collected on Celite, washed with H₂O (2 × 5 mL), EtOH (3 mL), and Et₂O (5 mL) and redissolved in CH₃CN. Removal of solvent gave the product as a red solid (8.2 mg, 4.6 μmol, 38%).

¹H NMR (400 MHz, CD₃CN) δ 9.12 (s, 4H, H^{B3}), 9.07 (s, 4H, H^{B3'}), 8.97 (d, *J* = 5.0 Hz, 4H, H^{C2}), 8.75 – 8.65 (m, 8H, H^{A3+A3'}), 8.41 (d, *J* = 8.0 Hz, 4H, H^{C3'}), 8.31 (s, 1H, H^{D2}), 8.23 (d, *J* = 7.9 Hz, 4H, H^{C2'}), 8.15 (d, *J* = 5.5 Hz, 4H, H^{C3}), 8.03 – 7.93 (m, 10H, 8H^{A4+A4'}+2H^{D4'}), 7.78 (t, *J* = 7.6 Hz, 1H, H^{D5}), 7.53 – 7.40 (m, 8H, H^{A6+A6'}), 7.27 – 7.16 (m, 8H, H^{A5+A5'}). ¹³C NMR (151 MHz, CD₃CN) δ 159.15 (C^{A2/A2'}), 158.98 (C^{A2/A2'}), 156.86 (C^{B2/B2'}), 156.36 (C^{B2/B2'}), 153.53 (C^{A6/A6'}), 153.42 (C^{A6/A6'}), 152.12 (C^{C2}), 149.38 (C^{C4'}), 146.29 (C^{B4}), 145.07 (C^{C4}), 143.20 (C^{B4'}), 142.16 (C^{D1}), 139.14 (C^{A4+A4'}), 138.64 (C^{C1}), 131.34 (C^{D5}), 128.63 (C^{C3'/C2'}), 128.47 (C^{C3'/C2'}), 128.13 (C^{A5+A5'}), 127.67 (C^{D4}), 127.30 (C^{D2}), 125.70 (C^{A3/A3'}), 125.66 (C^{A3/A3'}), 122.98 (C^{C3}), 122.89 (C^{B3}), 122.81 (C^{B3'}). LR-ESI-MS (in CH₃CN): *m/z* 1951.40 [M - PF₆]⁺ requires 1951.22; *m/z* 903.26 [M - 2PF₆]²⁺ requires 903.13; *m/z* 553.84 [M -

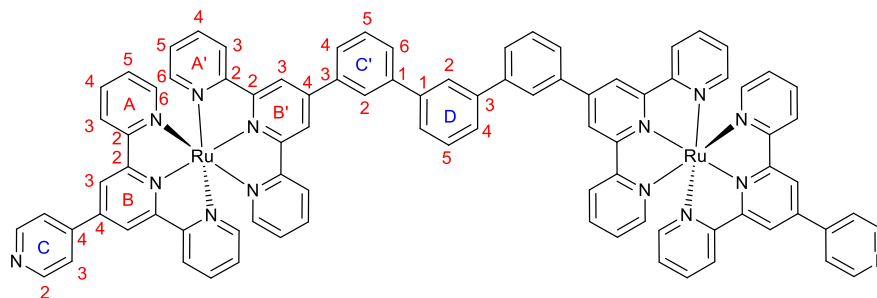
$3\text{PF}_6\text{]}^{3+}$ requires 553.76; m/z 379.20 $[\text{M} - 4\text{PF}_6\text{]}^{4+}$ requires 379.08. *Anal.* Calc. for $\text{C}_{88}\text{H}_{60}\text{F}_{24}\text{N}_{14}\text{P}_4\text{Ru}_2 \cdot 2.3\text{H}_2\text{O} \cdot 0.7\text{CH}_3\text{CN}$: C, 45.65; H, 3.47; N, 9.47. Found: C, 45.24; H, 3.12; N, 9.49%.

3.9.11. $[(\mathbf{3})\text{Ru}(\mathbf{12})\text{Ru}(\mathbf{3})](\text{PF}_6)_4$



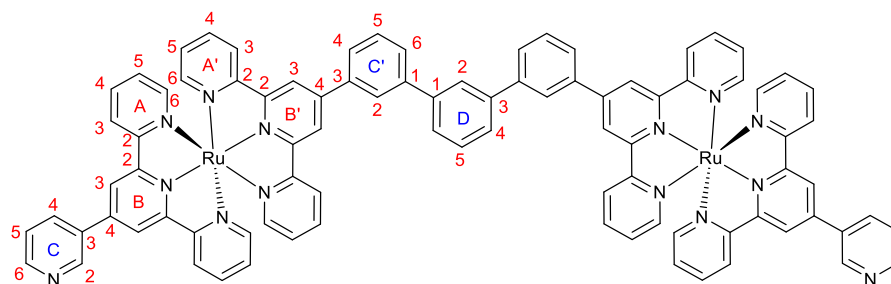
The preparation of cross-coupling reaction of $[\text{Ru}(\mathbf{6b})(\mathbf{3})](\text{PF}_6)_2$ with 1,3-dibromobenzene was as for this ruthenium complexes, starting with $[\text{Ru}(\mathbf{6b})(\mathbf{3})](\text{PF}_6)_2$ (50 mg, 47 μmol) and 1,3-dibromobenzene (2.8 mg, 12 μmol). The product was isolated as a red solid (9.7 mg, 5.4 μmol , 45%). ^1H NMR (400 MHz, CD_3CN) δ 9.41 (d, $J = 2.4$ Hz, 2H, $\text{H}^{\text{C}2}$), 9.13 (s, 4H, $\text{H}^{\text{B}3}$), 9.07 (s, 4H, $\text{H}^{\text{B}3'}$), 8.86 (d, $J = 4.8$ Hz, 2H, $\text{H}^{\text{C}6}$), 8.76 – 8.64 (m, 8H, $\text{H}^{\text{A}3+\text{A}3'}$), 8.56 (dt, $J = 8.0, 2.0$ Hz, 2H, $\text{H}^{\text{C}4}$), 8.41 (d, $J = 8.0$ Hz, 4H, $\text{H}^{\text{C}3'}$), 8.31 (s, 1H, $\text{H}^{\text{D}2}$), 8.22 (d, $J = 8.3$ Hz, 4H, $\text{H}^{\text{C}2'}$), 8.03 – 7.93 (m, 10H, $8\text{H}^{\text{A}4+\text{A}4'} + 2\text{H}^{\text{D}4}$), 7.82 – 7.72 (m, 3H, $2\text{H}^{\text{C}5} + 1\text{H}^{\text{D}5}$), 7.52 – 7.42 (m, 8H, $\text{H}^{\text{A}6+\text{A}6'}$), 7.26 – 7.18 (m, 8H, $\text{H}^{\text{A}5+\text{A}5'}$). ^{13}C NMR (151 MHz, CD_3CN) δ 159.20 ($\text{C}^{\text{A}2/\text{A}2'}$), 159.09 ($\text{C}^{\text{A}2/\text{A}2'}$), 156.70 ($\text{C}^{\text{B}2/\text{B}2'}$), 156.46 ($\text{C}^{\text{B}2/\text{B}2'}$), 153.51 ($\text{C}^{\text{A}6/\text{A}6'}$), 153.46 ($\text{C}^{\text{A}6/\text{A}6'}$), 152.17 ($\text{C}^{\text{C}6}$), 149.70 ($\text{C}^{\text{C}2}$), 148.79 ($\text{C}^{\text{C}4'}$), 146.30 ($\text{C}^{\text{B}4}$), 143.61 ($\text{C}^{\text{B}4'}$), 141.62 ($\text{C}^{\text{D}1}$), 139.16 ($\text{C}^{\text{A}4/\text{A}4'}$), 139.13 ($\text{C}^{\text{A}4/\text{A}4'}$), 137.01 ($\text{C}^{\text{C}1}$), 136.24 ($\text{C}^{\text{C}4}$), 130.99 ($\text{C}^{\text{D}5}$), 129.42 ($\text{C}^{\text{C}3'/\text{C}2'}$), 129.36 ($\text{C}^{\text{C}3'/\text{C}2'}$), 128.59 ($\text{C}^{\text{A}5/\text{A}5'}$), 128.51 ($\text{C}^{\text{A}5/\text{A}5'}$), 126.91 ($\text{C}^{\text{D}4}$), 125.64 ($\text{C}^{\text{A}3/\text{A}3'}$), 125.63 ($\text{C}^{\text{A}3/\text{A}3'}$), 125.34 ($\text{C}^{\text{D}2}$), 122.83 ($\text{C}^{\text{B}3}$), 122.54 ($\text{C}^{\text{B}3'}$). LR-ESI-MS (in CH_3CN): m/z 1951.28 $[\text{M} - \text{PF}_6]^+$ requires 1951.22; m/z 903.25 $[\text{M} - 2\text{PF}_6]^{2+}$ requires 903.13; m/z 553.58 $[\text{M} - 3\text{PF}_6]^{3+}$ requires 553.76; m/z 379.25 $[\text{M} - 4\text{PF}_6]^{4+}$ requires 379.08. *Anal.* Calc. for $\text{C}_{88}\text{H}_{60}\text{F}_{24}\text{N}_{14}\text{P}_4\text{Ru}_2 \cdot 0.5\text{H}_2\text{O}$: C, 47.58; H, 3.36; N, 8.83. Found: C, 47.47; H, 3.24; N, 8.97%.

3.9.12. [(4)Ru(11)Ru(4)](PF₆)₄



The preparation of cross-coupling reaction of [Ru(**5b**)(**4**)](PF₆)₂ with 1,3-dibromobenzene was as for this ruthenium complexes, starting with [Ru(**5b**)(**4**)](PF₆)₂ (50 mg, 47 μmol) and 1,3-dibromobenzene (2.8 mg, 12 μmol). The product was isolated as a red solid (8.7 mg, 4.8 μmol, 40%). ¹H NMR (400 MHz, CD₃CN) δ 9.15 (s, 4H, H^{B3}), 9.06 (s, 4H, H^{B3'}), 8.97 (d, *J* = 5.0 Hz, 4H, H^{C2}), 8.75 – 8.63 (m, 8H, H^{A3+A3'}), 8.63 (s, 2H, H^{C2'}), 8.41 (s, 1H, H^{D2}), 8.26 (d, *J* = 2.8 Hz, 2H, H^{C4'}), 8.16 – 8.12 (m, 6H, 4H^{C3}+2H^{D4}), 8.05 (dd, *J* = 7.7, 1.8 Hz, 2H, H^{C6'}), 8.00 – 7.88 (m, 10H, 8H^{A4+A4'}+2H^{C5'}), 7.82 (t, *J* = 7.7 Hz, 1H, H^{D5}), 7.50 – 7.39 (m, 8H, H^{A6+A6'}), 7.23 – 7.12 (m, 8H, H^{A5+A5'}). ¹³C NMR (151 MHz, CD₃CN) δ 159.15(C^{A2/A2'}), 158.99 (C^{A2/A2'}), 156.88(C^{B2/B2'}), 156.37 (C^{B2/B2'}), 153.54 (C^{A6/A6'}), 153.45 (C^{A6/A6'}), 152.11 (C^{C2}), 148.93 (C^{C3'}), 146.26 (C^{B4}), 145.09 (C^{C4}), 143.64 (C^{D1}), 141.61(C^{B4'}), 139.17 (C^{A4+A4'}), 136.99 (C^{C1'}), 130.98 (C^{C6'}), 129.42 (C^{A5/A5'}), 129.37 (C^{A5/A5'}), 128.66 (C^{D4/C4'}), 128.50 (C^{D4/C4'}), 128.09 (C^{C2'}), 126.93 (C^{D2}), 125.71 (C^{A3/A3'}), 125.64 (C^{A3/A3'}), 122.91 (C^{B3'}), 122.79 (C^{C3}), 122.56 (C^{B3}). LR-ESI-MS (in CH₃CN): *m/z* 1951.24 [M - PF₆]⁺ requires 1951.22; *m/z* 903.33 [M - 2PF₆]²⁺ requires 903.13; *m/z* 554.25 [M - 3PF₆]³⁺ requires 553.76; *m/z* 379.25 [M - 4PF₆]⁴⁺ requires 379.08. *Anal. Calc.* for C₈₈H₆₀F₂₄N₁₄P₄Ru₂·0.2H₂O·0.4CH₃CN: C, 49.12; H, 3.32; N, 8.23. Found: C, 49.17; H, 3.02; N, 8.59%.

3.9.13. [(3)Ru(11)Ru(3)](PF₆)₄



The preparation of cross-coupling reaction of [Ru(5b)(3)](PF₆)₂ with 1,3-dibromobenzene was as for this ruthenium complexes, starting with [Ru(5b)(4)](PF₆)₂ (50 mg, 47 μmol) and 1,3-dibromobenzene (2.8 mg, 12 μmol). The product was isolated as a red solid (9.5 mg, 5.3 μmol, 44%). ¹H NMR (400 MHz, CD₃CN) δ 9.43 (dd, *J* = 2.5, 0.9 Hz, 2H, H^{C2}), 9.19 (s, 4H, H^{B3}), 9.08 (s, 4H, H^{B3'}), 8.89 (dd, *J* = 4.8, 1.6 Hz, 2H, H^{C6}), 8.77 – 8.65 (m, 10H, 8H^{A3+A3'}+2H^{C2'}). 8.58 (ddd, *J* = 8.0, 2.5, 1.6 Hz, 2H, H^{C4}), 8.45 (t, *J* = 1.8 Hz, 1H, H^{D2}), 8.30 (ddd, *J* = 7.8, 2.0, 1.0 Hz, 1H), 8.17 (ddd, *J* = 7.8, 1.8, 1.0 Hz, 1H), 8.07 (dd, *J* = 7.8, 1.8 Hz, 1H), 8.02 – 7.91 (m, 10H, 8H^{A4+A4'}+2H^{D4}), 7.85 (t, *J* = 7.7 Hz, 1H, H^{D5}), 7.77 (ddd, *J* = 8.0, 4.8, 0.9 Hz, 2H, H^{C5}), 7.55 – 7.43 (m, 8H, ^{A6+A6'}), 7.27 – 7.15 (m, 8H, H^{A5+A5'}). ¹³C NMR (151 MHz, CD₃CN) δ 159.20(C^{A2/A2'}), 159.07(C^{A2/A2'}), 156.68 (C^{B2/B2'}), 156.44 (C^{B2/B2'}), 153.48 (C^{A6/A6'}), 153.43 (C^{A6/A6'}), 152.19 (C^{C6}), 149.72 (C^{C2}), 149.26 (C^{C3'}), 146.33 (C^{B4}), 143.20 (C^{D1}), 142.17 (C^{B4'}), 139.12 (C^{A4/A4'}), 139.06 (C^{A4/A4'}), 138.67 (C^{C1'}), 136.20 (C^{C4}), 133.72 (C^{C3}), 131.33 (C^{C5'}), 130.95 (C^{D5}), 130.26 (C^{C6'}), 128.57 (C^{A5/A5'}), 128.47 (C^{A5/A5'}), 128.13 (C^{D4+C4'}), 127.68 (C^{C2'}), 127.31(C^{D2}), 125.63 (C^{A3+A3'}), 125.30 (C^{C5}), 122.96 (C^{B3}), 122.83 (C^{B3'}). LR-ESI-MS (in CH₃CN): *m/z* 1951.26 [M - PF₆]⁺ requires 1951.22; *m/z* 903.25 [M - 2PF₆]²⁺ requires 903.13; *m/z* 553.92 [M - 3PF₆]³⁺ requires 553.76; *m/z* 379.25 [M - 4PF₆]⁴⁺ requires 379.08. *Anal. Calc.* for C₈₈H₆₀F₂₄N₁₄P₄Ru₂·4H₂O: C, 48.36; H, 3.17; N, 8.97. Found: C, 48.36; H, 3.17; N, 8.97%.

4. Chapter four

The formation of supramolecular assemblies with planar, tetra-functionalised cores

4.1. Introduction

Pyrene or pyrene derivatives have attracted much attention due to their planarity, symmetry and interesting chromophore properties. This π -conjugated system can act as a linker working as a typical fluorescent probe and has been used in many applications due to its photostability and absorption and emission in the UV-visible region.^[80] In order to meet the requirements of these applications, the pyrene can be functionalized at 1-, 3-, 6-, 8- positions.^[81] Some substituents such as trimethylsilylethynyl^[82] or 3-hydroxy-1-propynyl^[82] can expand the conjugated system. Other substituents such as trimethylsilyl group may result in tuning of luminescence properties.^[83]

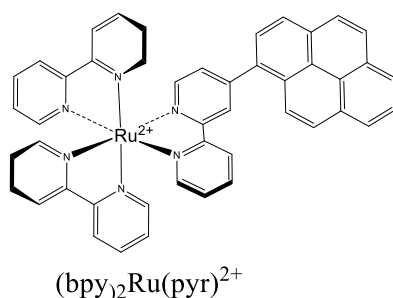


Figure 39 : $(bpy)_2Ru(pyr)^{2+}$ ruthenium complex

$[Ru(bpy)_3]^{2+}$ and $[Ru(bpy)_2(phen)]^{2+}$ (bpy = 2,2'-bipyridine; phen = 1,10-phenanthroline) exhibit red luminescence with excited state lifetimes about 600 ns to 1 μ s.^[84] When pyrene substituted Ru(II) complexes are irradiated, photoinduced electron/energy transfer occurs where by the ruthenium centre is excited from the ground state to the long-lived ³MLCT state via intersystem crossing, promoted by spin-orbital coupling of the heavy ruthenium atom. The appended pyrene allows intramolecular energy transfer from the excited ³MLCT excited state to a pyrene-based ³($\pi - \pi^*$) state of linked pyrene which has a significantly longer excited lifetime than ³MLCT excited state of $[Ru(bpy)_3]^{2+}$.^[85] The excited intraligand triplet state is reported to have a lower energy or equal energy to the ³MLCT state.^[85]

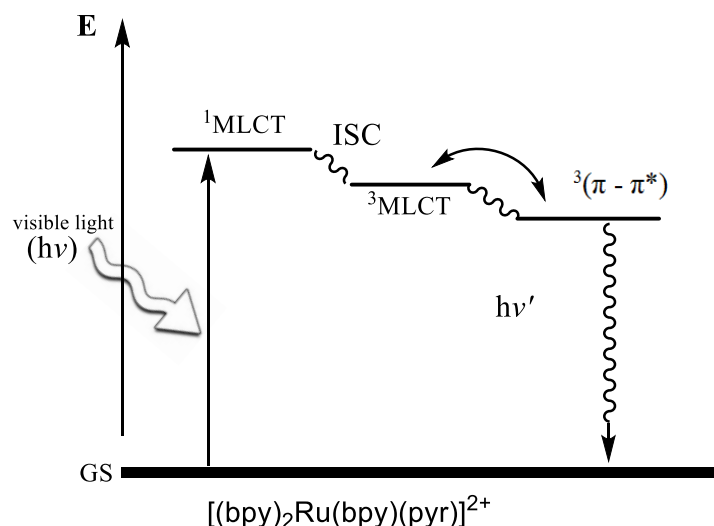


Figure 40 : Diagrams of $[(bpy)_2Ru(bpy)(pyr)]^{2+}$ (MLCT = metal to ligand charge transfer, ISC = intersystem crossing, GS = ground state, bpy = 2,2'-bipyridine, pyr = pyrene)

Tetraphenylethene (**14**) is known as a fluorescent chromophore. This compound has a weak emission in the solid or concentrated solution due to aggregation-induced quenching^[86] but has a strong emission in dilute solution.^[87] However, restriction of intermolecular rotation in some tetraphenylethene derivatives is responsible for the high fluorescence caused by the aggregation-induced emission which is opposite to the aggregation-caused quenching effect.^[88] This phenomenon was observed by Tang and co-workers one decade ago.^[89] Since then, tetraphenylethene derivatives have attracted much interest and applied in sensor work,^[87, 90] such as derivative **15** which acts as a fluorescent probe.^[90a]

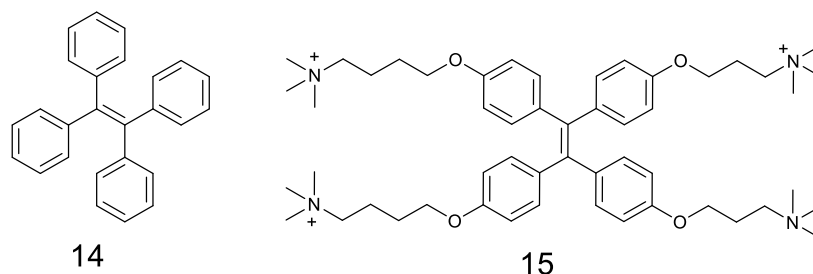


Figure 41 : Tetraphenylethene and an example of tetraphenylethene derivative as a fluorescent probe

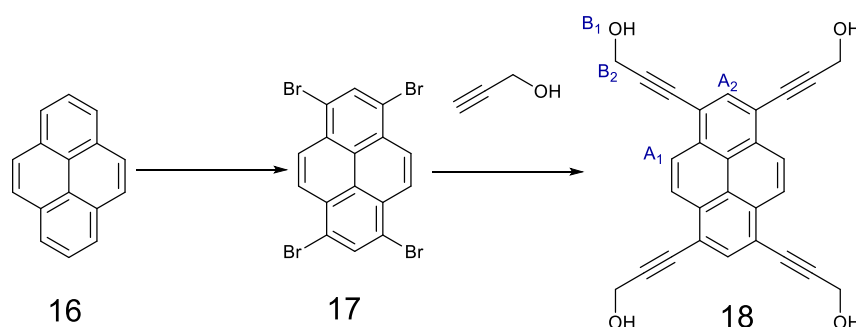
In this chapter, our endeavour was to design a conjugated, planar core with appended metal ion binding groups such that the unit can act as a molecular ‘panel’ for self-assembly of molecular cage structures. The $[\text{Ru}(\text{tpy})_2]^{2+}$ complexes have been discussed in Chapter 1 which have weak luminescence due to the effective energy transfer from the excited $^3\text{MLCT}$ to the ^3MC state. Introduction of the pyrene or tetraphenylethene unit aims to allow transfer of energy to the ^3LC state which may act as an energy reservoir to increase the excited state lifetime and improve the luminescent properties of $[\text{Ru}(\text{tpy})_2]^{2+}$ complexes.

Importantly, these types of rigid, planar metalloligands also have potential to act as molecular panels to form self-assembled structures such as molecular cages. In this chapter studies into the formation of large polynuclear assemblies are reported using either pyrene or TPE-based ligands.^[79]

4.2. Synthesis of pyrene derivatives

4.2.1. Synthesis and hydrogenation of pyrene derivatives

1,3,6,8-Tetrabromopyrene was prepared following the previously reported procedure.^[91] This product has poor solubility in common organic solvents and was used in subsequent reactions after being triturated with chloroform, filtered and washed with H_2O .



Scheme 4 : bromolyation of pyrene and Sonogashira cross coupling reaction of tetrabromopyrene with propargyl alcohol

1,3,6,8-Tetrakis(3-hydroxy-1-propynyl)pyrene was prepared following a reported procedure.^[81b] Tetrabromopyrene was reacted under standard conditions for Sonogashira coupling reaction to attach propargyl alcohol (THF, 5% $\text{Pd}(\text{PPh}_3)_4$, 5% CuI , diisopropylamine, an argon atmosphere, and 70°C for 42

h). The product was isolated by triturating with CHCl_3 and filtration. ^1H NMR spectroscopy confirmed the identity of the product (Figure 42), in agreement with literature.^[81b]

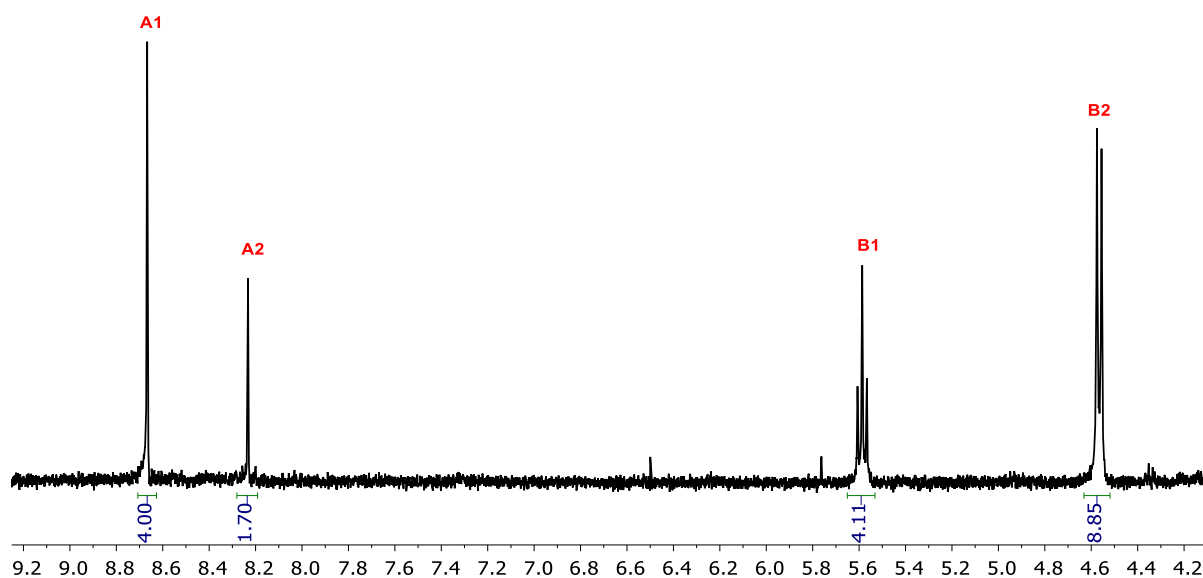
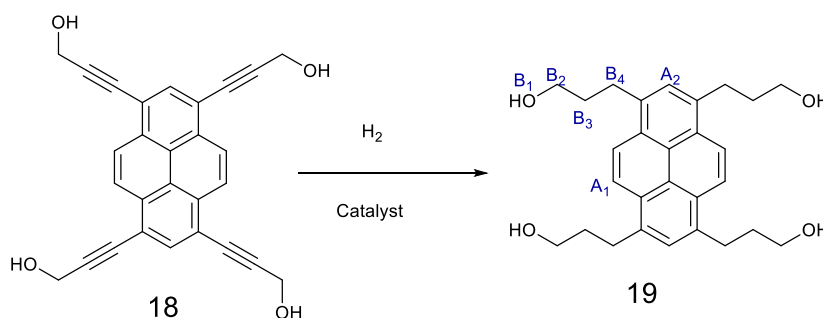


Figure 42 : ^1H NMR (DMSO- d_6 , 300MHz) spectrum of 1,3,6,8-tetrakis(3-hydroxy-1-propynyl)pyrene



Scheme 5 : Hydrogenation of 1,3,6,8-Tetrakis(3-hydroxy-1-propynyl)pyrene

Hydrogenation of this compound should give the more flexible alkyl chain and OH functionalized groups may have potential uses. The hydrogenation of 1,3,6,8-tetrakis(3-hydroxy-1-propynyl)pyrene was attempted using Pd/C as a catalyst in THF under a H_2 atmosphere for 42 hr at room temperature. After removal of the catalyst by filtration, solvent was removed to give a pale yellow solid. Analysis by ^1H NMR spectroscopy (Figure 43) showed the formation of new unidentified peaks but also a substantial proportion of starting material remained. However, when the reaction was catalysed by PtO_2 , a light

yellow powder was obtained which displayed a ^1H NMR spectrum with significant differences to the starting material. The singlet signals corresponding to protons of the pyrene core were shifted significantly upfield from 8.66 ppm to 8.26 ppm; 8.22 ppm to 7.77 ppm). New peaks also appeared at 4.35(t) ppm and 3.54 (m) ppm which were assigned as the alcohol and protons in the alkyl chain. Other new signals in the aromatic region were not assigned. Possibly, the hydrogenation catalysed by PtO_2 could also hydrogenate the pyrene core (Figure 43).

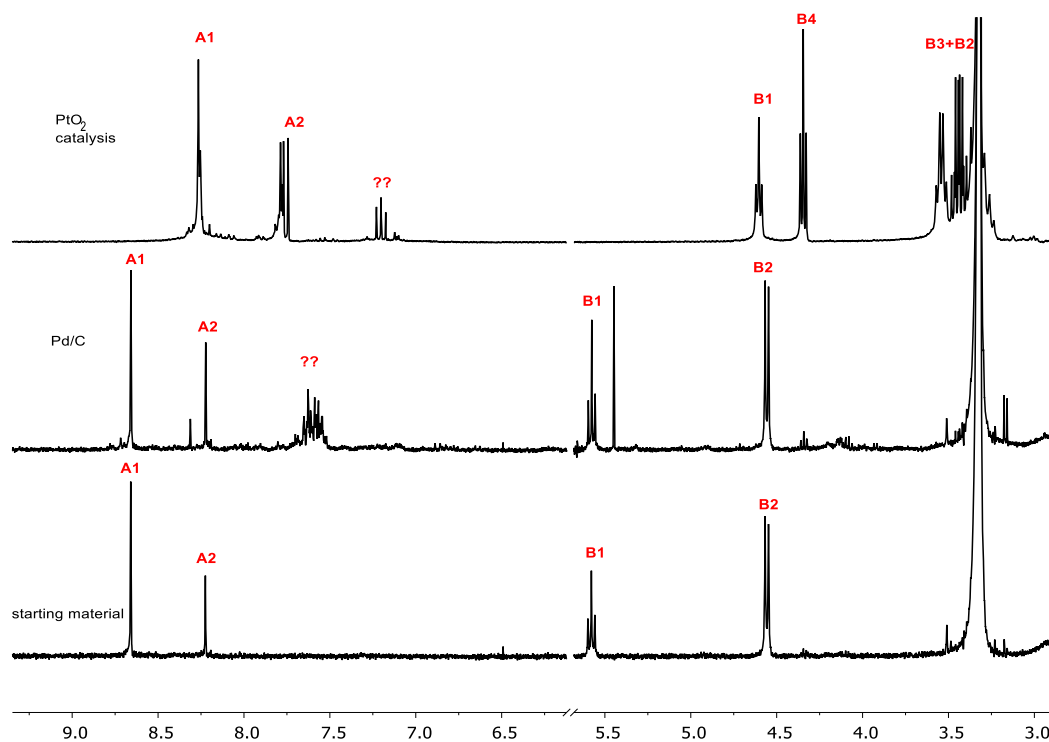
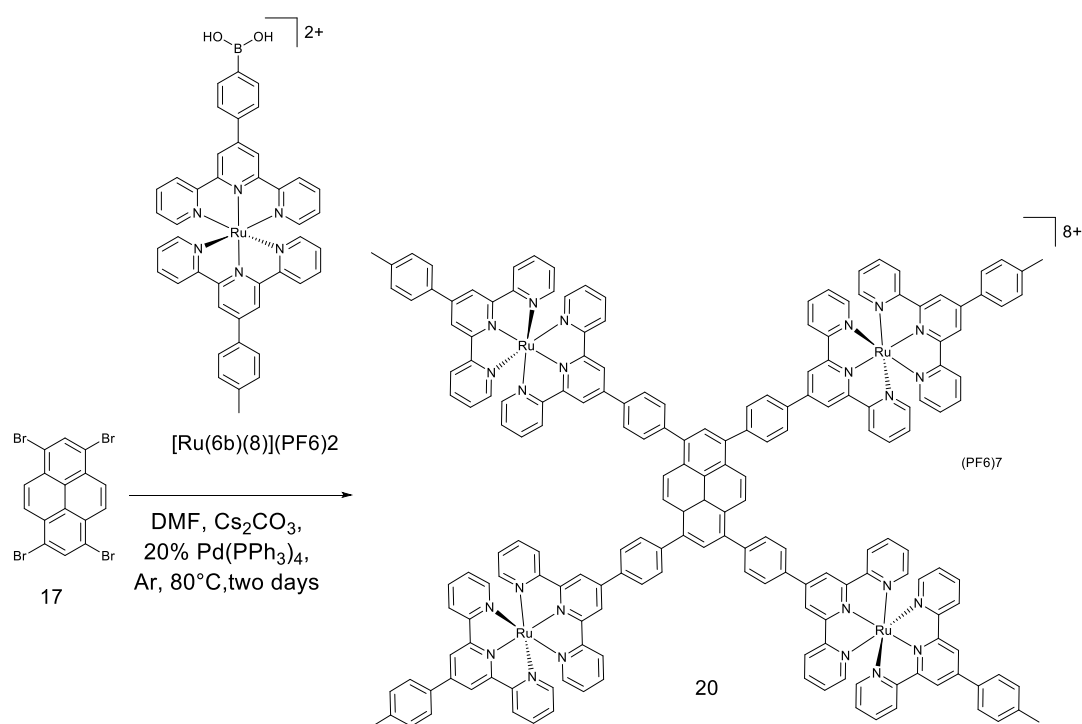


Figure 43 : ^1H NMR (DMSO- d_6 , 300MHz) Comparison of starting materials, hydrogenation catalyzed by Pd/C and by PtO_2

4.2.2. Suzuki or Sonogashiracross coupling reactions between tetrabromopyrene or tetraborylpyrene and functionalized ruthenium(II) complexes

The first attempt to synthesize the tetranuclear complex was based on Suzuki cross coupling reaction between 1,3,6,8-tetrabromopyrene and $[\text{Ru}(\mathbf{6b})(\mathbf{8})(\text{PF}_6)_2]$. This ruthenium(II) complex was shown to be readily coupled to aryl bromides to give dinuclear complexes (see Chapter 3) and therefore the optimised reaction conditions were also used for the coupling to tetrabromopyrene. The conditions of the Suzuki coupling reaction were tetrabromopyrene (1 eq.), $[\text{Ru}(\mathbf{6b})(\mathbf{8})(\text{PF}_6)_2]$ (6 eq.), DMF, Cs_2CO_3 (10 eq.), 20%

$\text{Pd}(\text{PPh}_3)_4$, under an argon atmosphere at 80°C for two days. After the anion exchange with PF_6^- , the crude product was dissolved in acetonitrile. The eluent of $\text{CH}_3\text{CN}:\text{KNO}_3:\text{H}_2\text{O}$ (5: 1: 1) was used for TLC analysis using mononuclear and dinuclear complexes from Chapter 2 as references. Five separate products were apparent under the UV including two complexes which were more polar than the dinuclear complexes. We propose these two species are the tri- and tetra-substituted pyrene products. However, the ESI-MS analysis did not show the expected (highly charged) ions, and lower charge ions would have mass/charge outside of the standard range (e.g. $[\mathbf{20}(\text{PF}_6)_7]^+ = 4136 \text{ m/z}$).



Scheme 6 : Attempted Suzuki cross coupling of tetrabromopyrene with $[\text{Ru}(\mathbf{6b})(\mathbf{8})](\text{PF}_6)_2$.

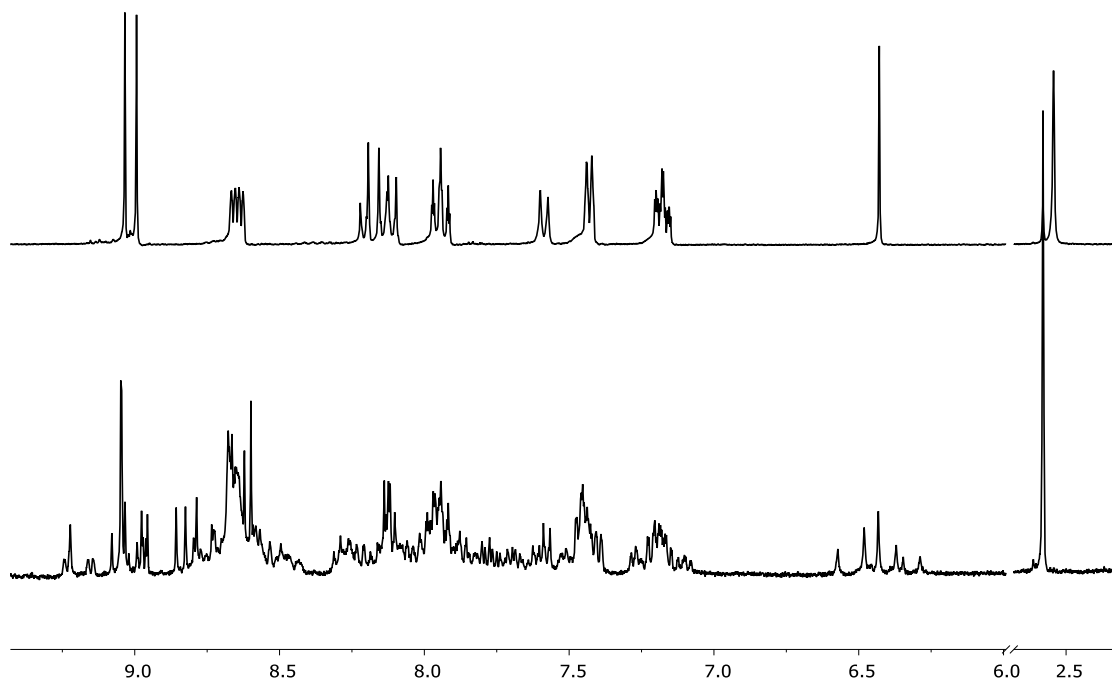
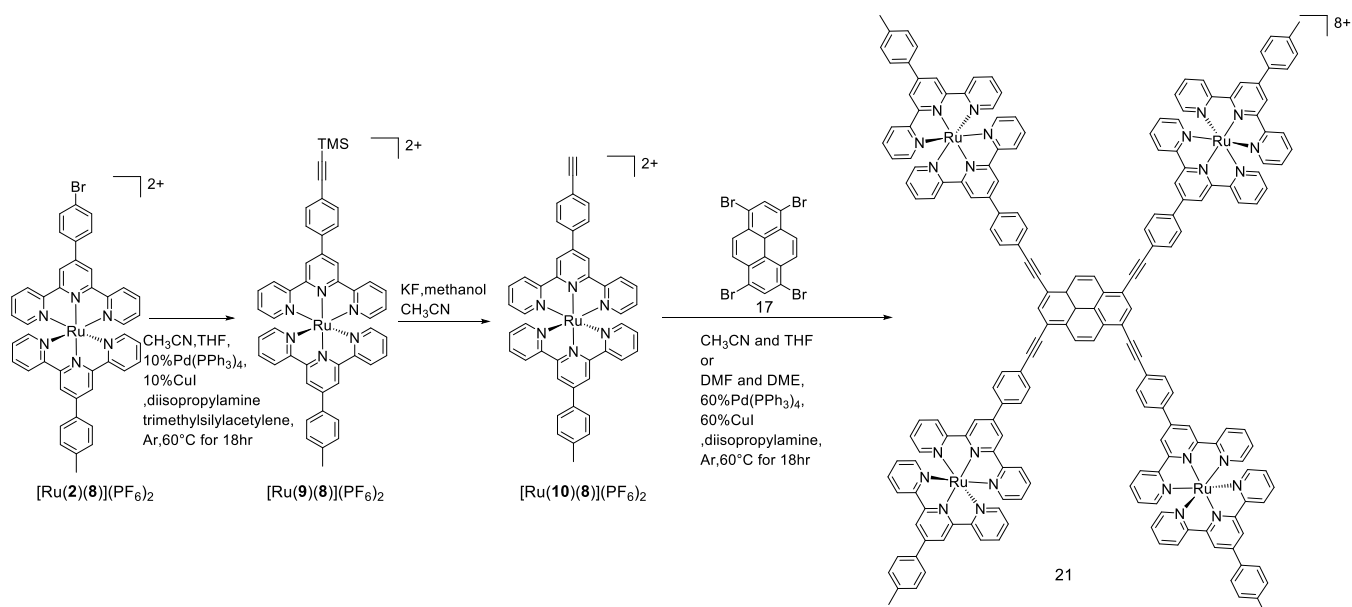


Figure 44 : ^1H NMR recorded spectra on 300MHz in CD_3CN , top, $[\text{Ru}(\mathbf{6b})(\mathbf{8})](\text{PF}_6)_2$; bottom, crude product of Suzuki cross coupling reaction between 1,3,6,8-tetrabromopyrene and $[\text{Ru}(\mathbf{6b})(\mathbf{8})](\text{PF}_6)_2$



Scheme 7 : Sonogashira cross coupling of tetrabromopyrene and its alkyne ruthenium(II) complex

As Suzuki coupling had proven difficult, an alternative approach was taken. The acetylene functionalised $[\text{Ru}(\mathbf{10})(\mathbf{8})](\text{PF}_6)_2$ complex was synthesized from the $[\text{Ru}(\mathbf{2})(\mathbf{8})](\text{PF}_6)_2$ over 2 steps. The first step was to synthesize the TMS protected $[\text{Ru}(\mathbf{9})(\mathbf{8})](\text{PF}_6)_2$ via Sonogashira coupling (CH_3CN , THF, 60%Pd(PPh₃)₄, 60%CuI, trimethylsilylacetylene, diisopropylamine, under an argon atmosphere at 60°C for two

days) before deprotection with KF. The deprotected alkyne is not stable for extended periods of time and must be reacted in the following step immediately after deprotection. The reaction conditions of the Sonogashira reactions onto pyrene were tetrabromopyrene (1 eq.), [Ru(**10**)(**8**)](PF₆)₂ (8 eq.), DMF, DME, diisopropylamine, 60% Pd(PPh₃)₄, 40% CuI under an argon atmosphere at 60°C for two days. The workup was exactly the same as for the Suzuki coupling reaction mentioned above. After anion exchange with KPF₆, a black crude product precipitated as sticky lumps. Analysis of the ESI-MS did not show the expected peaks. Analysis by TLC (CH₃CN: KNO₃: H₂O, 5: 1: 1) showed only two nonpolar red spots, assumed to be from the decomposed alkyne-functionalised ruthenium(II) complex.

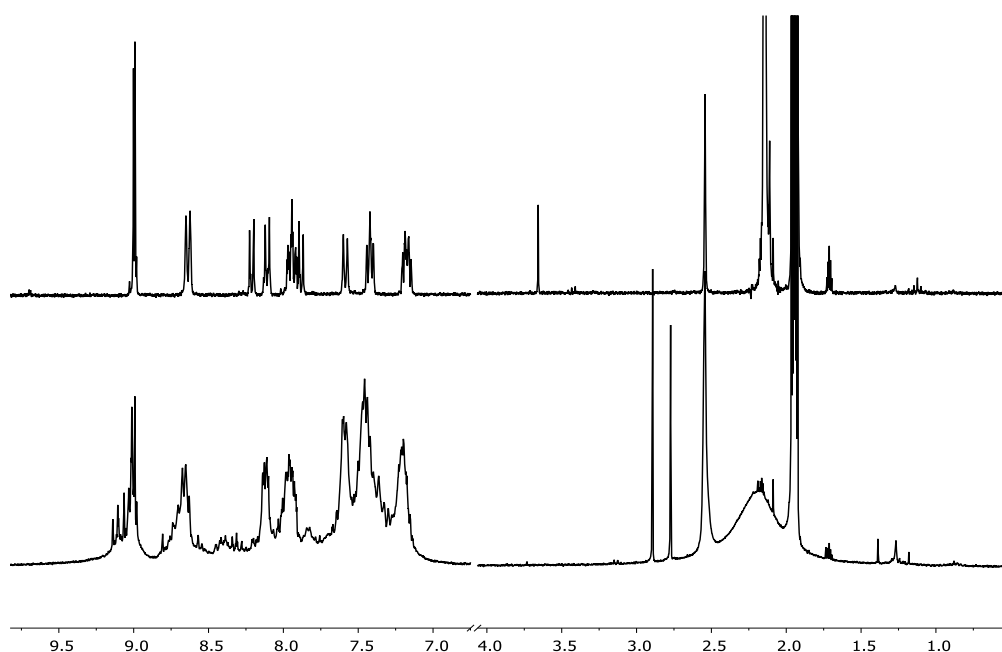
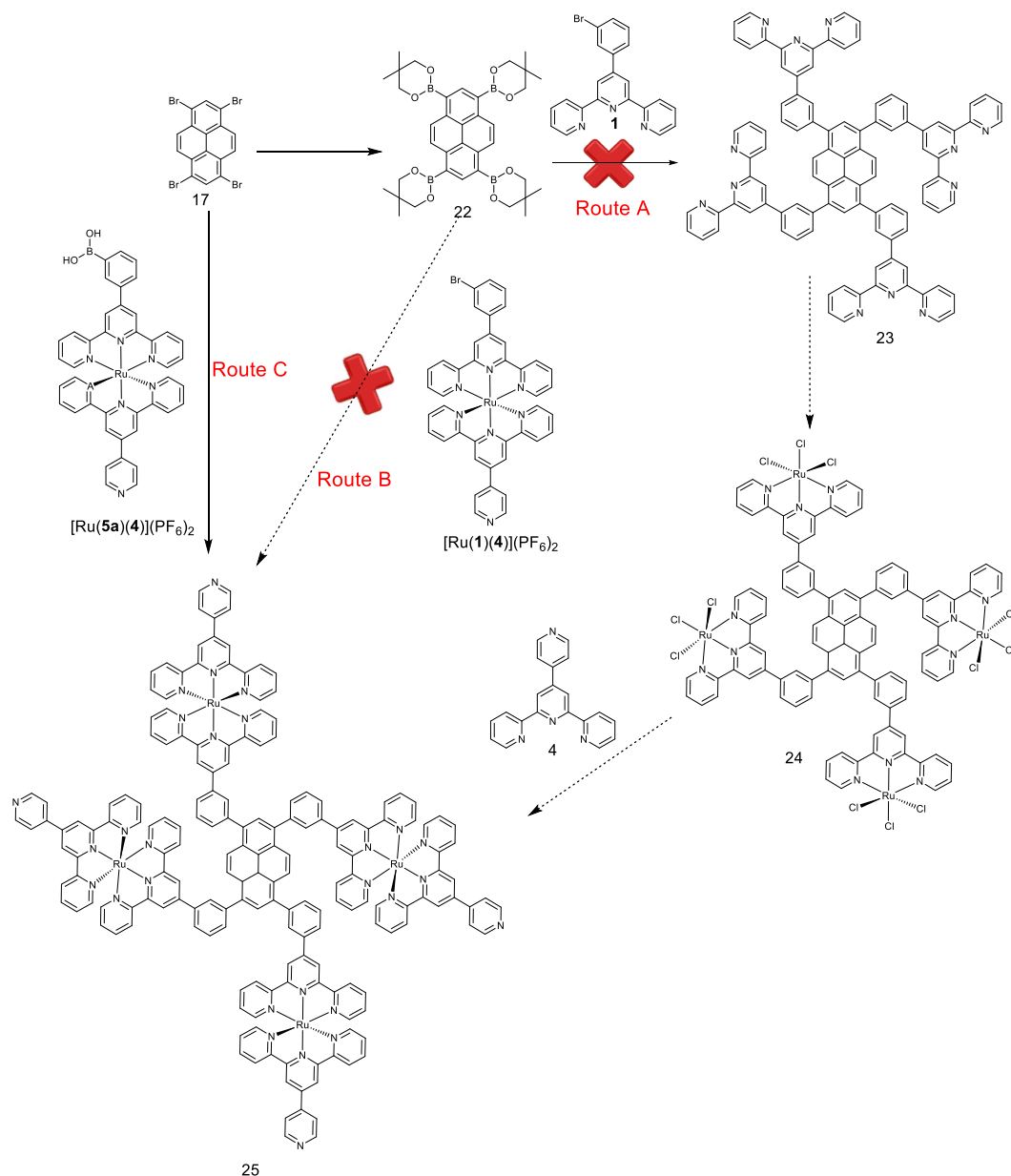


Figure 45 : ¹H NMR recorded spectra on 300MHz in CD₃CN, top, [Ru(**10**)(**8**)](PF₆)₂; bottom, crude product of Sonogashira cross coupling reaction between 1,3,6,8-tetrabromopyrene and [Ru(**10**)(**8**)](PF₆)₂

A potential cause of these poor coupling reactions could be the low solubility of 1,3,6,8-tetrabromopyrene. Borylation of this molecule was used to improve solubility before the Suzuki reaction. Therefore the neopentyl glycolato substituted pyrene (**22**) was prepared using a modification of a procedure of related compounds.^[91] Additionally, the 3-bromophenyl terpyridine derivative (rather than 4-bromophenylterpyridine) could also lead to different solubility.



Scheme 8 : Three attempts of Suzuki coupling reaction to build the pyrene tetramer

The synthesis of a pyrene-(2,2'-bipyridine) conjugates have been reported^[91] using Suzuki coupling between 5,5'-dibromo-2,2'-bipyridine and pinacolato functionalised pyrene. A similar method was attempted here to prepare pyrene-terpyridine derivatives (Scheme 8, Route A). Although ligand **1** has a good solubility in toluene, in the 20% water/toluene mixture which was reported^[91] a viscous slurry was formed. To overcome this, DMF was added (approximately 50% of total volume) in order to make the slurry less viscous before the freeze-pump-thaw cycles. The reaction was set under an argon atmosphere at 80°C with Cs_2CO_3 for 3 days, catalysed by 60% $\text{Pd}(\text{PPh}_3)_4$ per pyrene. The colour changed from bright

yellow-orange to brown. After dilution with DCM, followed by washing with H₂O, the organic layer was dried over Na₂SO₄. The colour changes from brown to bright yellow. Removing the solvent under the vacuum gave orange oil. ESI-MS analysis did not reveal the expected highly charged ions. TLC analysis (toluene: ethyl acetate, 1: 1) indicated all of the tetraborylpyrene was consumed and an intensely fluorescent yellow spot which remained on the baseline.

Table 1 : Attempts to couple functionalised pyrene units with Ru(II) complexes via

Route	Pyrene Starting Material	Ligand 1 , [Ru(5a)(4)](PF ₆) ₂ or [Ru(1)(4)] (PF ₆)	Reaction Conditions	Successful
A	1,3,6,8-tetrabromopyrene	6 eq.	Argon, 80°C, 3 days, DMF, 30% Pd(PPh ₃) ₄ , Cs ₂ CO ₃ ,	NO
A	1,3,6,8-tetrabromopyrene	12 eq.	Argon, 80°C, 3 days, DMF, 60% Pd(PPh ₃) ₄ , Cs ₂ CO ₃ ,	YES
B	1,3,6,8-tetraborylpyrene	12 eq.	Argon, 80°C, 3 days, DMF, 60% Pd(PPh ₃) ₄ , Cs ₂ CO ₃ ,	NO
C	1,3,6,8-tetraborylpyrene	12 eq.	Argon, 80°C, 3 days, DMF/toluene/H ₂ O, 60% Pd(PPh ₃) ₄ , Cs ₂ CO ₃ ,	NO

Our next approach was to perform the coupling reaction directly upon the Ru(II) complex, which would ensure good solubility in polar solvents (Scheme 8, Route B). The Suzuki reaction of [Ru(**1**)(**4**)](PF₆)₂ with tetraborylpyrene in was performed in DMF with Cs₂CO₃, 60% Pd(PPh₃)₄ per pyrene, under an argon atmosphere at 80°C for 3 days. The colour changed from pale red to deep red to brown. After the reaction was finished, the mixture was poured into saturated KPF₆ solution. The precipitate was collected on Celite, and then washed with H₂O, ethanol and ether. The precipitate was redissolved in acetonitrile for ESI-MS. No peak corresponds to the expected ions. Analysis by TLC (CH₃CN: KNO₃: H₂O, 5: 1: 1) showed only two red spots, one of which corresponds to the [Ru(**1**)(**4**)](PF₆)₂ starting material and the other could not be identified.

Having had little success with these routes, another approach was needed. We returned to our first method of coupling tetrabromopyrene with boronic acid functionalised terpyridine, but this time using the 3-boronic acid derivative in place of the 4-boronic acid (Scheme 8, Route C). This Suzuki reaction between

[Ru(**5b**)(**4**)](PF₆)₂ and the insoluble tetrabromopyrene was conducted in DMF with Cs₂CO₃, 60% Pd(PPh₃)₄ per pyrene, under an argon atmosphere at 80°C for 3 days. No colour change was observed. After the reaction was finished, the red slurry was poured into saturated KPF₆ solution. The precipitate was collected on Celite, and then washed with H₂O, ethanol and ether. The precipitate was redissolved in acetonitrile for ESI-MS. Peaks corresponding to the desired complex **25** were observed with sequential loss of PF₆⁻ counter anions: [M-2PF₆]²⁺, [M-3PF₆]³⁺, [M-4PF₆]⁴⁺, [M-5PF₆]⁵⁺, [M-6PF₆]⁶⁺, [M-7PF₆]⁷⁺. The attempt to purify the compound by chromatography (SiO₂, CH₃CN: H₂O: saturated aqueous KNO₃: TEA 5: 1: 1: 0.01) resulted in the most polar red band remaining on the SiO₂ even if the polarity of eluent was increased to CH₃CN: H₂O: saturated aqueous KNO₃: TEA, 1: 1: 1: 0.01. Attempts to recover the red coloured band from the column using polar solvent mixtures were also unsuccessful.

4.2.3. *M₈L₆ cage synthesis via metal-template imine bond formation*

The Nitschke group has reported many examples of self-assembled structures where aryl amines and 2-pyridylcarboxaldehyde are reacted to form pyridyl-imine ligands which form stable complexes with iron(II) salts including FeSO₄,^[10e, 92] Fe(NTf)₂,^[5a, 93] Fe(OTf)₂.^[93-94] Other ions such as Co(SO₄) and Ni(OAc)₂ are also suitable for synthesis of self-assembled cages.^[10e, 94] In one example, **26** (Figure 46) is reacted with 2-pyridylcarboxaldehyde and Fe(II) salts in DMF at 70°C overnight to give M₈L₆ cages where the porphyrin groups act as faces of the cube.^[95] Related metal template structures have been also prepared in DMF, DMSO and CH₃CN.^[5a, 96]

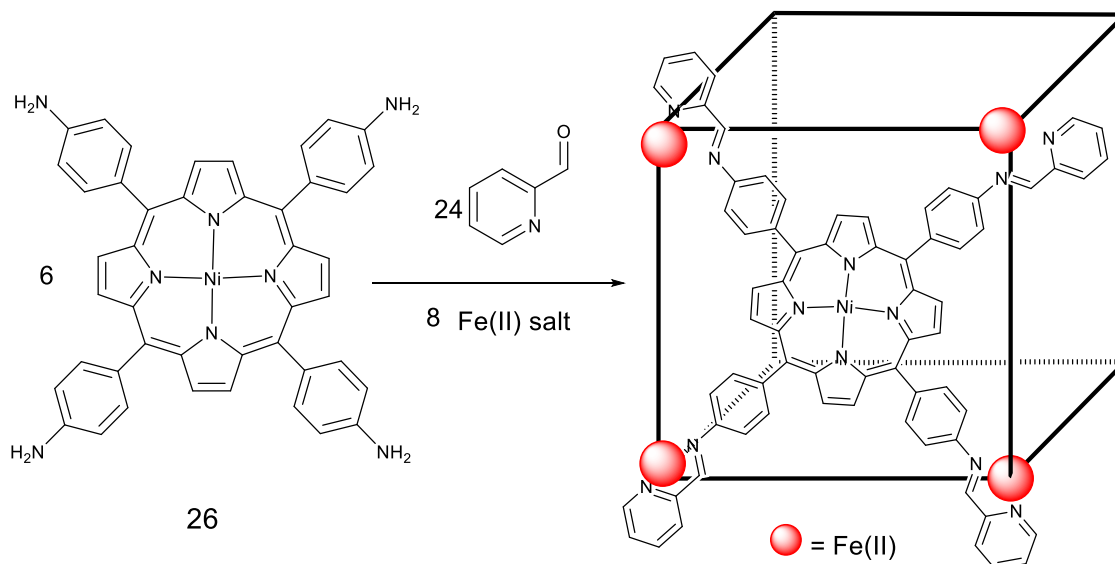


Figure 46 : Self-assembled M_8L_6 cubic cage by Jonathan Nitschke's group^[95]

Following the synthetic difficulties faced with pyrene derivatives, we looked for an alternative planar core to prepare molecular cages. Tetraphenylethene (**14**) has attractive photoproperties and can be readily functionalized to form tetra-substituted ligands. A potential complication is that this molecule possesses two-fold symmetry, compared with the four-fold symmetry of tetraphenylporphyrin derivatives. This could lead to the formation of isomers should a M_8L_6 cage be synthesized.

Following a reported procedure,^[97] the tetraamine functionalized ligand (**27**) was prepared.

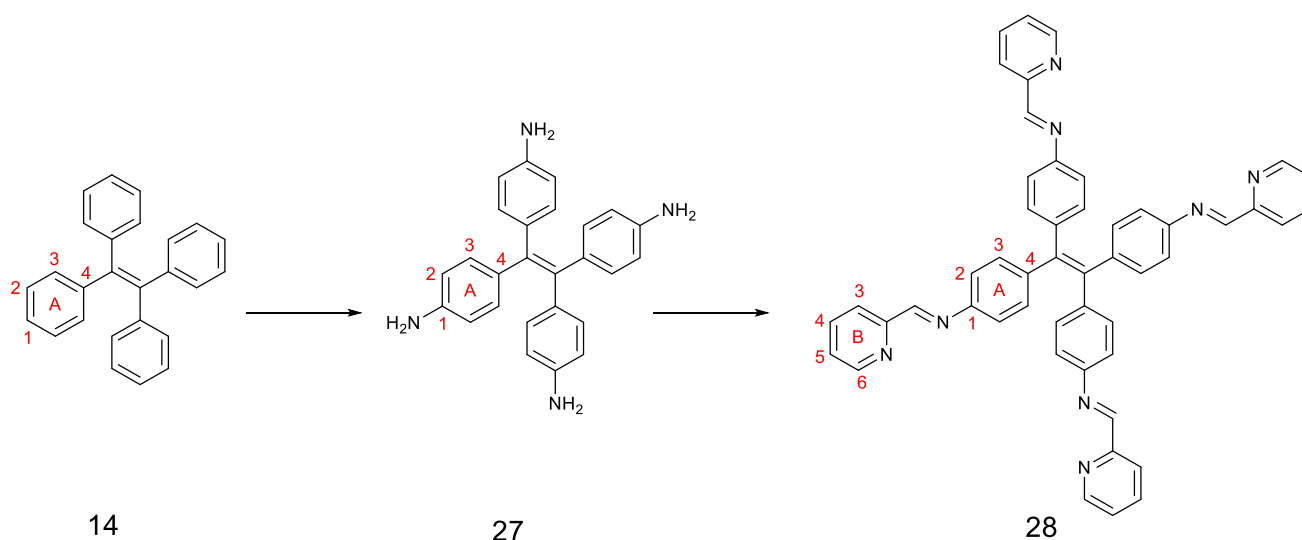


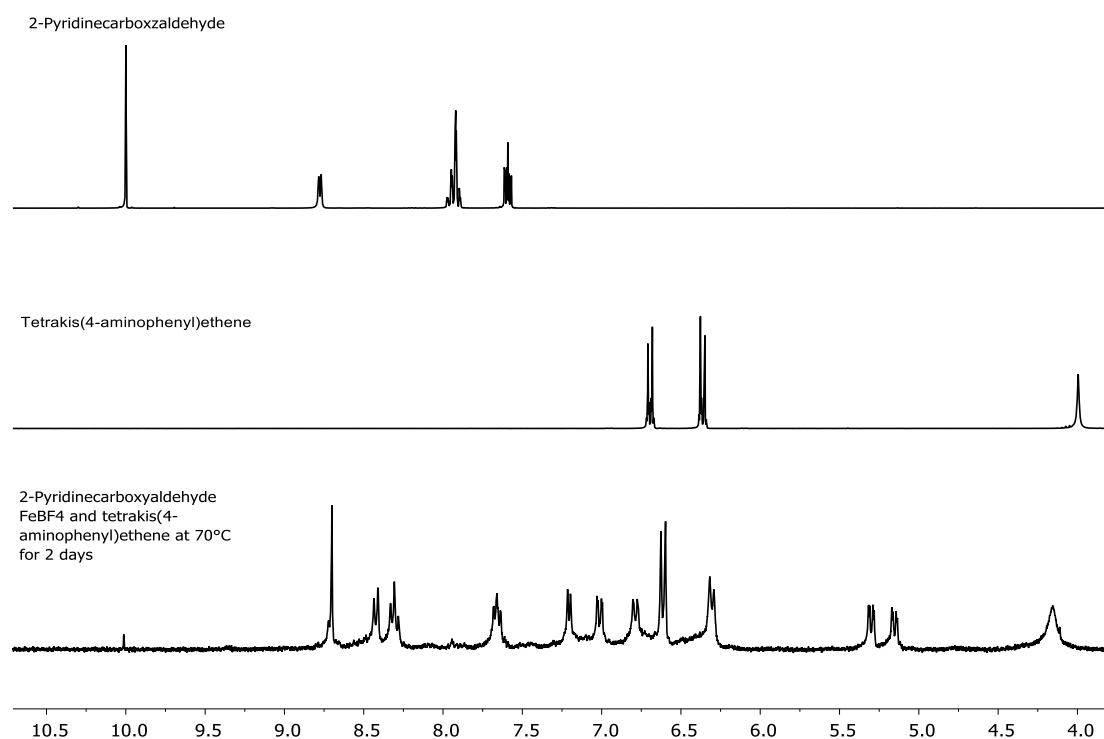
Figure 47 : Left, tetrakis(4-aminophenyl)ethene; Right, TPE imine ligand.

The reaction of **27** with 2-pyridinecarboxaldehyde and Fe(II) salts was examined in detail.

Table 2: Summary of reaction conditions to synthesize the cage

Entry	Tetramine (equiv.)	2-pyridylaldehyde (equiv.)	Fe(BF ₄)·6H ₂ O(equiv.)	T (°C)	Solvent	Time (hr)	Successful?
1	6	24	8	70	DMF	24	No
2	6	24	8	70	DMF	48	YES?
3	6	24	8	25	DMF	48	YES
4	6	24	8	70	DMSO	24	NO
5	6	24	8	70	DMSO	36	NO
6	6	24	8	25	CD ₃ CN	24	NO
7	6	24	8	70	CD ₃ CN	24	NO

The reaction was attempted using conditions reported by Nitschke for the porphyrin-containing cage shown in Figure 46.^[95] Specifically, 6 equivalents of **27**, 24 equivalents of 2-pyridinecarboxaldehyde and 8 equivalents of Fe(BF₄)₂·6H₂O were reacted in DMF at 70 °C for 2 days. The aqueous saturated KPF₆ solution was added to the solvent mixture. The precipitate was collected on Celite, and then washed with H₂O, DCM and ether. The precipitate was redissolved in acetonitrile. TLC analysis showed a large brown spot and a purple spot using eluent of CH₃CN: H₂O: saturated aqueous KNO₃, 5: 1: 1.

**Figure 48 :** ¹H NMR (CD₃CN, 300 MHz) spectra of (top): tetrakis(4-aminophenyl)ethene; (middle): 2-pyridinecarboxaldehyde; (bottom): mixture of 2-pyridinecarboxaldehyde, FeBF₄·6H₂O and tetrakis(4-aminophenyl) ethene (24:8:6) at 70°C in DMF for two days, followed by workup and dissolution in CD₃CN.

From the stacked ^1H NMR spectra (Figure 48) peaks corresponding to the aromatic rings from tetrakis(4-aminophenyl)ethene and signals corresponding to pyridine rings from 2-pyridine carboxaldehyde disappeared with the appearance of new peaks in the aromatic region.

Compared with starting materials, signals corresponding to the pyridine rings in the product were assigned as H^{B6} at 8.42 ppm, H^{B5} at 8.31 ppm, H^{B4} at 7.65 ppm and H^{B4} at 7.21 ppm. The signal at 8.71 ppm was assigned as protons of imines (H^{B7}). The identity of this structure was discussed later in this chapter.

This reaction was repeated in other solvents to investigate the tolerance of the self-assembly process to solvent changes. Reactions in acetonitrile or DMSO were performed.

The reaction of $\text{FeBF}_4 \cdot 6\text{H}_2\text{O}$ (8 equivalents), tetrakis(4-aminophenyl)ethene (6 equivalents) and 2-pyridinecarboxaldehyde (24 equivalents) is performed in 1:1 $\text{CD}_3\text{CN}/\text{DMF}$ at room temperature for 24 hours, followed by heating at 70°C for 24h. The reaction was monitored by ^1H NMR as the colour changed from brown to purple. ^1H NMR indicated the presence of 2-pyridinecarboxaldehyde, and the expected coupling pattern for the pyridine rings with the disappearance of signals corresponding to aromatic rings of TPE. The proton spectrum after further heating at 70°C for another 24 hours was the same as that at room temperature.

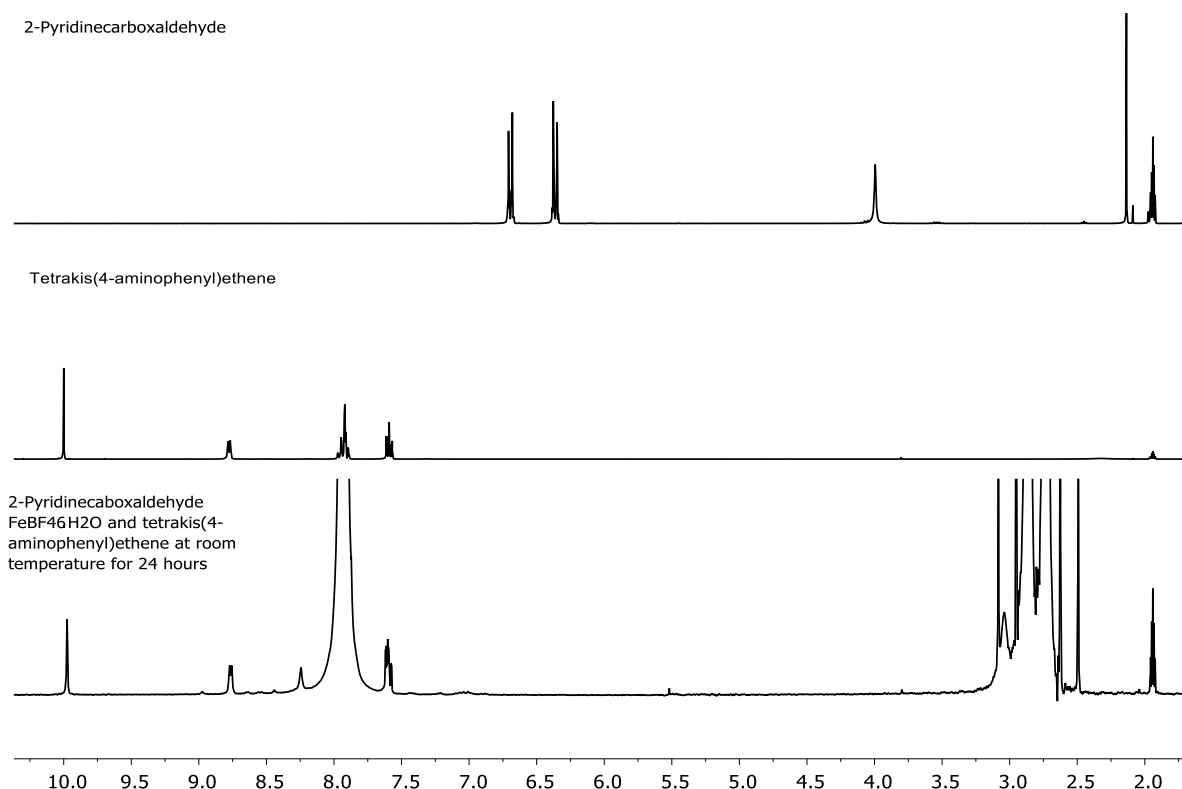
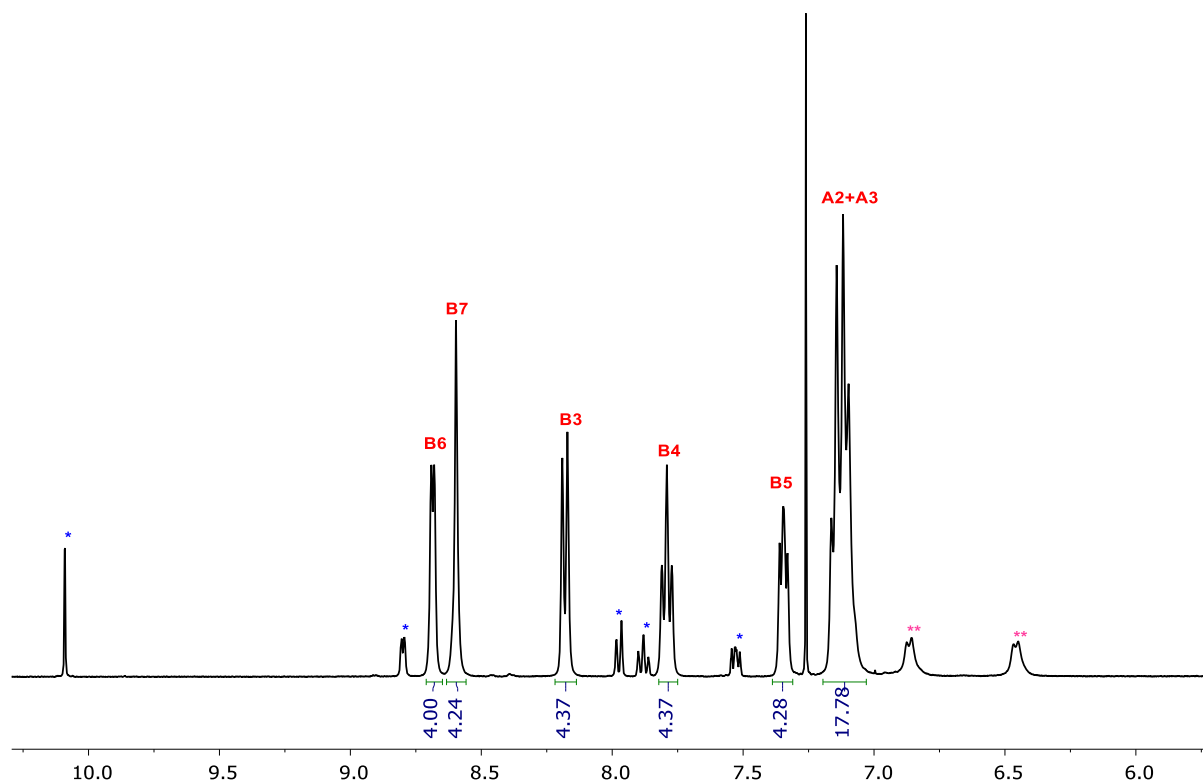


Figure 49 : ¹H NMR spectra recorded on 300MHz, top, tetrakis(4-aminophenyl)ethene in CD₃CN; middle, 2-pyridinecarboxaldehyde; bottom, mixture of 2-pyridinecarboxaldehyde(prepared the stock solution in DMF), FeBF₄·6H₂O and tetrakis(4-aminophenyl)ethene at room temperature for 24 hours.

Attempts to synthesize the cage in CD₃CN/DMF at room temperature resulted in a colour change from brown to intense purple, suggestive of the formation of a low-spin Fe(L)₃ complex. However ¹H NMR (See Figure 49) confirmed no significant changes in the signals around the pyridine rings with the disappearance of signals corresponding to aromatic rings of TPE. DCM probably washed the starting material, 27, away during the work up.

The reaction was also attempted in DMSO-d₆ as related self-assembled Fe(diimine) structures have been successfully prepared in this solvent.^[98] The reaction was attempted using a 24:6:8 ratio of 2-pyridinecarboxaldehyde: TPE: FeBF₄·6H₂O, which corresponds to the stoichiometry of the M₈L₆ cage, and stirring at 70°C for 24 hours. The ¹H NMR spectrum contained only broad poorly resolved signals, suggesting the formation of polymeric products.

The imine ligand (**28**) was prepared by reaction of **27** and 2-pyridinecarboxaldehyde in ethanol at 80°C for 16h. This ligand was characterized by ^1H NMR in CDCl_3 (See Scheme 9), and found to readily hydrolyse in wet solvent. This pre-formed imine (**28**) ligand was used in the self-assembly with Fe(II) ions to ensure the ratio of amine : aldehyde was ideal for the self-assembly reaction.



Scheme 9 : ^1H NMR (CDCl_3 , 400MHz) of **28**. Peaks corresponding to 2-pyridinecarboxaldehyde are indicated *; those corresponding to **27** are marked with **

This imine ligand (6 equiv.) was reacted with $\text{Fe}(\text{BF}_4)_2 \cdot 6\text{H}_2\text{O}$ (8 equiv.) in DMSO-d_6 at 70°C, with periodic monitoring by ^1H NMR. After 36 hours no further ^1H NMR spectral changes were observed and the reaction was assumed to have reached completion.

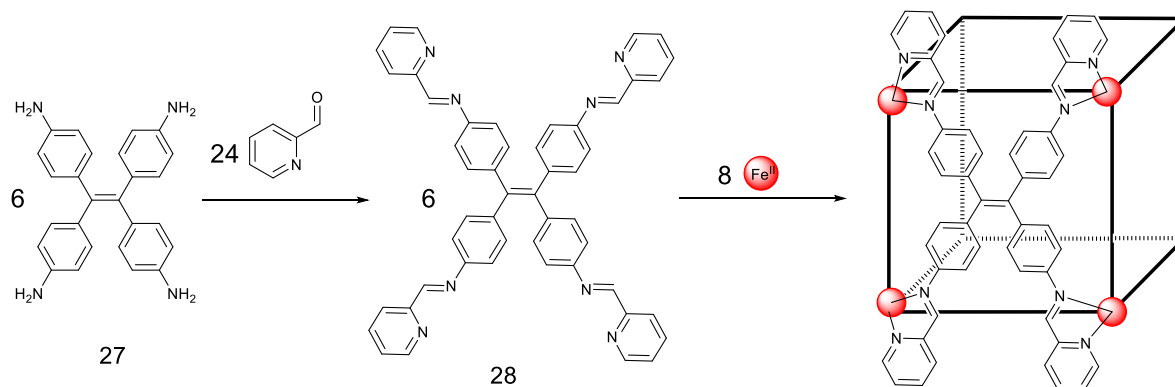


Figure 50 : The proposed self-assembly of a M_8L_6 cubic cage based on tetraanilineethene .

Excess aqueous saturated KPF_6 was added to the reaction mixture. The precipitate was collected on Celite, and washed with H_2O , DCM and ether. The precipitate was redissolved in acetonitrile for ESI-MS, although no signals corresponding to the (highly charged) expected ions were observed. The hydrolysis of the imine was observed by 1H NMR due to presence of H_2O in the $DMSO-d_6$ (Figure 51, top spectrum). The appearance of new signals at 5.20 ppm indicates the formation of a significantly deshielded environment.

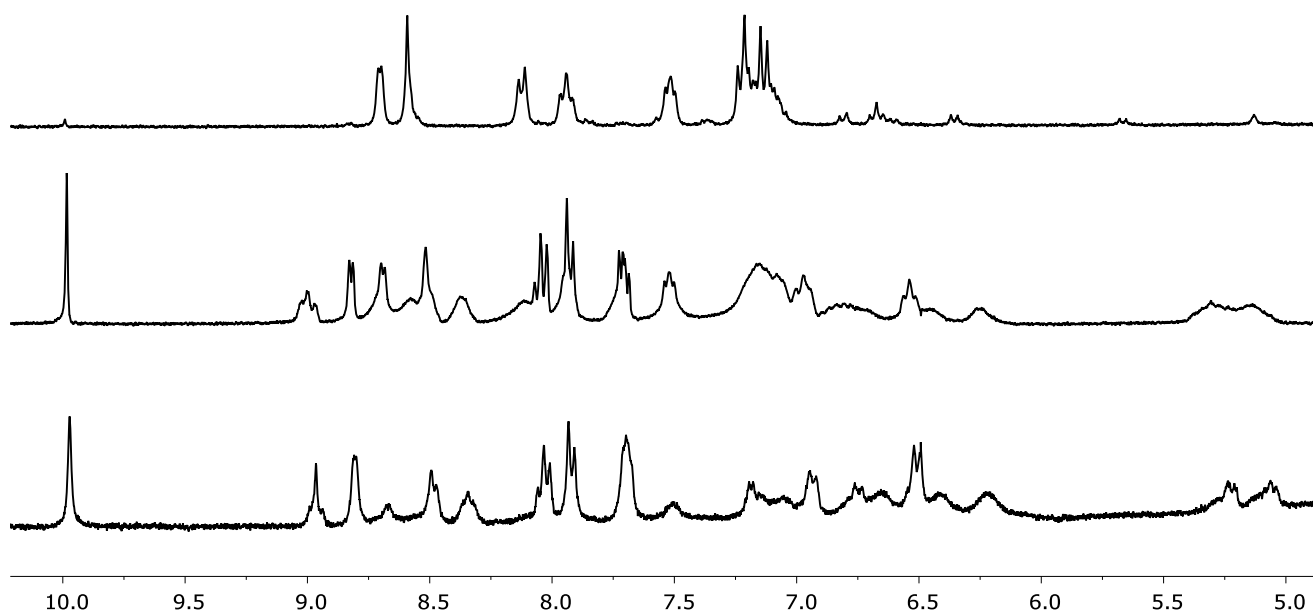


Figure 51 : 1H NMR spectra (300 MHz, $DMSO-d_6$) top to bottom: imine ligand 28, mixture of TPE imine ligand and $FeBF_4 \cdot 6H_2O$ after heating at $70^\circ C$ for 24 hours (middle) and 36h (bottom).

Based on the attempts to synthesize the cage in different reaction conditions, the reaction in pure DMF appeared to give the most promising results. Therefore, further work was done to investigate formation of the cage in different ratio of **27**, 2-pyridinecarboxaldehyde and $\text{Fe}(\text{BF}_4)\cdot 6\text{H}_2\text{O}$ (see Table 3). The ideal ratio to form the M_8L_6 cage analogous to the porphyrin containing example of Nitschke would be 3: 12: 4 of tetraamine: aldehyde: Fe(II).

Table 3 : Six attempts to optimize the reaction conditions for synthesizing the Fe_2L_3 cage

Entry	Tetraamine (equiv.)	Pyridylaldehyde (equiv.)	$\text{Fe}(\text{BF}_4)\cdot 6\text{H}_2\text{O}$ (equiv.)	T (°C)	Solvent	Time (hr)	Successful?
1	3	6	1.5	25	DMF	48	YES
2	3	6	3	25	DMF	48	YES
3	3	6	6	25	DMF	48	YES
4	3	12	1.5	25	DMF	48	YES
5	3	12	3	25	DMF	48	YES
6	3	12	6	25	DMF	48	NO

The general procedure for the workup was as follows: after the reaction was finished, the red slurry was poured into saturated KPF_6 solution. The dark brown precipitate was collected on Celite, and then washed with H_2O , DCM and ether. The precipitate was redissolved in acetonitrile and analysed by NMR (Figure 52). Entries 1-3, which have an excess of amine and/or Fe(II) with respect to the tetraamine, each showed the formation of a single, highly symmetric product, which we propose to be the dimeric structure shown in Figure 53. When the ratio of Fe(II) and/or aldehyde added are changed from 3:6 to 3:12, the ^1H NMR spectra are very broad which is presumably caused by the formation of paramagnetic Fe(II) complexes as well as polymeric products. In the case of entry 6, which is close to the “ideal” stoichiometry for the reaction, the reaction mixture formed an insoluble brown solid, consistent with the formation of polymeric products.

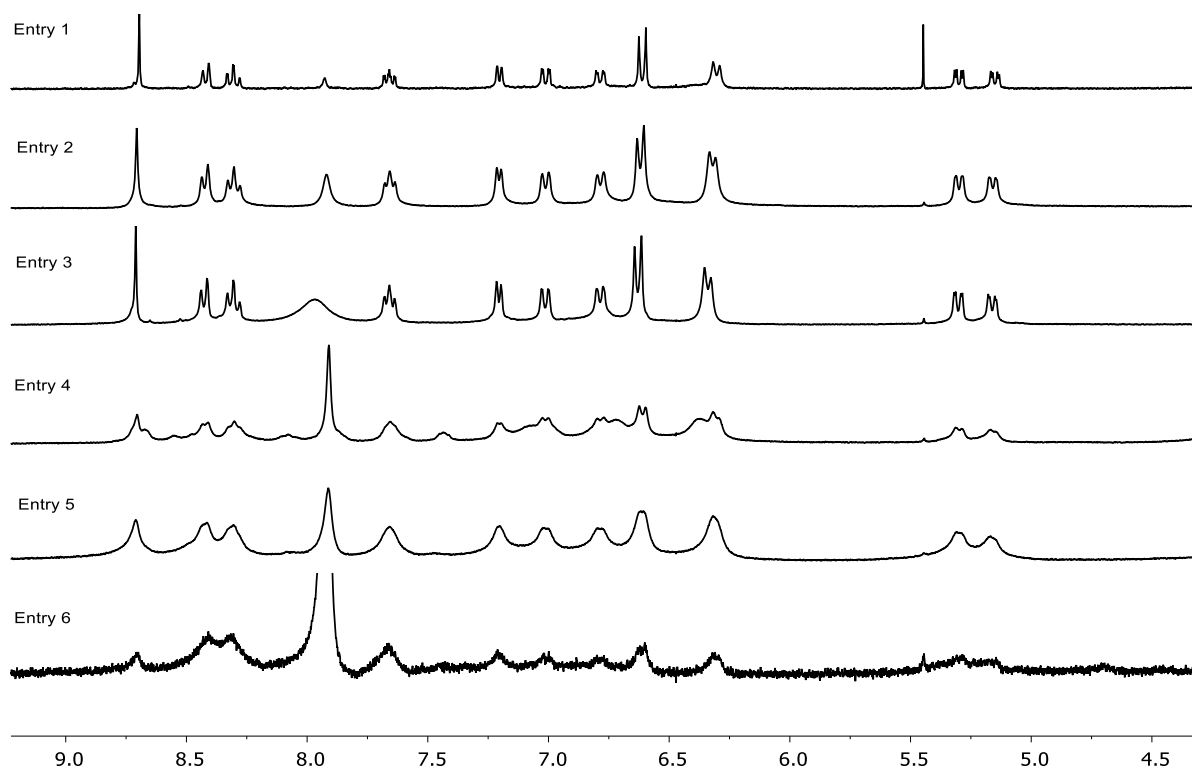


Figure 52 : ^1H NMR (CD_3CN , 300MHz) spectra the reaction mixtures (in DMF) from different ratios (See **Table 3**) of **27**, 2-pyridinecarboxaldehyde and $\text{Fe}(\text{BF}_4) \cdot 6\text{H}_2\text{O}$, after workup.

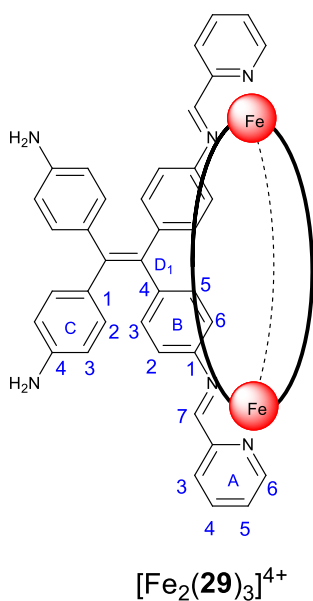


Figure 53 : The structure of the $\text{Fe}_2(\mathbf{29})_3$ cage formed by reaction of TPE with 2-pyridinecarboxaldehyde and $\text{Fe}(\text{BF}_4)_2 \cdot 6\text{H}_2\text{O}$.

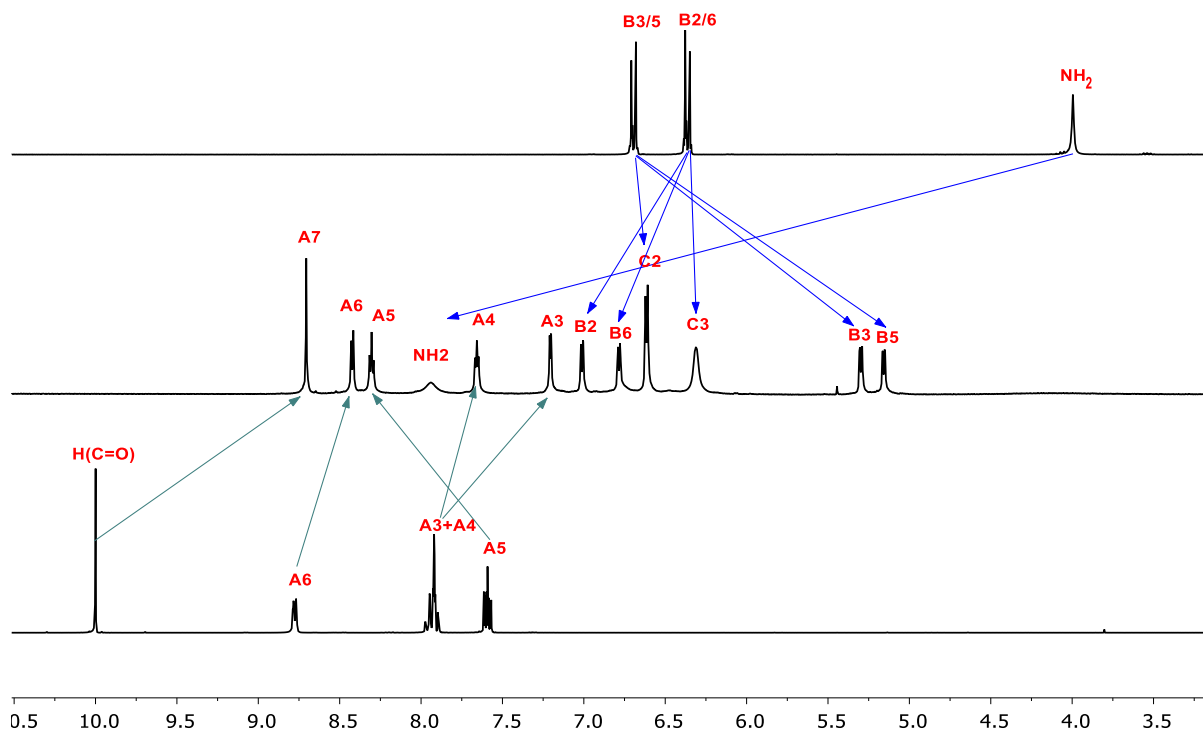


Figure 54 : ^1H NMR (CD_3CN , 300MHz), top, **27**; middle, Fe_2L_3 cage; bottom, 2-pyridinecarboxaldehyde.

The NMR of the isolated product from entry 1 was shown in Figure 54, which showed a comparison with the tetraamine and aldehyde starting materials. Very significant peak shifts were observed, with the signals from the tetraamine shifting upfield by up to 1.55 ppm. More significantly, the signals of the tetraamine were split into three non-equivalent para-substituted aromatic rings, in a 1:1:2 ratio, and the formation of a sharp imine peak at 8.75 ppm was also in keeping with the formation of a metal complex with this ligand. The identity of this product was established using 2D NMR techniques. Specifically ^1H NMR, ^{13}C NMR, COSY, HSQC, HMBC and NOESY techniques in CD_3CN were used for structural assignment. The COSY spectrum was shown in Figure 55. This is consistent with the formation of a $\text{Fe}(\text{L})_3$ type structure where the rotation of the aniline ring is restricted, as reported in the porphyrin-containing cage.^[95]

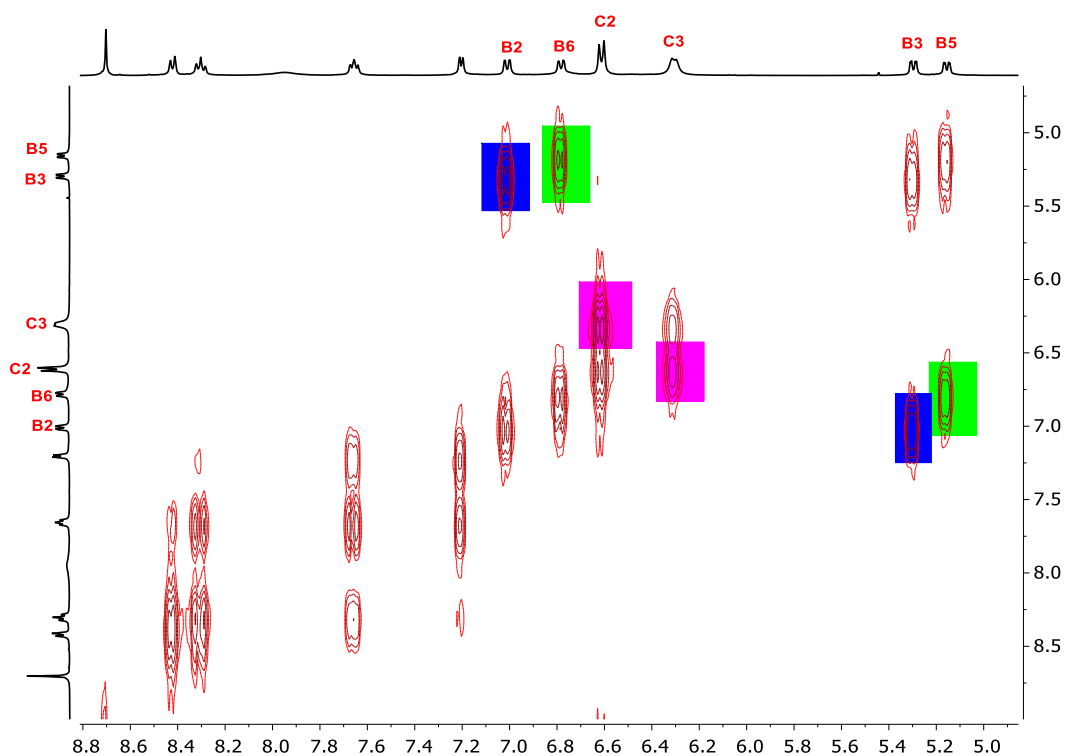


Figure 55 : COSY spectrum (400 MHz, CD₃CN) of the Fe₂L₃ Cage

The signal at 8.00 ppm was assigned as a NH₂ peak and this assignment was supported by the HSQC spectrum, which showed this signal was not attached to a carbon atom (Figure 56).

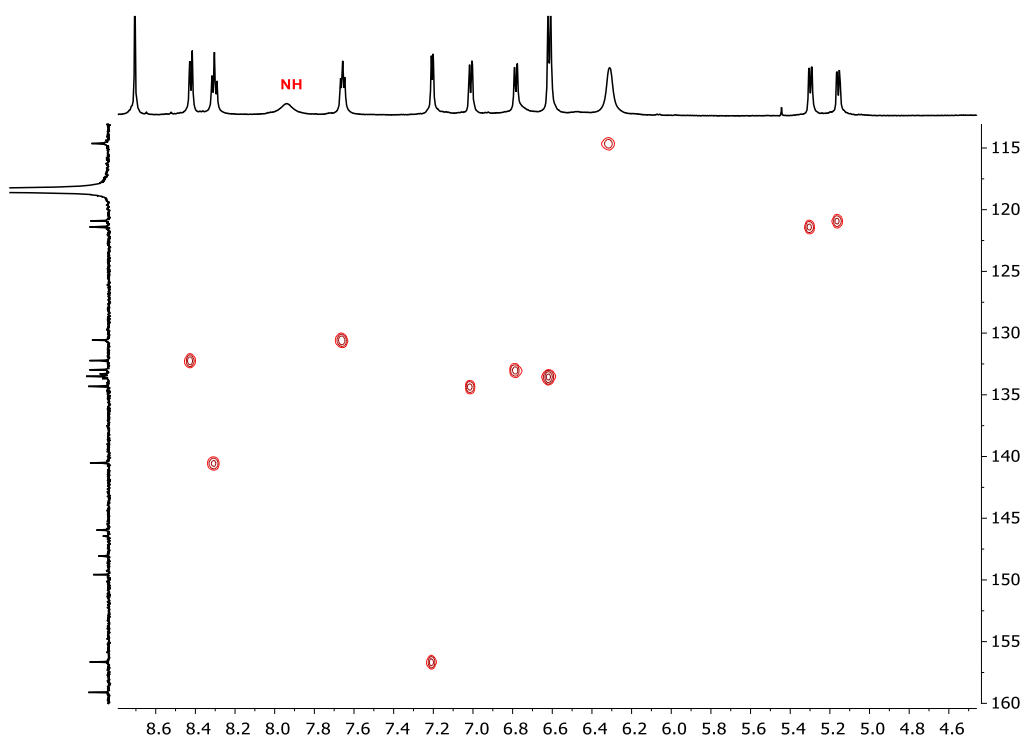


Figure 56 : ¹H-¹³C HSQC (600 MHz, CD₃CN) spectrum of the cage shows there is no cross peak of the peak in ¹H NMR spectrum at 8.00 ppm.

The ^1H NMR signals corresponding to pyridyl ring $\text{H}^{\text{A}6}$, $\text{H}^{\text{A}4}$ and $\text{H}^{\text{A}3}$ were shifted upfield from 8.77 ppm to 8.42 ppm, 7.93 ppm to 7.65 ppm and 7.92 ppm to 7.20 ppm. While the signal of $\text{H}^{\text{A}5}$ had a chemical shift at 8.30 ppm (shifted downfield from 7.59 ppm in Figure 54, bottom). Signals corresponding to tetraamine core were split into three sets. Signals at 6.61 ppm and 6.31 ppm were integrated as 12 protons, respectively, which represented the $\text{H}^{\text{C}2}$ and $\text{H}^{\text{C}3}$ protons. Signals at 6.79 ppm and 5.16 ppm were assigned $\text{H}^{\text{B}6}$ and $\text{H}^{\text{B}5}$ both of which were strongly shielded upon coordination. The rest of the signals correspond to $\text{H}^{\text{B}2}$ and $\text{H}^{\text{B}3}$. A ^1H - ^1H NOESY (Figure 57) spectrum confirmed the $\text{H}^{\text{B}2}/\text{H}^{\text{B}6}$ and $\text{H}^{\text{B}3}/\text{H}^{\text{B}5}$ were close in space (or in exchange), consistent with their assignment as belonging to the same aromatic ring.

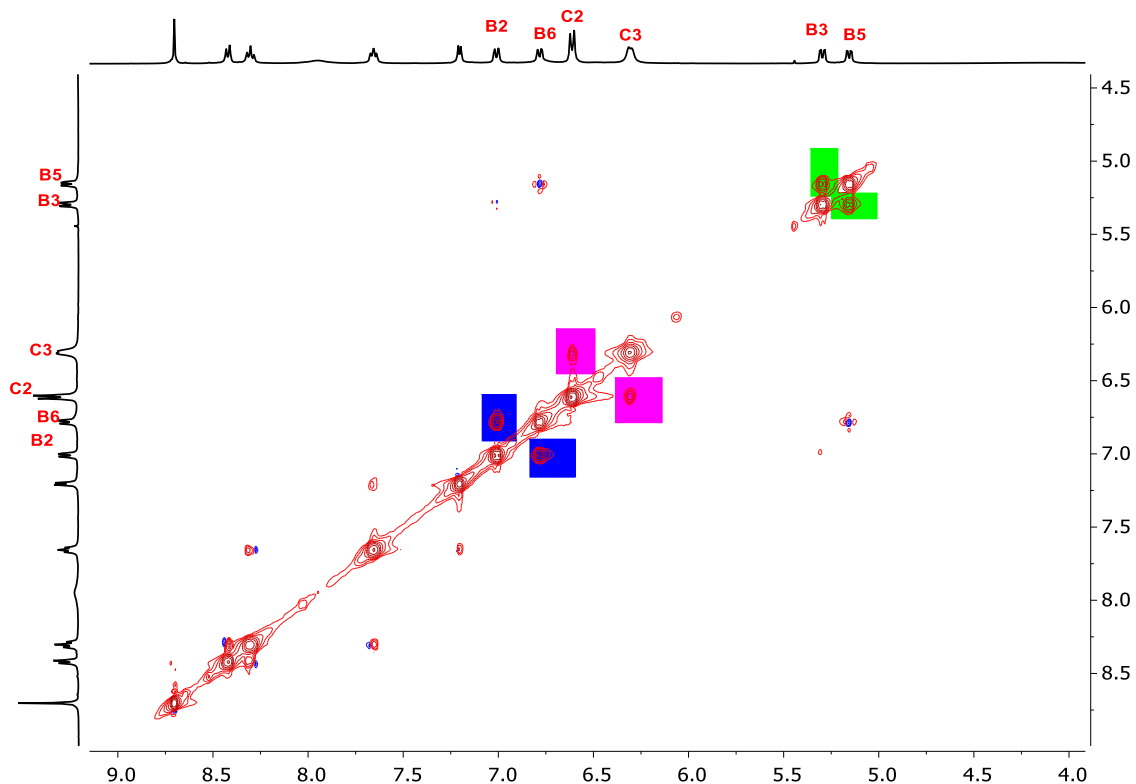


Figure 57 : NOESY spectrum of the Fe_2L_3 cage

Finally, ESI-MS was used to provide further information regarding the identity of this species. Charged ions with m/z at 1056.17, 663.26 and 455.91 were observed, corresponding to $[\text{M}-2\text{PF}_6]^{2+}$, $[\text{M}-3\text{PF}_6]^{3+}$, $[\text{M}-4\text{PF}_6]^{4+}$ formed by the sequential loss of PF_6^- counter anions from the dimeric structure. This structure is also in complete agreement with the NMR assignments discussed above.

This new dimeric helical cage may find applications in guest binding as well as being a useful building block for the formation of larger, extended structures.

4.3. Summary and conclusion

Although the hydrogenation of 1,3,6,8-tetrakis(3-hydroxy-1-propynyl)pyrene appears to proceed, some evidence of the reduction of pyrene core were also observed by ^1H NMR, suggesting this was not a good route for developing pyrene-containing building blocks. Further purification needed to be done in the future. Attempts to perform Suzuki coupling reactions between either tetraborylpyrene or tetrabromopyrene and either a 4-bromophenyl-functionalized Ru(II) complex or a 4-boronic acid functionalised Ru(II) complex were unsuccessful.

Suzuki coupling reaction between a 3-(boronic acid)phenyl functionalized mononuclear Ru(II) complex and tetrabromopyrene did form the desired tetrasubstituted product. However, purification of this highly polar species remained a significant challenge to be overcome. Sonogashira coupling reactions between alkyne functionalized mononuclear Ru(II) complexes and tetrabromopyrene was found to proceed slowly, with the formation of a complex mixture of reaction by-products.

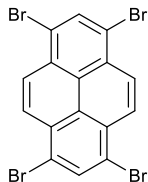
The synthesis of a new type of molecular cage featuring planar, conjugated TPE units was successful using metal-template imine bond formation with Fe(II) ions. The reaction conditions have been optimized by using the ratio of **27** (3 equivalents), 2-pyridinecarboxaldehyde (6 equivalents) and $\text{Fe}(\text{BF}_4) \cdot 6\text{H}_2\text{O}$ (3 equivalents) to synthesize exclusively the Fe_2L_3 cage as the sole product (by NMR). This new type of self-assembled structure could be useful for guest binding, as well as forming Ru(II) complexes in future. The presence of amine groups in direct conjugation with the metal centre may also allow, for example, pH to be used to modulate electrochemical properties of the resulting complexes.

The work presented in this thesis has demonstrated a ready synthetic route to prepare large, discrete metallocsupramolecular structures which contain $\text{Ru}(\text{tpy})_2$ units. Future work will allow new types of cages to be prepared and their use for small molecule catalysis will be explored.

4.4. Experimental

4.4.1. 1,3,6,8-tetrabromopyrene

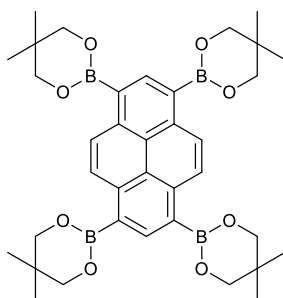
Prepared following a literature procedure^[83]



Pyrene (1.0 g, 4.9 mmol) was dissolved in nitrobenzene (20 mL). Bromine (3.5 g, 22 mmol) was added dropwisely to the solution. The mixture was stirred vigorously at 120°C for 4h. After being cooled to room temperature, the slurry was filtered. The pale-green precipitate was collected on a glass frit, and washed with ethanol (20 mL). Drying under vacuum in the desiccator gave the pale-green solid in 85% yield (2.15 g, 4.2 mmol). Due to the poor solubility in all organic solvents, it was used for next reaction without further purification.

4.4.2. 1,3,6,8-tetrakis(5,5-dimethyl-1,3,2-dioxaborinan-2-yl)pyrene

Prepared following a literature procedure^[91]

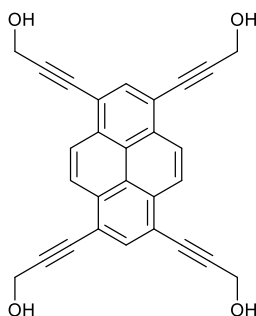


Borylation of pyrene was performed using the same procedure as that for the related compound. 1,3,6,8-tetrabromopyrene (0.30 g, 0.50 mmol) was reacted with bis(neopentyl glycolato)diboron (0.68 g, 3 mmol) with Pd(dppf)Cl₂ (27 mg, 30 μmol) and potassium acetate (0.58 g, 5.8 mmol) in toluene (7 mL) at 80°C for 24 hr under an argon atmosphere. The solution was diluted with CH₂Cl₂ (30 mL), washed with H₂O (4

× 30 mL), and organic phase was dried over Na₂SO₄. The solvent was removed by rotary evaporation. The crude product was purified by column chromatography on silica using DCM/hexane 1:1 as eluent. A yellow product was obtained (0.23 g, 0.35 mmol, 70%). ¹H NMR (300 MHz, CDCl₃) δ 9.12 (s, 4H), 8.98 (s, 2H), 3.99 (s, 16H), 1.17 (s, 24H).

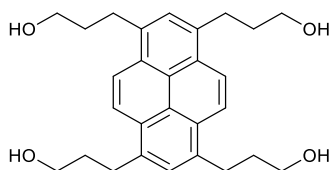
4.4.3. 1,3,6,8-Tetrakis(3-hydroxy-1-propynyl)pyrene

Prepared following a literature procedure^[81b]



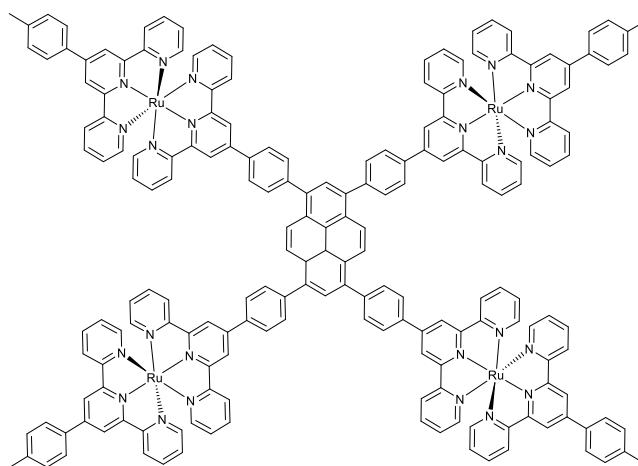
1,3,6,8-tetrabromopyrene (0.50 g, 0.97 mmol), propargyl alcohol (0.33 g, 5.8 mmol) was dissolved in THF (10 mL) and diisopropylamine (10 mL). After the mixture solution was degassed via three freeze-pump-thaw cycles, Pd(PPh₃)₄ (55 mg, 0.048 mmol) and CuI (9.0 mg, 0.048 mmol) were quickly added under an argon atmosphere. The resulting mixture was stirred at 70°C for 42 h. The mixture was cooled to the room temperature, triturated with CHCl₃ (13 mL) and filtered. Washing with water and drying under the vacuum gave the 1,3,6,8-Tetrakis(3-hydroxy-1-propynyl)pyrene as an orange solid (0.12 g, 0.29 mmol, 29%). ¹H NMR (300 MHz, DMSO-*d*₆) δ 8.67 (s, 4H), 8.23 (s, 2H), 5.59 (t, *J* = 6.0 Hz, 4H), 4.57 (d, *J* = 5.9 Hz, 8H).

4.4.4. Attempted hydrogenation of 1,3,6,8-Tetrakis(3-hydroxy-1-propynyl)pyrene



1,3,6,8-Tetrakis(3-hydroxy-1-propynyl)pyrene (50 mg, 0.12mmol) was dissolved in THF (3 mL) and CH₃OH (3 mL). The solution was degassed under argon for 20 min. The catalyst, palladium on charcoal (0.60 mg) or PtO₂ (4.5 mg, 20 ummol), was quickly added. The suspension was stirred at room temperature under a H₂ atmosphere. The mixture was filtered followed by evaporation of the solvent to yield a yellow solid. Recrystallization from hexane and DCM gave the starting material or the compound with impurities which are the reduced pyrene core compound.

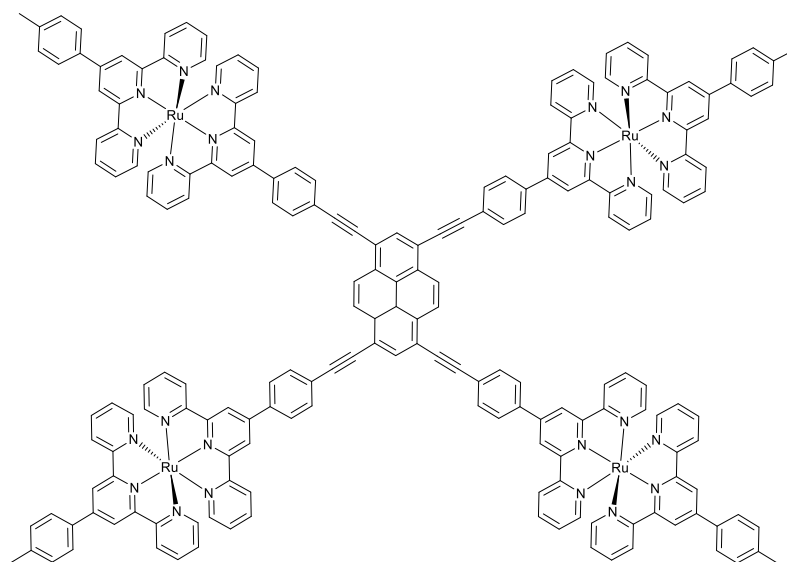
4.4.5. Suzuki cross coupling reaction between 1,3,6,8-tetrabromopyrene and [Ru(6b)(8)](PF₆)₂



1,3,6,8-tetrabromopyrene (2.8 mg, 5.5 μmol), Cs₂CO₃ (18 mg, 55 μmol), DMF (5 mL) and [Ru(6b)(8)](PF₆)₂ (35 mg, 33 μmol) were placed in a dry Schlenk tube. The solution was degassed via three freeze-pump-thaw cycles, followed by addition of Pd(PPh₃)₄ (3.8 mg, 3.3 μmol). The reaction was

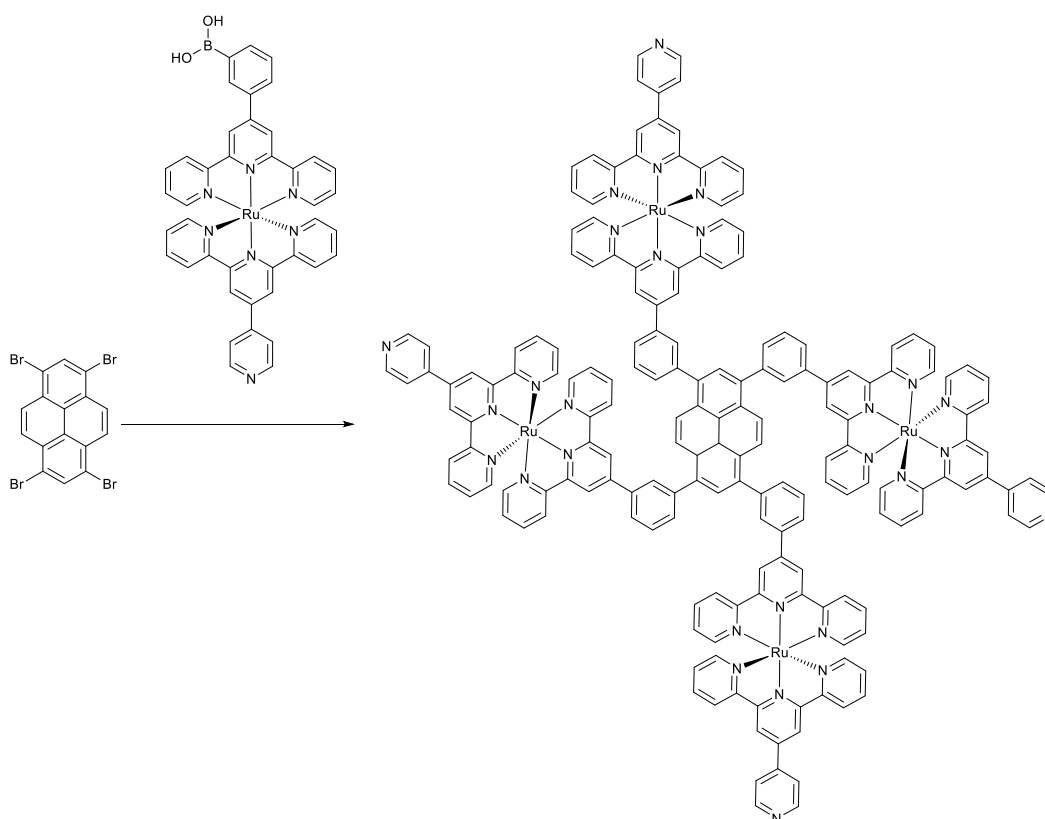
stirred under an argon atmosphere at 80°C for 2 days, cooled to room temperature and evaporated to give a red residue. An aqueous solution of saturated KPF₆ was poured into the residue. The precipitate was collected on Celite, washed with H₂O (5 mL), EtOH (2 mL) and ether (5 mL). The cake was redissolved in acetonitrile. Removal of the solvent yielded a bright red product. Attempts to characterise by ¹H-NMR and ESI-MS revealed a mixture of unidentified products.

4.4.6. Sonogashira cross coupling reaction between 1,3,6,8-tetrabromopyrene and [Ru(10)(8)](PF₆)₂



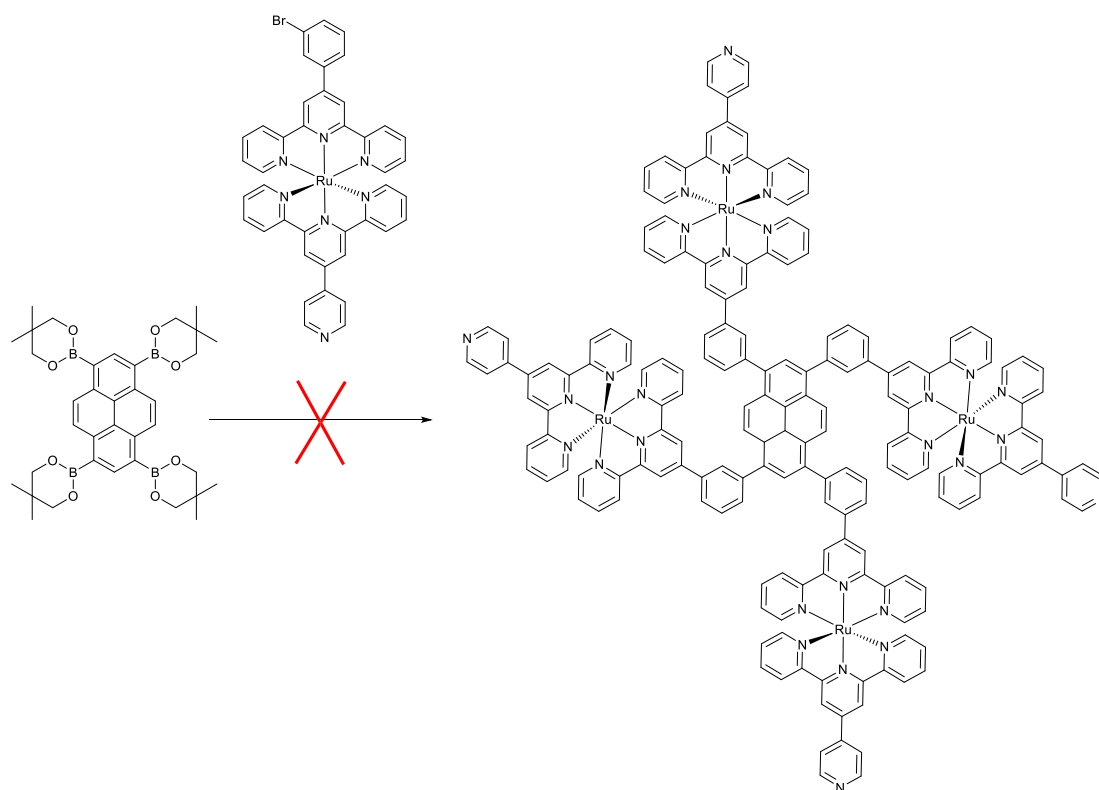
[Ru(10)(8)](PF₆)₂ (46 mg, 44 μmol) was dissolved in CH₃CN (10 mL), THF (5 mL) and diisopropylamine (5 mL). After the solution was degassed via three freeze-pump-thaw cycles, 1,3,6,8-tetrabromopyrene (2.8 mg, 5.5 μmol), Pd(PPh₃)₄ (3.8 mg, 3.3 μmol) and CuI (0.62 mg, 3.3 μmol) were quickly added under an argon atmosphere. The resulting mixture was stirred at 60°C for 3 days. The solution was cooled to the room temperature. An aqueous solution of saturated KPF₆ was poured into the slurry. The precipitate was collected on Celite, washed with H₂O (5 mL), EtOH (2 mL) and ether (5 mL). The cake was redissolved in acetonitrile. Removal of the solvent yields a black product. Attempts to characterise by ¹H-NMR and ESI-MS revealed a mixture of unidentified products.

4.4.7. Suzuki cross coupling reaction between 1,3,6,8-tetrabromopyrene and $[Ru(\mathbf{5b})(\mathbf{4})](PF_6)_2$



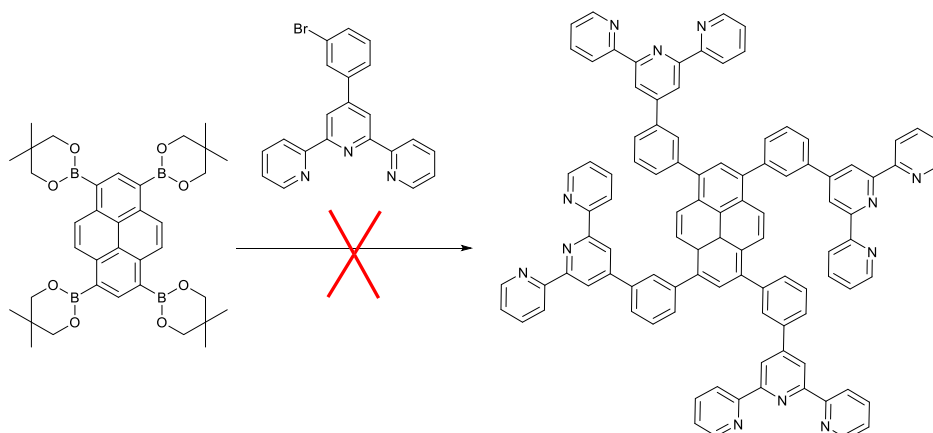
Route A: 1,3,6,8-tetrabromopyrene (2.8 mg, 5.5 μmol), Cs_2CO_3 (18 mg, 55 μmol), DMF (5 mL) and $[Ru(\mathbf{5b})(\mathbf{4})](PF_6)_2$ (69 mg, 66 μmol) were placed in a dry Schlenk tube. The solution was degassed via three freeze-pump-thaw cycles, following which $\text{Pd}(\text{PPh}_3)_4$ (3.8 mg, 3.3 μmol) was added. The reaction was stirred under an argon atmosphere at 80°C for 3 days, cooled to room temperature and evaporated to give a red residue. An aqueous solution of saturated KPF_6 was poured into the residue. The precipitate was collected on Celite, washed by H_2O (5 mL), EtOH (2 mL) and ether (5 mL). The cake was redissolved in acetonitrile. Removal of the solvent yields a bright red product. LR-ESI-MS (in CH_3CN): m/z 1974.71 $[\text{M} - 2\text{PF}_6]^{2+}$ requires 1974.72; m/z 1268.30 $[\text{M} - 3\text{PF}_6]^{3+}$ requires 1268.16; m/z 914.57 $[\text{M} - 4\text{PF}_6]^{4+}$ requires 914.88; m/z 702.83 $[\text{M} - 5\text{PF}_6]^{5+}$ requires 702.91; m/z 561.50 $[\text{M} - 6\text{PF}_6]^{6+}$ requires 561.60; m/z 460.53 $[\text{M} - 7\text{PF}_6]^{7+}$ requires 460.66; $[\text{M} - 8\text{PF}_6]^{8+}$ lost

4.4.8. Suzuki cross coupling reaction between 1,3,6,8-tetrakis(5,5-dimethyl-1,3,2-dioxaborinan-2-yl)pyrene and Ru[1][4](PF₆)₂



Route B: 1,3,6,8-tetraborylpyrene (3.5 mg, 5.5 μmol), Cs₂CO₃ (18 mg, 55 μmol), DMF (5 mL) and [Ru(1)(4)](PF₆)₂ (72 mg, 66 μmol) were placed in a dry Schlenk tube. The solution was degassed via three freeze-pump-thaw cycles, following which Pd(PPh₃)₄ (3.8 mg, 3.3 μmol) was added. The reaction was stirred under an argon atmosphere at 80°C for 3 days, cooled to room temperature and evaporated to give a red residue. An aqueous solution of saturated KPF₆ was poured into the residue. The precipitate was collected on Celite, washed by H₂O (5 mL), EtOH (2 mL) and ether (5 mL). The cake was redissolved in acetonitrile. Removal of the solvent yields a deep brown product. Attempts to characterise by ¹H-NMR and ESI-MS revealed a mixture of unidentified products.

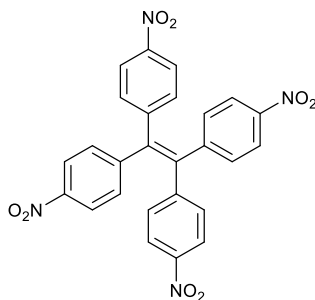
4.4.9. Suzuki cross coupling reaction between 1,3,6,8-tetrakis(5,5-dimethyl-1,3,2-dioxaborinan-2-yl)pyrene and Ligand 1



Route C: 1,3,6,8-tetraborylpyrene (0.10 g, 0.15 mmol), Cs_2CO_3 (1.0 g, 3.1 mmol), DMF (5 mL), toluene (5 mL), H_2O (3 mL) and ligand **1** (0.59 g, 1.5 mmol) were placed in a dry Schlenk tube. The solution was degassed via three freeze-pump-thaw cycles, following which $\text{Pd}(\text{PPh}_3)_4$ (3.8 mg, 3.3 μmol) were added. The reaction was stirred under an argon atmosphere at 105°C for 48h, cooled to room temperature. The slurry was diluted with CH_2Cl_2 (50 mL) and washed with H_2O (4×50 mL). The organic layer was dried over Na_2SO_4 . Removal of the solvent gave the orange oil. The oil was used for ESI-MS analysis. No peak was found matching the expected peak.

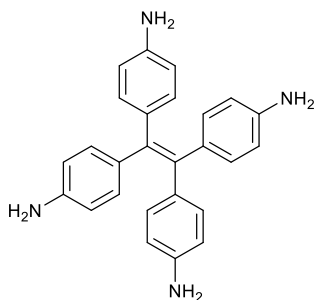
4.4.10. Tetrakis(4-nitrophenyl)ethene

Prepared following a literature procedure^[97]



Nitric acid (6.5 mL) was added into a round bottom flask and cooled in an iced bath. Tetraphenylethene (2.50 g, 7.8 mmol), acetic anhydride (3 mL) and glacial anhydride (4 mL) were added dropwisely under vigorous stirring. The mixture was stirred overnight, and then was diluted with glacial acetic acid (8 mL). The crude product was collected by filtration, followed by washing with H₂O (4 × 20 mL) to afford the yellow solid (1.5 g, 3.0 mmol, 38%). ¹H NMR (300 MHz, CD₃Cl) δ 8.07 (d, *J* = 8.6 Hz, 4H), 7.19 (d, *J* = 8.7 Hz, 4H).

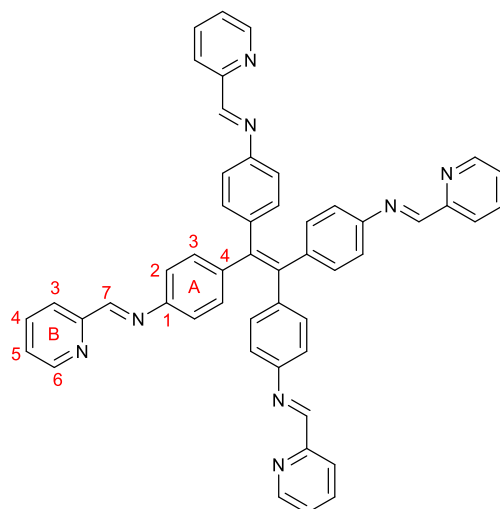
4.4.11. Tetrakis(4-aminophenyl)ethene



Prepared following a literature procedure^[97]

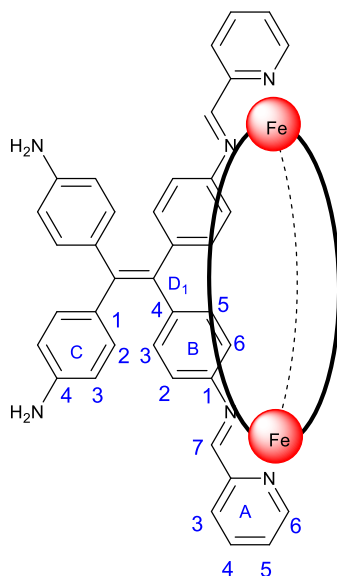
Tetrakis(4-nitrophenyl)ethene(0.25 g, 0.50 mmol) was dissolved in THF (5.0 mL). Raney nickel (1.5 g) and hydrazine monohydrate (0.34 g, 6.7 mmol) were added. The reaction mixture was refluxed for 2 h. The mixture solution was cooled to room temperature, followed by filtration. The filtrate was evaporated under the vacuum to afford a white solid. (0.16 g, 0.41 mmol, 81%). ¹H NMR (300 MHz, CD₃CN) δ 6.69 (d, *J* = 8.3 Hz, 8H), 6.36 (d, *J* = 8.4 Hz, 8H), 4.00 (s, 8H).

4.4.12. TPE imine ligand (**28**)



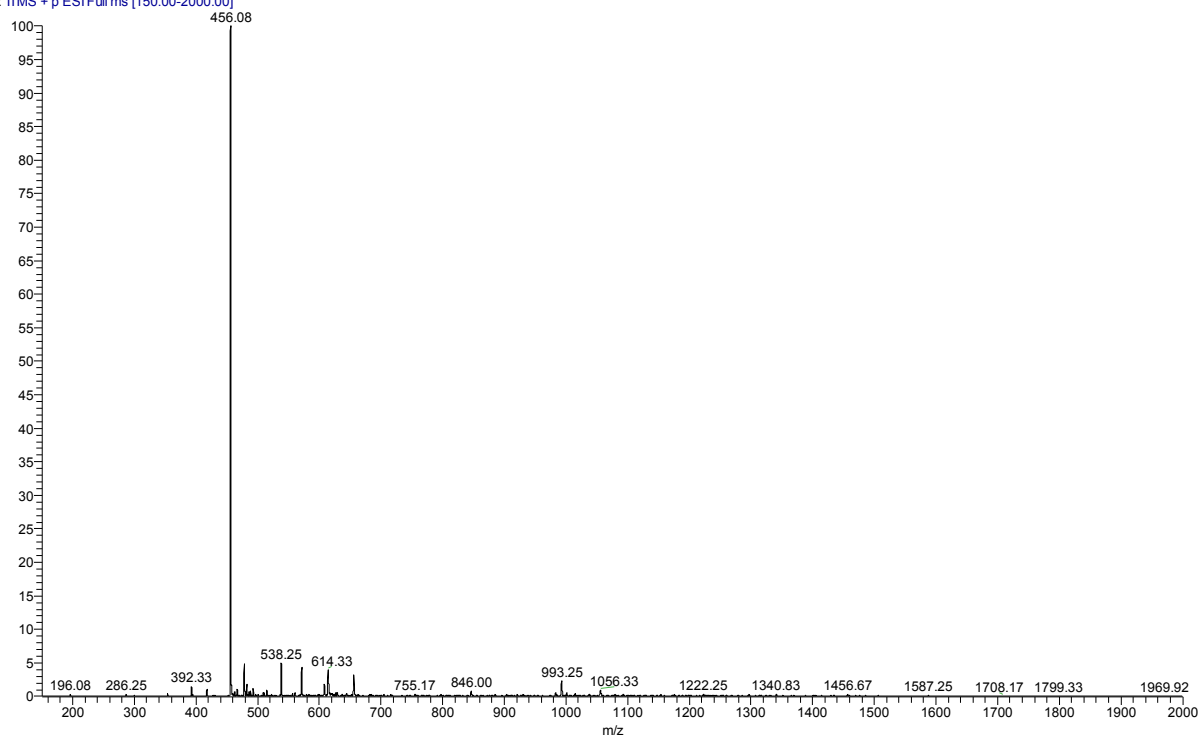
Tetrakis(4-nitrophenyl)ethene (0.13 g, 0.33 mmol) and 2-pyridinecarboxaldehyde (0.20 g, 1.9 mmol) were added to EtOH (10 mL). The solution was refluxed for 2h. The solution was cooled to room temperature. The precipitate was collected by filtration, followed by washing with EtOH (2×5 mL) to give the yellow solid (0.23 g, 0.31 mmol, 95%). ^1H NMR (400 MHz, CDCl_3) δ 8.69 (dt, $J = 4.6, 1.4$ Hz, 4H, $\text{H}^{\text{B}6}$), 8.60 (s, 4H, $\text{H}^{\text{B}7}$), 8.18 (dt, $J = 7.9, 1.1$ Hz, 4H, $\text{H}^{\text{B}3}$), 7.79 (td, $J = 7.7, 1.7$ Hz, 4H, $\text{H}^{\text{B}4}$), 7.35 (ddd, $J = 7.6, 4.9, 1.2$ Hz, 4H, $\text{H}^{\text{B}5}$), 7.13 (m, 16H, $\text{H}^{\text{A}2+\text{A}3}$). ^{13}C NMR (101 MHz, CDCl_3) δ 160.24 ($\text{C}^{\text{B}7}$), 154.79 ($\text{C}^{\text{B}2}$), 149.75 ($\text{C}^{\text{B}6}$), 149.26 ($\text{C}^{\text{A}1}$), 142.50 ($\text{C}^{\text{A}4}$), 140.53 ($\text{C}^{\text{C}=\text{C}}$), 136.78 ($\text{C}^{\text{B}4}$), 132.59 ($\text{C}^{\text{A}2}$), 125.16 ($\text{C}^{\text{B}5}$), 121.95 ($\text{C}^{\text{B}3}$), 120.98 ($\text{C}^{\text{A}3}$). LR-ESI-MS (in CHCl_3): m/z 749.10 $[\text{M} + \text{H}]^+$ requires 749.31.

4.4.13. Self-assembled M_2L_3 cage



Tetraamine (**27**) (20 mg, 51 μmol), 2-pyridinecarboxaldehyde (9.5 μL , 0.10 mmol) and $\text{Fe}(\text{BF}_4) \cdot 6\text{H}_2\text{O}$ (17 mg, 51 μmol) was dissolved in 20 mL DMF. The reaction mixture was stirred at room temperature for two days. An aqueous solution of saturated KPF_6 was poured into the residue. The precipitate was collected on Celite, washed with H_2O (10 mL), DCM (10 mL) and ether (20 mL). The cake was redissolved in acetonitrile. Removal of the solvent yielded a brown solid (89 mg, 37 μmol , 73%). ^1H NMR (600 MHz, CD_3CN) δ 8.71 (s, 6H, $\text{H}^{\text{A}7}$), 8.42 (d, $J = 7.7$ Hz, 6H, $\text{H}^{\text{A}6}$), 8.30 (t, $J = 7.8$ Hz, 6H, $\text{H}^{\text{A}5}$), 7.94 (s, 6H, H^{NH}), 7.66 (t, $J = 6.9$ Hz, 6H, $\text{H}^{\text{A}4}$), 7.21 (d, $J = 5.6$ Hz, 6H, $\text{H}^{\text{A}3}$), 7.01 (d, $J = 8.3$ Hz, 6H, $\text{H}^{\text{B}2}$), 6.78 (d, $J = 8.4$ Hz, 6H, $\text{H}^{\text{B}6}$), 6.61 (d, $J = 8.1$ Hz, 12H, $\text{H}^{\text{C}2}$), 6.31 (s, 12H, $\text{H}^{\text{C}3}$), 5.30 (d, $J = 8.3$ Hz, 6H, $\text{H}^{\text{B}3}$), 5.16 (d, $J = 8.3$ Hz, 6H, $\text{H}^{\text{B}5}$). ^{13}C NMR (151 MHz, CD_3CN) δ 159.11 ($\text{C}^{\text{A}2}$), 156.65 ($\text{C}^{\text{A}3}$), 149.57 ($\text{C}^{\text{B}3}$), 148.07 ($\text{C}^{\text{C}1}$), 146.46 ($\text{C}^{\text{D}1}$), 145.96 ($\text{C}^{\text{B}4}$), 140.52 ($\text{C}^{\text{A}5}$), 134.32 ($\text{C}^{\text{B}2}$), 133.50 ($\text{C}^{\text{C}2}$), 132.97 ($\text{C}^{\text{B}6}$), 132.23 ($\text{C}^{\text{A}6}$), 130.57 ($\text{C}^{\text{A}4}$), 121.40 ($\text{C}^{\text{B}3}$), 120.91 ($\text{C}^{\text{B}5}$), 114.64 ($\text{C}^{\text{C}3}$). LR-ESI-MS (in CH_3CN): m/z 1056.17 $[\text{M}-2\text{PF}_6]^{2+}$ requires 1056.78; 655.26 $[\text{M}-3\text{PF}_6]^{3+}$ requires 656.20. 455.91 $[\text{M}-4\text{PF}_6]^{4+}$ requires 455.91.

promising cage_2455a #265-319 RT: 1.22-1.46 AV: 55 NL: 1.33E5
T: FTMS + p ESIFull ms [150.00-2000.00]



CS 4-1 full_046 #104-148 RT: 4.28-5.71 AV: 45 NL: 4.60E5
T: FTMS + p ESIFull ms [200.00-2000.00]

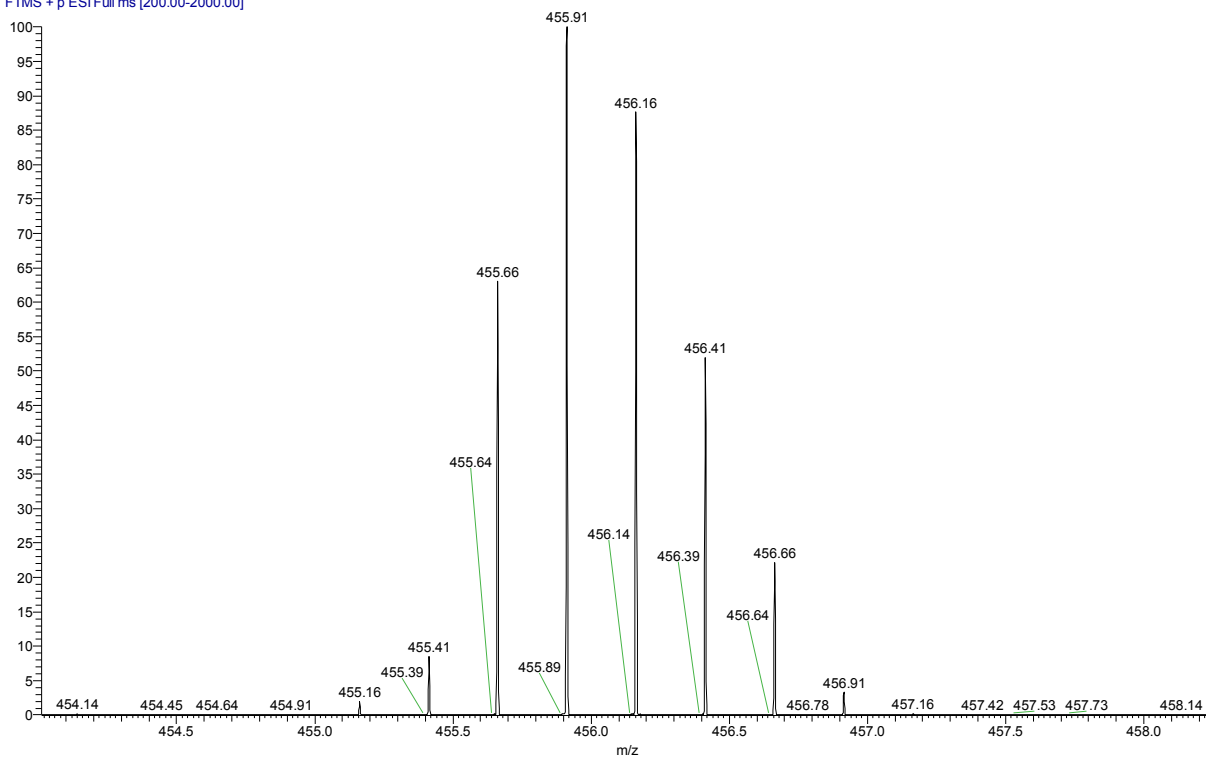


Figure 58 : ESI-MS of $[\text{Fe}_2(29)_3]^{4+}$. Zoom of the 455.91 peak. Calc.455.91

5. Conclusions and Future Work

The work described in this thesis was focussed on new ruthenium(II) containing metalloligands for supramolecular chemistry.

In chapter 2, eight new bromo functionalized and boronic acid functionalised ruthenium(II) heteroleptic complexes with a pendent pyridyl site were reported and characterised. All of complexes are suitable for Suzuki cross coupling reactions and Sonogashira coupling reactions. In chapter 3, the first expanded ligand, $[\text{Ru}(\mathbf{6b})(\mathbf{4})](\text{PF}_6)_2$, with two ruthenium(II) cores and two pendent pyridyl sites were reported via Suzuki cross coupling reaction. Its structural isomers have been prepared using the same reaction conditions. The first use of dinuclear Ru(II) complexes as expanded ligands was reported, with the clean assembly of a Pd(II)-templated supramolecular assembly, although its unambiguous identification remains future work.

In chapter 4, cages based on panels formed from conjugated and planar cores were attempted to be prepared via Pd(0) cross coupling reactions using the mononuclear complexes described in Chapter 2. Attempts to synthesize and characterize the pyrene based tetranuclear ruthenium(II) complexes were challenging, in part due to purification difficulties of the higher polar products. Pleasingly, the use of a tetraphenylethene core instead of pyrene allowed the construction of a Fe_2L_3 cage, which was characterised in detail by 2D NMR and ESI-MS. Optimization of conditions for synthesizing the cage has been reported, opening the door for future exploration in this class of assemblies.

Future work will involve the solid state structure determination of these new supramolecular assemblies, and investigations of their guest potential binding properties.

6. References

- [1] A. Fotin, Y. Cheng, P. Sliz, N. Grigorieff, S. C. Harrison, T. Kirchhausen, T. Walz, *Nature* **2004**, *432*, 573-579.
- [2] R. W. Saalfrank, A. Stark, M. Bremer, H.-U. Hummel, *Angew. Chem. Int. Ed.* **1990**, *29*, 311-314.
- [3] R. W. Saalfrank, B. Hörner, D. Stalke, J. Salbeck, *Angew. Chem. Int. Ed.* **1993**, *32*, 1179-1182.
- [4] aM. Yamanaka, Y. Yamada, Y. Sei, K. Yamaguchi, K. Kobayashi, *J. Am. Chem. Soc.* **2006**, *128*, 1531-1539; bM. Fujita, *Chem. Soc. Rev.* **1998**, *27*, 417-425; cM. Fujita, N. Fujita, K. Ogura, K. Yamaguchi, *Nature* **1999**, *400*, 52-55; dK. Kumazawa, K. Biradha, T. Kusukawa, T. Okano, M. Fujita, *Angew. Chem. Int. Ed.* **2003**, *42*, 3909-3913.
- [5] aT. K. Ronson, A. B. League, L. Gagliardi, C. J. Cramer, J. R. Nitschke, *J. Am. Chem. Soc.* **2014**, *136*, 15615-15624; bR. M. Yeh, J. Xu, G. Seeber, K. N. Raymond, *Inorg. Chem.* **2005**, *44*, 6228-6239; cF. I. Andersson, D. G. Pina, A. L. Mallam, G. Blaser, S. E. Jackson, *FEBS* **2009**, *276*, 2625-2635; dC. Klein, C. Gütz, M. Bogner, F. Topić, K. Rissanen, A. Lützen, *Angew. Chem. Int. Ed.* **2014**, *53*, 3739-3742.
- [6] aT. Kusukawa, M. Fujita, *J. Am. Chem. Soc.* **2002**, *124*, 13576-13582; bD. Moon, S. Kang, J. Park, K. Lee, R. P. John, H. Won, G. H. Seong, Y. S. Kim, G. H. Kim, H. Rhee, M. S. Lah, *J. Am. Chem. Soc.* **2006**, *128*, 3530-3531; cK. Li, L.-Y. Zhang, C. Yan, S.-C. Wei, M. Pan, L. Zhang, C.-Y. Su, *J. Am. Chem. Soc.* **2014**, *136*, 4456-4459.
- [7] M. Tominaga, K. Suzuki, M. Kawano, T. Kusukawa, T. Ozeki, S. Sakamoto, K. Yamaguchi, M. Fujita, *Angew. Chem. Int. Ed.* **2004**, *43*, 5621-5625.
- [8] aM. Otte, P. F. Kuijpers, O. Troeppner, I. Ivanovic-Burmazovic, J. N. Reek, B. de Bruin, *Chem.-Eur. J.* **2013**, *19*, 10170-10178; bK. Suzuki, M. Tominaga, M. Kawano, M. Fujita, *Chem. Commun.* **2009**, 1638-1640.
- [9] aN. Takeda, K. Umemoto, K. Yamaguchi, M. Fujita, *Nature* **1999**, *398*, 794-796; bS.-Y. Yu, T. Kusukawa, K. Biradha, M. Fujita, *J. Am. Chem. Soc.* **2000**, *122*, 2665-2666.
- [10] aP. P. Neelakandan, A. Jimenez, J. R. Nitschke, *Chem. Sci.* **2014**, *5*, 908-915; bA. M. Castilla, N. Ousaka, R. A. Bilbeisi, E. Valeri, T. K. Ronson, J. R. Nitschke, *J. Am. Chem. Soc.* **2013**, *135*, 17999-18006; cA. Jiménez, R. A. Bilbeisi, T. K. Ronson, S. Zarra, C. Woodhead, J. R. Nitschke, *Angew. Chem. Int. Ed.* **2014**, *53*, 4556-4560; dS. Ma, M. M. J. Smulders, Y. R. Hristova, J. K. Clegg, T. K. Ronson, S. Zarra, J. R. Nitschke, *J. Am. Chem. Soc.* **2013**, *135*, 5678-5684; eT. K. Ronson, C. Giri, N. K. Beyeh, A. Minkkinen, F. Topic, J. J. Holstein, K. Rissanen, J. R. Nitschke, *Chem.-Eur. J.* **2013**, *19*, 3374-3382; fI. A. Riddell, M. M. J. Smulders, J. K. Clegg, Y. R. Hristova, B. Breiner, J. D. Thoburn, J. R. Nitschke, *Nat Chem* **2012**, *4*, 751-756.
- [11] aT. N. Parac, M. Scherer, K. N. Raymond, *Angew. Chem. Int. Ed.* **2000**, *39*, 1239-1242; bD. W. Johnson, J. Xu, R. W. Saalfrank, K. N. Raymond, *Angew. Chem. Int. Ed.* **1999**, *38*, 2882-2885; cC. Brückner, R. E. Powers, K. N. Raymond, *Angew. Chem. Int. Ed.* **1998**, *37*, 1837-1839; dA. V. Davis, K. N. Raymond, *J. Am. Chem. Soc.* **2005**, *127*, 7912-7919.
- [12] aD. H. Leung, R. G. Bergman, K. N. Raymond, *J. Am. Chem. Soc.* **2008**, *130*, 2798-2805; bM. D. Pluth, K. N. Raymond, *Chem. Soc. Rev.* **2007**, *36*, 161-171; cA. V. Davis, D. Fiedler, G. Seeber, A. Zahl, R. van Eldik, K. N. Raymond, *J. Am. Chem. Soc.* **2006**, *128*, 1324-1333; dV. M. Dong, D. Fiedler, B. Carl, R. G. Bergman, K. N. Raymond, *J. Am. Chem. Soc.* **2006**, *128*, 14464-14465.
- [13] aT. Murase, S. Sato, M. Fujita, *Angew. Chem., Int. Ed.* **2007**, *46*, 5133-5136; bM. Yoshizawa, S. Miyagi, M. Kawano, K. Ishiguro, M. Fujita, *J. Am. Chem. Soc.* **2004**, *126*, 9172-9173; cM. Yoshizawa, Y. Takeyama, T. Okano, M. Fujita, *J. Am. Chem. Soc.* **2003**, *125*, 3243-3247.
- [14] aM. Yoshizawa, M. Tamura, M. Fujita, *Science* **2006**, *312*, 251-254; bC. J. Hastings, M. D. Pluth, R. G. Bergman, K. N. Raymond, *J. Am. Chem. Soc.* **2010**, *132*, 6938-6940.
- [15] S. Horiuchi, T. Murase, M. Fujita, *J. Am. Chem. Soc.* **2011**, *133*, 12445-12447.
- [16] aM. Yoshizawa, T. Kusukawa, M. Fujita, S. Sakamoto, K. Yamaguchi, *J. Am. Chem. Soc.* **2001**, *123*, 10454-10459; bT. Furusawa, M. Kawano, M. Fujita, *Angew. Chem. Int. Ed.* **2007**, *46*, 5717-5719; cM. Yoshizawa, J. K. Klosterman, M. Fujita, *Angew. Chem., Int. Ed.* **2009**, *48*, 3418-3438.
- [17] C. Zhao, Q.-F. Sun, W. M. Hart-Cooper, A. G. DiPasquale, F. D. Toste, R. G. Bergman, K. N. Raymond, *J. Am. Chem. Soc.* **2013**, *135*, 18802-18805.
- [18] aY. Nishioka, T. Yamaguchi, M. Kawano, M. Fujita, *J. Am. Chem. Soc.* **2008**, *130*, 8160-8161; bA. V. Davis, D. Fiedler, M. Ziegler, A. Terpin, K. N. Raymond, *J. Am. Chem. Soc.* **2007**, *129*, 15354-15363.
- [19] T. Liu, Y. Liu, W. Xuan, Y. Cui, *Angew. Chem., Int. Ed.* **2010**, *49*, 4121-4124.
- [20] S. Wan, L.-R. Lin, L. Zeng, Y. Lin, H. Zhang, *Chem. Commun.* **2014**, *50*, 15301-15304.

- [21] E. C. Constable, *Coord. Chem. Rev.* **2008**, *252*, 842-855.
- [22] J. E. Beves, E. C. Constable, S. Decurtins, E. L. Dunphy, C. E. Housecroft, T. D. Keene, M. Neuburger, S. Schaffner, J. A. Zampese, *CrystEngComm* **2009**, *11*, 2406-2416.
- [23] D. Philp, J. F. Stoddart, *Angew. Chem. Int. Ed.* **1996**, *35*, 1154-1196.
- [24] aE. C. Constable, E. L. Dunphy, C. E. Housecroft, M. Neuburger, S. Schaffner, F. Schaper, S. R. Batten, *Dalton Trans.* **2007**, 4323-4332; bM. Beley, C. A. Bignozzi, G. Kirsch, M. Alebbi, J. C. Raboin, *Inorg. Chim. Acta* **2001**, *318*, 197-200.
- [25] aE. C. Constable, C. E. Housecroft, M. Neuburger, A. G. Schneider, M. Zehnder, *J. Chem. Soc., Dalton Trans.* **1997**, 2427-2434; bE. C. Constable, C. E. Housecroft, M. Neuburger, A. G. Schneider, B. Springler, M. Zehnder, *Inorg. Chim. Acta* **2000**, *300-302*, 49-55.
- [26] aA. C. Benniston, A. Harriman, P. Li, C. A. Sams, *J. Phys. Chem. A* **2005**, *109*, 2302-2309; bE. Narr, A. Godt, G. Jeschke, *Angew. Chem. Int. Ed.* **2002**, *41*, 3907-3910.
- [27] aD. M. Schultz, T. P. Yoon, *Science* **2014**, *343*; bC. K. Prier, D. A. Rankic, D. W. C. MacMillan, *Chem. Rev.* **2013**, *113*, 5322-5363; cJ. M. R. Narayanam, C. R. J. Stephenson, *Chem. Soc. Rev.* **2011**, *40*, 102-113; dT. P. Yoon, M. A. Ischay, J. Du, *Nature Chem.* **2010**, *2*, 527-532.
- [28] S. Fukuzumi, S. Mochizuki, T. Tanaka, *J. Phys. Chem.* **1990**, *94*, 722-726.
- [29] aA. McNally, C. K. Prier, D. W. C. MacMillan, *Science* **2011**, *334*, 1114-1117; bA. G. Condie, J. C. González-Gómez, C. R. J. Stephenson, *J. Am. Chem. Soc.* **2010**, *132*, 1464-1465.
- [30] aD. Hvasanov, J. R. Peterson, P. Thordarson, *Chem. Sci.* **2013**, *4*, 3833-3838; bA. Breivogel, C. Kreitner, K. Heinze, *Eur. J. Inorg. Chem.* **2014**, *2014*, 5468-5490.
- [31] M. Maestri, N. Armaroli, V. Balzani, E. C. Constable, A. M. W. C. Thompson, *Inorg. Chem.* **1995**, *34*, 2759-2767.
- [32] E. A. Medlycott, G. S. Hanan, *Chem. Soc. Rev.* **2005**, *34*, 133-142.
- [33] J. Yang, J. K. Clegg, Q. Jiang, X. Lui, H. Yan, W. Zhong, J. E. Beves, *Dalton Trans.* **2013**, *42*, 15625-15636.
- [34] aA. J. Metherell, M. D. Ward, *Chem. Commun.* **2014**, *50*, 10979-10982; bA. J. Metherell, M. D. Ward, *Chem. Commun.* **2014**, *50*, 6330-6332; cT.-Z. Xie, S.-Y. Liao, K. Guo, X. Lu, X. Dong, M. Huang, C. N. Moorefield, S. Z. D. Cheng, X. Liu, C. Wesdemiotis, G. R. Newkome, *J. Am. Chem. Soc.* **2014**, *136*, 8165-8168; dB. Therrien, *Eur. J. Inorg. Chem.* **2009**, *2009*, 2445-2453.
- [35] H. W. Roesky, M. Andruh, *Coord. Chem. Rev.* **2003**, *236*, 91-119.
- [36] I. Eryazici, O. K. Farha, O. C. Compton, C. Stern, J. T. Hupp, S. T. Nguyen, *Dalton Trans.* **2011**, *40*, 9189-9193.
- [37] J. E. Beves, E. C. Constable, C. E. Housecroft, C. J. Kepert, D. J. Price, *CrystEngComm* **2007**, *9*, 456-459.
- [38] J. E. Beves, E. C. Constable, C. E. Housecroft, M. Neuburger, S. Schaffner, *CrystEngComm* **2008**, *10*, 344-348.
- [39] J. E. Beves, E. C. Constable, C. E. Housecroft, C. J. Kepert, M. Neuburger, D. J. Price, S. Schaffner, J. A. Zampese, *Dalton Trans.* **2008**, 6742-6751.
- [40] K. Harris, D. Fujita, M. Fujita, *Chem. Commun.* **2013**, *49*, 6703-6712.
- [41] aJ. Veliks, O. Blacque, J. S. Siegel, *Inorg. Chem.* **2014**, *53*, 12122-12126; bJ. Veliks, J.-C. Tseng, K. I. Arias, F. Weisshar, A. Linden, J. S. Siegel, *Chem. Sci.* **2014**, *5*, 4317-4327.
- [42] aJ. E. Beves, E. C. Constable, C. E. Housecroft, C. J. Kepert, D. J. Price, *CrystEngComm* **2007**, *9*, 456-459; bJ. E. Beves, E. C. Constable, C. E. Housecroft, C. J. Kepert, M. Neuburger, D. J. Price, S. Schaffner, J. A. Zampese, *Dalton Trans.* **2008**, 6742-6751; cJ. E. Beves, E. C. Constable, S. Decurtins, E. L. Dunphy, C. E. Housecroft, T. D. Keene, M. Neuburger, S. Schaffner, *CrystEngComm* **2008**, *10*, 986-990; dJ. E. Beves, D. J. Bray, J. K. Clegg, E. C. Constable, C. E. Housecroft, K. A. Jolliffe, C. J. Kepert, L. F. Lindoy, M. Neuburger, D. J. Price, S. Schaffner, F. Schaper, *Inorg. Chim. Acta* **2008**, *361*, 2582-2590.
- [43] aG. R. Newkome, T. J. Cho, C. N. Moorefield, G. R. Baker, R. Cush, P. S. Russo, *Angew. Chem., Int. Ed.* **1999**, *38*, 3717-3721; bS.-H. Hwang, C. N. Moorefield, F. R. Fronczek, O. Lukoyanova, L. Echegoyen, G. R. Newkome, *Chem. Commun.* **2005**, 713-715; cS.-H. Hwang, P. Wang, C. N. Moorefield, L. A. Godínez, J. Manriquez, E. Bustos, G. R. Newkome, *Chem. Commun.* **2005**, 4672-4674.
- [44] aM. W. Cooke, D. Chartrand, G. S. Hanan, *Coord. Chem. Rev.* **2008**, *252*, 903-921; bG. R. Newkome, T. J. Cho, C. N. Moorefield, R. Cush, P. S. Russo, L. A. Godínez, M. J. Saunders, P. Mohapatra, *Chem.-Eur. J.* **2002**, *8*, 2946-2954; cG. R. Newkome, T. J. Cho, C. N. Moorefield, P. P. Mohapatra, L. A. Godínez, *Chem.-Eur. J.* **2004**, *10*, 1493-1500; dI. Eryazici, G. R. Newkome, *New J. Chem.* **2009**, *33*, 345 - 357; eA. Schultz, X. Li, B. Barkakaty, C. N. Moorefield, C. Wesdemiotis, G. R. Newkome, *J. Am. Chem. Soc.* **2012**, *134*, 7672-

- 7675;fX. Lu, X. Li, K. Guo, T.-Z. Xie, C. N. Moorefield, C. Wesdemiotis, G. R. Newkome, *J. Am. Chem. Soc.* **2014**.
- [45] J. Yang, J. K. Clegg, Q. Jiang, X. Lui, H. Yan, W. Zhong, J. E. Beves, *Dalton Trans.* **2013**, 42, 15625-15636.
- [46] aM. Fujita, M. Tominaga, A. Hori, B. Therrien, *Acc. Chem. Res.* **2005**, 38, 369-378; bY. Inokuma, M. Kawano, M. Fujita, *Nature Chem.* **2011**, 3, 349-358; cR. Chakrabarty, P. S. Mukherjee, P. J. Stang, *Chem. Rev.* **2011**, 111, 6810-6918.
- [47] aC. Patoux, J.-P. Launay, M. Beley, S. Chodorowski-Kimmes, J.-P. Collin, S. James, J.-P. Sauvage, *J. Am. Chem. Soc.* **1998**, 120, 3717-3725; bC. J. Aspley, J. A. G. Williams, *New J. Chem.* **2001**, 25, 1136-1147; cK. J. Arm, J. A. G. Williams, *Dalton Trans.* **2006**, 2172-2174; dY.-W. Zhong, N. Vila, J. C. Henderson, S. Flores-Torres, H. D. Abrunna, *Inorg. Chem.* **2007**, 46, 10470-10472; eO. Johansson, R. Lomoth, *Inorg. Chem.* **2008**, 47, 5531-5533; fW. Leslie, A. S. Batsanov, J. A. K. Howard, J. A. G. Williams, *Dalton Trans.* **2004**, 623-631; gV. L. Whittle, J. A. G. Williams, *Inorg. Chem.* **2008**, 47, 6596-6607; hV. L. Whittle, J. A. G. Williams, *Dalton Trans.* **2009**, 3929-3940.
- [48] J. Wang, G. S. Hanan, *Synlett* **2005**, 2005, 1251-1254.
- [49] J. Wang, G. S. Hanan, *Synlett* **2005**, 2005, 1251-1254.
- [50] W. Spahni, G. Calzagerri, *Helv. Chim. Acta* **1984**, 67, 450-454.
- [51] S. Bonnet, J.-P. Collin, J.-P. Sauvage, *Chem. Commun.* **2005**, 3195-3197.
- [52] W. Goodall, J. A. G. Williams, *J. Chem. Soc., Dalton Trans.* **2000**, 2893-2895.
- [53] E. C. Constable, A. M. W. C. Thompson, *J. Chem. Soc., Dalton Trans.* **1992**, 2947-2950.
- [54] F. Wehmeier, J. Mattay, *Beilstein Journal of Organic Chemistry* **2010**, 6, 53.
- [55] M. Vrábel, M. Hocek, L. Havran, M. Fojta, I. Votruba, B. Klepetářová, R. Pohl, L. Rulíšek, L. Zendlová, P. Hobza, I. h. Shih, E. Mabery, R. Mackman, *Eur. J. Inorg. Chem.* **2007**, 2007, 1752-1769.
- [56] H.-J. Cantow, H. Hillebrecht, S. N. Magonov, H. W. Rotter, M. Drechsler, G. Thiele, *Angew. Chem., Int. Ed. Engl.* **1990**, 29, 537-541.
- [57] C. J. Aspley, J. A. Gareth Williams, *New J. Chem.* **2001**, 25, 1136-1147.
- [58] J. E. Beves, E. L. Dunphy, E. C. Constable, C. E. Housecroft, C. J. Kepert, M. Neuburger, D. J. Price, S. Schaffner, *Dalton Trans.* **2008**, 386-396.
- [59] Y.-Q. Zou, J.-R. Chen, X.-P. Liu, L.-Q. Lu, R. L. Davis, K. A. Jørgensen, W.-J. Xiao, *Angew. Chem., Int. Ed.* **2012**, 51, 784-788.
- [60] K. Inamoto, K. Nozawa, M. Yonemoto, Y. Kondo, *Chem. Commun.* **2011**, 47, 11775-11777.
- [61] A. D. Chowdhury, S. M. Mobin, S. Mukherjee, S. Bhaduri, G. K. Lahiri, *Eur. J. Inorg. Chem.* **2011**, 2011, 3232-3239.
- [62] aN. Mulakayala, Ismail, K. M. Kumar, R. K. Rapolu, B. Kandagatla, P. Rao, S. Oruganti, M. Pal, *Tetrahedron Lett.* **2012**, 53, 6004-6007; bM. Gohain, M. du Plessis, J. H. van Tonder, B. C. B. Bezuidenhout, *Tetrahedron Lett.* **2014**, 55, 2082-2084.
- [63] R. E. Maleczka, F. Shi, D. Holmes, M. R. Smith, *J. Am. Chem. Soc.* **2003**, 125, 7792-7793.
- [64] C. Zhu, R. Wang, J. R. Falck, *Org. Lett.* **2012**, 14, 3494-3497.
- [65] E. Kianmehr, M. Yahyaei, K. Tabatabai, *Tetrahedron Lett.* **2007**, 48, 2713-2715.
- [66] S. Liatard, J. Chauvin, F. Balestro, D. Jouvenot, F. Loiseau, A. Deronzier, *Langmuir* **2012**, 28, 10916-10924.
- [67] E. C. Constable, A. M. W. C. Thompson, *J. Chem. Soc., Dalton Trans.* **1992**, 3467-3475.
- [68] A. Schultz, Y. Cao, M. Huang, S. Z. D. Cheng, X. Li, C. N. Moorefield, C. Wesdemiotis, G. R. Newkome, *Dalton Trans.* **2012**, 41, 11573-11575.
- [69] X. Lu, X. Li, J.-L. Wang, C. N. Moorefield, C. Wesdemiotis, G. R. Newkome, *Chem. Commun.* **2012**, 48, 9873-9875.
- [70] aM. Han, R. Michel, B. He, Y.-S. Chen, D. Stalke, M. John, G. H. Clever, *Angew. Chem., Int. Ed.* **2013**, 52, 1319-1323; bD. A. McMorran, P. J. Steel, *Angew. Chem., Int. Ed.* **1998**, 37, 3295-3297; cJ. D. Crowley, E. L. Gavey, *Dalton Trans.* **2010**, 39, 4035-4037; dH. S. Sahoo, D. K. Chand, *Dalton Trans.* **2010**, 39, 7223-7225; eM. Han, R. Michel, G. H. Clever, *Chem.-Eur. J.* **2014**, 20, 10640-10644; fD. M. Engelhard, S. Freye, K. Grohe, M. John, G. H. Clever, *Angew. Chem., Int. Ed.* **2012**, 51, 4747-4750; gG. H. Clever, S. Tashiro, M. Shionoya, *Angew. Chem.* **2009**, 121, 7144-7146; hS. O. Scott, E. L. Gavey, S. J. Lind, K. C. Gordon, J. D. Crowley, *Dalton Trans.* **2011**, 40, 12117-12124.
- [71] aZ. Li, N. Kishi, K. Hasegawa, M. Akita, M. Yoshizawa, *Chem. Commun.* **2011**, 47, 8605-8607; bZ. Li, N. Kishi, K. Yoza, M. Akita, M. Yoshizawa, *Chem.-Eur. J.* **2012**, 18, 8358-8365; cM. Frank, J. Hey, I. Balcioglu, Y.-S.

- Chen, D. Stalke, T. Suenobu, S. Fukuzumi, H. Frauendorf, G. H. Clever, *Angew. Chem., Int. Ed.* **2013**, *52*, 10102-10106.
- [72] aJ. E. M. Lewis, A. B. S. Elliott, C. J. McAdam, K. C. Gordon, J. D. Crowley, *Chem. Sci.* **2014**, *5*, 1833-1843; bG. H. Clever, S. Tashiro, M. Shionoya, *Angew. Chem. Int. Ed.* **2009**, *48*, 7010-7012.
- [73] aJ. E. M. Lewis, E. L. Gavey, S. A. Cameron, J. D. Crowley, *Chem. Sci.* **2012**, *3*, 778-784; bG. H. Clever, M. Shionoya, *Chem.-Eur. J.* **2010**, *16*, 11792-11796; cJ. E. M. Lewis, J. D. Crowley, *Supramol. Chem.* **2013**, *26*, 173-181.
- [74] M. Han, J. Hey, W. Kawamura, D. Stalke, M. Shionoya, G. H. Clever, *Inorg. Chem.* **2012**, *51*, 9574-9576.
- [75] aM. Tominaga, K. Suzuki, T. Murase, M. Fujita, *J. Am. Chem. Soc.* **2005**, *127*, 11950-11951; bT. Kikuchi, T. Murase, S. Sato, M. Fujita, *Supramol. Chem.* **2008**, *20*, 81-94.
- [76] A. M. Johnson, R. J. Hooley, *Inorg. Chem.* **2011**, *50*, 4671-4673.
- [77] P. Liao, B. W. Langloss, A. M. Johnson, E. R. Knudsen, F. S. Tham, R. R. Julian, R. J. Hooley, *Chem. Commun.* **2010**, *46*, 4932-4934.
- [78] aK. Harris, Q.-F. Sun, S. Sato, M. Fujita, *J. Am. Chem. Soc.* **2013**, *135*, 12497-12499; bQ.-F. Sun, T. Murase, S. Sato, M. Fujita, *Angew. Chem. Int. Ed.* **2011**, *50*, 10318-10321.
- [79] J. Yang, M. Bhadbhade, W. A. Donald, H. Iranmanesh, E. G. Moore, H. Yan, J. E. Beves, *Chem. Commun.* **2015**, *51*, 4465-4468.
- [80] aM. Sassaroli, M. Ruonala, J. Virtanen, M. Vauhkonen, P. Somerharju, *Biochemistry* **1995**, *34*, 8843-8851; bAndrew C. Benniston, A. Harriman, Donald J. Lawrie, Sarah A. Rostron, *Eur. J. Org. Chem.* **2004**, *2004*, 2272-2276; cE. Rivera, M. Belletête, X. Xia Zhu, G. Durocher, R. Giasson, *Polymer* **2002**, *43*, 5059-5068; dC. Diner, D. E. Scott, R. R. Tykwinski, M. R. Gray, J. M. Stryker, *J. Org. Chem.* **2015**, *80*, 1719-1726; eS. A. Ingale, F. Seela, *J. Org. Chem.* **2012**, *77*, 9352-9356.
- [81] aY. Niko, S. Kawauchi, S. Otsu, K. Tokumaru, G. Konishi, *J. Org. Chem.* **2013**, *78*, 3196-3207; bG. Venkataramana, S. Sankararaman, *Eur. J. Org. Chem.* **2005**, *2005*, 4162-4166.
- [82] M. Shimizu, H. Tatsumi, K. Mochida, T. Hiyama, *Chem. Commun.* **2008**, 2134-2136.
- [83] H. Maeda, T. Maeda, K. Mizuno, K. Fujimoto, H. Shimizu, M. Inouye, *Chem.-Eur. J.* **2006**, *12*, 824-831.
- [84] J. A. Simon, S. L. Curry, R. H. Schmehl, T. R. Schatz, P. Piotrowiak, X. Jin, R. P. Thummel, *J. Am. Chem. Soc.* **1997**, *119*, 11012-11022.
- [85] J. Gu, J. Chen, R. H. Schmehl, *J. Am. Chem. Soc.* **2010**, *132*, 7338-7346.
- [86] G. v. Büнау, *Berichte der Bunsengesellschaft für physikalische Chemie* **1970**, *74*, 1294-1295.
- [87] J. Zhao, D. Yang, Y. Zhao, X.-J. Yang, Y.-Y. Wang, B. Wu, *Angew. Chem. Int. Ed.* **2014**, *53*, 6632-6636.
- [88] E. A. Jares-Erijman, T. M. Jovin, *Nat Biotech* **2003**, *21*, 1387-1395.
- [89] Y. Hong, J. W. Y. Lam, B. Z. Tang, *Chem. Soc. Rev.* **2011**, *40*, 5361-5388.
- [90] aP. Wang, X. Yan, F. Huang, *Chem. Commun.* **2014**, *50*, 5017-5019; bF. Sun, G. Zhang, D. Zhang, L. Xue, H. Jiang, *Org. Lett.* **2011**, *13*, 6378-6381.
- [91] B. A. G. Hammer, M. Baumgarten, K. Mullen, *Chem. Commun.* **2014**, *50*, 2034-2036.
- [92] J. L. Bolliger, A. M. Belenguer, J. R. Nitschke, *Angew. Chem. Int. Ed.* **2013**, *52*, 7958-7962.
- [93] J. K. Clegg, J. Cremers, A. J. Hogben, B. Breiner, M. M. J. Smulders, J. D. Thoburn, J. R. Nitschke, *Chem. Sci.* **2013**, *4*, 68-76.
- [94] N. Ousaka, S. Grunder, A. M. Castilla, A. C. Whalley, J. F. Stoddart, J. R. Nitschke, *J. Am. Chem. Soc.* **2012**, *134*, 15528-15537.
- [95] W. Meng, B. Breiner, K. Rissanen, J. D. Thoburn, J. K. Clegg, J. R. Nitschke, *Angew. Chem., Int. Ed.* **2011**, *50*, 3479-3483.
- [96] aD. M. Wood, W. Meng, T. K. Ronson, A. R. Stefankiewicz, J. K. M. Sanders, J. R. Nitschke, *Angew. Chem. Int. Ed.* **2015**, *54*, 3988-3992; bJ. L. Bolliger, T. K. Ronson, M. Ogawa, J. R. Nitschke, *J. Am. Chem. Soc.* **2014**, *136*, 14545-14553; cD. A. Roberts, A. M. Castilla, T. K. Ronson, J. R. Nitschke, *J. Am. Chem. Soc.* **2014**, *136*, 8201-8204.
- [97] A. Schreivogel, J. Maurer, R. Winter, A. Baro, S. Laschat, *Eur. J. Org. Chem.* **2006**, *2006*, 3395-3404.
- [98] aJ. E. Beves, C. J. Campbell, D. A. Leigh, R. G. Pritchard, *Angew. Chem., Int. Ed.* **2013**, *52*, 6464-6467; bJ.-F. Ayme, J. E. Beves, D. A. Leigh, R. T. McBurney, K. Rissanen, D. Schultz, *J. Am. Chem. Soc.* **2012**, *134*, 9488-9497; cJ.-F. Ayme, J. E. Beves, D. A. Leigh, R. T. McBurney, K. Rissanen, D. Schultz, *Nature Chem.* **2012**, *4*, 15-20.